Motor flexibility: neuronal control of walking direction and walking speed in an insect

Inaugural-Dissertation

zur

Erlangung des Doktorgrades

der Mathematisch-Naturwissenschaftlichen Fakultät

der Universität zu Köln

vorgelegt von

Philipp Rosenbaum

aus Soest

Köln

Mai 2013

Berichterstatter:
Prof. Dr. Ansgar Büschges
Prof. Dr. Peter Kloppenburg

Tag der mündlichen Prüfung:

05. Juli 2013.

Abstract

The neuronal basis of locomotion is largely investigated in many different vertebrate and invertebrate species. Especially studying the neuronal control of adaptive locomotor behaviors is important to reveal general insights into nervous system function. In this thesis, the stick insects *Carausius morosus* and *Cuniculina impigra* were used to investigate how important parts of the locomotor network generate different walking directions and walking speeds. In order to study which parameters have to be changed to generate the different behaviors, leg muscle, motoneuron, and premotor nonspiking interneuron activity was recorded.

In the first part, leg muscle activity during forward, backward, and curve walking was studied in a slippery surface setup, in which the animal is stationary about a slippery substrate and all legs can freely move. Muscle activity and timing was compared during different walking directions. The main change was observed in protractor and retractor muscles which move the leg in anterior and posterior direction. These muscles almost completely reverse their phase of activity with the change of walking direction, and intermediate changes occur in the inside leg during curve walking, depending on the steepness of the curve.

In the second and third part, leg motoneuron and interneuron activity was recorded intracellularly in the single-leg preparation, in which only one leg is able to move in the vertical plane on a treadwheel. Fictive forward and backward walking can be reliably elicited in this preparation. It is known that leg motoneurons receive tonic depolarizing synaptic inputs from higher centers throughout walking, and additional phasic excitatory and inhibitory inputs from leg sense organs, as well as phasic inhibitory inputs from the rhythm generating network. It could be shown that similar inputs shape the motoneuron modulation pattern also during backward walking. The phase of the step cycle in which the phasic inputs to protractor and retractor MNs occur reverses during backward walking. It was shown previously that stepping velocity in the single-leg preparation is correlated to flexor MN activity (stance) but not extensor MN (swing) activity. These findings are confirmed in this thesis and also held for backward walking. No such influences could be shown for other stance phase motoneurons. Furthermore, premotor nonspiking interneurons were recorded to investigate their contribution to the generation of different walking directions and walking speeds. These neurons are known to integrate signals from descending, central, and sensory sources and thus contribute to the control of timing and magnitude of the motor output. Previously identified (E3, E4, E5, E7, I1, I2), as well as newly described nonspiking interneurons providing synaptic drive to motoneurons of all leg joints were recorded during forward and backward stepping. Interestingly, neurons could be identified which contribute

to the change in protractor and retractor muscle activity. Furthermore it could be shown that all recorded nonspiking interneurons contribute to the motor output during walking in both directions, suggesting that the same premotor network is responsible for the generation of both behaviors. NSI activity also underlies tonic and phasic synaptic inputs. Additionally, the contribution of NSIs to the generation of different stepping velocities was investigated.

Zusammenfassung

Die neuronale Kontrolle der Fortbewegung wird seit langer Zeit an vielen Vertebraten und Invertebraten untersucht. Die Untersuchung der neuronalen Kontrolle von adaptivem Laufverhalten kann helfen generelle Aussagen über die Funktion von Nervensystemen zu erlangen. In dieser Dissertation wurde anhand der Stabheuschreckenarten *Carausius morosus* und *Cuniculina impigra* untersucht, wie verschiedene Ebenen des motorischen Netzwerks der Laufkontrolle zur Generation verschiedener Laufrichtungen und Laufgeschwindigkeiten beitragen. Um herauszufinden, welche Parameter verändert werden müssen um verschiedene Verhaltensweisen zu generieren wurden Muskel-, Motorneuron- und Interneuronableitungen durchgeführt.

Im ersten Teil der Arbeit wurde die Beinmuskelaktivität während Vorwärts-, Rückwärts- und Kurvenlaufen in einem Glitschplattensetup untersucht. In diesem Versuchsaufbau ist das Tier stationär über einer glitschigen Oberfläche gehaltert und alle Beine können sich frei bewegen. Der Hauptunterschied in der Muskelaktivität zwischen den verschiedenen Laufrichtungen wurde in den Protractor- und Retractormuskeln gefunden, die das Bein in anteriore, bzw. posteriore Richtung bewegen. Ihre Aktivität während des Schrittzykluses wurde mit Änderung der Laufrichtung annähernd umgekehrt. Bei dem in der Kurveninnenseite laufenden Bein treten Zwischenformen in der Protractor- und Retractoraktivität auf.

Weiterhin wurde in einem Einbeinpräparat, in dem nur ein Bein in der vertikalen Ebene Schrittbewegungen auf einem Laufband ausüben kann, Beinmotorneurone und prämotorische nichtspikende Interneurone intrazellulär abgeleitet. In dieser Präparation kann fiktives Vor- und Rückwärtslaufen zuverlässig ausgelöst werden. Es ist bereits bekannt, dass Beinmotorneurone während des Laufens tonisch depolarisiert werden und zusätzlich phasische erregende und hemmende Einflüsse von Beinsinnesorganen, sowie hemmende Einflüsse von dem Rhythmus generierendem Netzwerk erhalten. In dieser Arbeit konnte gezeigt werden, dass diese synaptischen Eingänge auch der Motorneuronaktivität während des Rückwärts-

laufens zugrundeliegen. Der einzige Unterschied in der Motorneuronaktivität während der beiden Laufrichtungen besteht, wie bei den Muskeln, in der Phasenumkehr der Protractor- und Retractoraktivität. Weiterhin ist bereits bekannt, dass die Laufgeschwindigkeit auf dem Laufband von der Aktivität der Flexormotorneurone (in der Stemmphase), aber nicht von der Aktivität der Extensormotorneurone (in der Schwingphase) abhängig ist. Dies konnte in meinen Untersuchungen bestätigt werden, jedoch wurde kein Zusammenhang zwischen der Aktivität anderer Stemmphasenmotorneurone und der Laufgeschwindigkeit gefunden. Um mehr über die synaptischen Eingänge der Motorneurone für die Generierung verschiedener Laufrichtungen und Laufgeschwindigkeiten herauszufinden, wurden die prämotorischen nichtspikenden Interneurone in derselben Präparation untersucht. Diese lokalen Neurone erhalten ihrerseits synaptische Eingänge von absteigenden Neuronen, Beinsinnesorganen und dem Rhythmus generierendem Netzwerk, integrieren diese und tragen somit zur Kontrolle der Magnitude und zeitlichen Koordinierung des motorischen Ausgangs bei. Bereits beschriebene Nichtspiker (E3, E4, E5, E7, I1, I2), sowie neu identifizierte nichtspikende Interneurone, die Einfluss auf Motorneurone aller Beingelenke ausüben, wurden während Vorwärts- und Rückwärtslaufen untersucht. Dabei konnten Neurone identifiziert werden, die zu der unterschiedlichen Ansteuerung der Protraktor- und Retraktormotorneurone während der verschiedenen Laufrichtungen beitragen. Außerdem konnte gezeigt werden, dass alle abgeleiteten Interneurone während beider Laufrichtungen zur Kontrolle der Beinbewegung beitragen. Dies lässt vermuten, dass das selbe prämotorische Netzwerk an der Generierung beider Laufrichtungen beteiligt ist. Der Aktivität der nichtspikenden Interneurone unterliegen ebenfalls tonische und phasische synaptische Eingänge. Außerdem wurde die Beteiligung der nichtspikenden Interneurone an der Kontrolle der Laufgeschwindigkeit untersucht.

Contents

List of Abbreviations

CTr	coxa-trochanter
CPG	central pattern generator
EMG	electromyogram
fCO	femoral chordotonal organ
fCS	femoral campaniform sensilla
FTi	femur-tibia
MN	motoneuron
MP	membrane potential
NSI	nonspiking interneuron
RMP	resting membrane potential
ThC	thorax-coxa
trCS	trochanteral campaniform sensilla

1 Introduction

Locomotion is one of the most important behaviors an animal can perform. Many different forms of locomotion exist, such as walking, swimming, flying, and crawling. Locomotion has to be very finely tuned to optimally adapt the behavior of the animal to the environmental needs. As a consequence, animals do not constantly perform straight walks, but also walk in curves, climb or are tunneling under objects. Therefore, it is a challenge to find out how the great adaptability is generated by the nervous system, which will also help to a better understanding about the general function of nervous systems. Despite considerable work devoted to understanding how behavioral plasticity arises (humans: van Deursen et al., 1998; Lamb and Yang, 2000; salamander: Ashley-Ross and Lauder, 1997; fish: Orger et al., 2008; lamprey: Islam et al., 2006; fruit fly: Frye and Dickinson, 2001, 2004; cockroach: Watson et al., 2002b,a; stick insect: Dürr and Ebeling, 2005; Gruhn et al., 2009a,b), the underlying mechanisms on the neuronal level are only at the advent of understanding (Schaefer and Ritzmann, 2001; Ridgel and Ritzmann, 2005; Pick and Strauss, 2005; Ridgel et al., 2007; Akay et al., 2007).

Most terrestrial animals locomote using legs. Not only the movement of one leg with its many joints has to be coordinated, but also the activity of the different legs with regard to each other. This results in different gaits. Quadrupedal animals change their gaits depending on the walking speed (Alexander, 1989). Insects use tetrapod and tripod gaits, and a multitude of intermediate forms, depending on the species, the developmental stage of the animal, and the walking speed (Hughes, 1952; Graham, 1985; Cruse, 1990; Grabowska et al., 2012; Wosnitza et al., 2013).

All forms of locomotion underlies a coordinated, rhythmic contraction of antagonistic muscles (Orlovsky et al., 1999). In vertebrates, the motor command centers in the brain, motor cortex, basal ganglia, and cerebellum, transmit signals via the brainstem to the spinal cord, in which local circuits, called central pattern generators (CPGs), are responsible for the coordinated motor output of the muscles (e.g. Grillner et al. 1995; Grillner 2003; Kiehn 2006). Also in insects, it is known that the brain and especially the central complex is responsible for higher loco-

motor function (Strauss, 2002), whereas the ventral nerve chord, which contains the rhythm generating networks, is responsible for the coordinated motor output of single legs and single leg joints (Bässler and Büschges, 1998).

Especially in insects, the neuronal control of walking has been investigated to some extent down to the single cell level. In the indian stick insect *Carausius morosus* and the closely related species *Cuniculina impigra*, detailed knowledge exists about the neuronal control of locomotion (reviews in Bässler and Büschges, 1998; Büschges, 2005; Büschges et al., 2008; Büschges and Gruhn, 2008). Furthermore, substantial information is available about leg kinematics during adaptive locomotor behaviors, such as different walking directions, turning, and gap climbing (Cruse, 1976a; Jander, 1982; Blaesing and Cruse, 2004; Dürr and Ebeling, 2005; Gruhn et al., 2009b; Cruse et al., 2009). In the stick insect, three main leg joints move the leg. In the thorax-coxa (ThC) joint, the protractor coxae moves the leg anteriorly and the retractor coxae posteriorly. The coxa-trochanter joint (CTr) lifts the leg using the levator trochanteris and depresses it by the depressor trochanteris. The extensor tibiae extends the tibia, while the flexor tibia bends the tibia around the femur-tibia (FTi) joint. The step cycle of a leg is divided into two phases. During forward walking, the leg is lifted and extended while moving in anterior direction in the swing phase. In the stance phase, in which propulsive force is generated to push the animal in the walking direction, the leg is depressed, flexed and moved backwards. This is the case for the forward walking front and middle legs of the stick insect, the movement kinematics of the hind legs differ from that to some extent (e.g. see Cruse and Bartling, 1995).

To achieve this coordinated movement, the muscles have to be activated in the right order and at the right time. In addition to the neuronal control of muscle activity, intrinsic muscle properties also play an important role in the generation of the movement (Guschlbauer et al., 2007; Hooper et al., 2007b,a, 2009). Each muscle is innervated by a set of motoneurons (MNs), three MNs innervate the extensor tibiae muscle and up to 25 the flexor tibia muscle (Goldammer et al., 2012). Descending signals from the brain and intersegmental signals from other legs lead to a general excitation of the leg MNs. The rhythm generating network, the central pattern generators, are responsible for the rhythmical activation of the leg MNs. Sensory signals from the legs, which measure load, strain, and posture, arrange the appropriate timing of the motor output (reviews in Bässler and Büschges, 1998; Ritzmann and Büschges, 2007; Büschges and Gruhn, 2008). In the following, these sources of input to the leg muscle control system are described in more detail.

Tonic descending drive The tonic background excitation in insect leg MNs is thought to derive from descending inputs (Ridgel and Ritzmann, 2005), similar to the glutamatergic excitation of spinal motoneurons in vertebrates descending from the brainstem (Roberts et al., 2008). The function of the tonic depolarization is to increase the membrane potential of the leg motoneurons for a higher responsiveness to further depolarizing inputs during walking. Previous studies showed that the tonic depolarization increases the membrane potential of leg motoneurons by up to 5 mV. It has a reversal potential in the range of -47 to -32 mV, which suggests that a mixed Na^+/K^+-ion current underlies its activation. This is mediated by metabotropic acetylcholine receptors in the leg motoneurons (Ludwar et al., 2005b; Westmark et al., 2009). Furthermore, the tonic depolarization is influenced by the neuromodulator octopamine. Thus, also neuromodulatory DUM (dorsal unpaired median) neurons, which release octopamine, might be involved in the generation of the tonic depolarization (Bräunig and Pflüger, 2001). It has also been shown that different leg motoneurons have different resting membrane potentials. For example, fast flexor MNs have a more negative resting potential than slow flexor MNs (Gabriel et al., 2003). Thus, when the flexor muscle has to be activated, the slow MNs first reach their firing threshold which is sufficient for slow movements, and only a stronger excitation brings the fast flexor MNs above the threshold to fire action potentials.

Central pattern generators The central pattern generating network in the thoracic ganglia of the stick insect provides inhibitory synaptic input to leg MNs. This has been studied in a preparation in which all legs of the insect were removed and the motor system of the stick insect was activated (Büschges et al., 2004). The central pattern generating circuit has not yet been identified in the stick insect, though some premotor nonspiking interneurons may contribute to its function (Büschges, 1995). In other invertebrates, cells have been identified the CPG is composed of (stomatogastric nervous system of crabs and lobsters (STG, Marder and Bucher, 2007); locust flight (Robertson and Pearson, 1985); swimmeret system of the crayfish (Mulloney and Smarandache-Wellmann, 2012); leech heartbeat (Kristan et al., 2005); sea slug Tritonia escape swimming (Getting et al., 1980)). Furthermore, in some vertebrates, although the CPG is not identified on the single cell level, a comprehensive overview about the rhythmic generation of locomotor output exists: lamprey swimming (Grillner et al., 1995; Grillner, 2003); frog tadpole swimming (Roberts et al., 1998); rodent walking (Kiehn, 2006); cat walking (Grillner and Zangger, 1979). A central pattern generating network can exert its drive by different mechanisms (Marder and Calabrese, 1996; Marder and Bucher, 2001; Goulding, 2009). Neurons, that are part of a CPG circuit, can show

rhythmicity because of their intrinsic membrane properties, such as endogenous bursting, postinhibitory rebound, spike frequency adaptation, or plateau potentials. The characteristics of a CPG network depend on such intrinsic properties of the neurons it is composed of and the synaptic interactions among them. Networks can either be pacemaker driven, like in the pyloric system of the STG (Marder and Eisen, 1984), or depend on reciprocal inhibition between CPG neurons (half-center oscillator) like in the spinal cord of the lamprey (Grillner, 1999). Furthermore, the output of such a network strongly depends on the action of neuromodulators, which change the intrinsic properties of neurons (Nusbaum et al., 2001). Some behaviors underlie the action of the same groups of muscles. In such cases it is also interesting to know if they share the same pattern generating network with different output properties, if one CPG for a certain behavior exists, or if CPGs are reconfigured in a task-dependent manner (Marder and Calabrese, 1996; Marder and Bucher, 2001; Goulding, 2009; Jing et al., 2011). In some systems, fictive rhythmicity can be induced in the isolated nerve cord, which largely resembles the one observed in the intact animal (like in the STG, Marder and Bucher, 2007). In other systems, only some aspects of the rhythm generation can be observed by pharmacologically activating the responsible network. Büschges et al. (1995) could show, that the thoracic nervous system of the stick insect becomes rhythmically active when activated with the muscarinic acetylcholine agonist pilocarpine. In that case, motoneurons are rhythmically bursting, though not in a manner that resembles fictive walking. However, the activity of antagonistic motoneuron pools show alternation, which led to the assumption that each leg joint in the stick insect is controlled by its own rhythm generating network (Büschges et al., 1995).

Afferent signals from leg sens organs The third source of synaptic inputs to leg MNs are sensory signals. Many studies investigated the effect of leg sense organs on the activation and inhibition of different motoneuron pools (reviewed in Büschges and Gruhn, 2008). All connections from mechanosensory neurons to central neurons are excitatory, whereas inhibitory effects are caused by intercalated interneurons which reverse the sign of the sensory output. Both spiking as well as nonspiking interneurons have receptive fields consisting of inputs from several leg mechanosensory signals and thus are processed in parallel (Burrows, 1996). One example is the femoral chordotonal organ (fCO) in the femur of the stick insect leg, which measures movements in the femur-tibia joint. In the quiescent animal, a leg flexion leads to a so called resistance reflex which activates extensor MNs and inhibits flexor activity. However, in the active animal, a leg flexion generates a so called reflex reversal (or active reaction) which further flexes the leg and inhibits extensor activity. Such a reinforcement of movement is thought to be an important

part of the control regime for the generation of single leg stepping (reviewed in Bässler, 1993). Recently, it was shown that this reflex is altered in the behavioral context of the leg during different walking directions (Hellekes et al., 2012). The fCO is also involved in inter-joint control, such that when it measures a leg flexion in the active animal, levator MNs are activated and depressor MNs are inhibited, and vice versa during an extension of the leg (Hess and Büschges, 1999). Other leg sense organs, like campaniform sensilla (CS) and hair plates (HP) have also been investigated and their roles in intra- and interleg joint coordination has been shown (e.g. CS: Akay et al., 2004, 2007; Zill et al., 2012; HP: Schmitz, 1986b; Büschges and Schmitz, 1991; Dean and Schmitz, 1992).

Premotor nonspiking interneurons The majority of these sources of synaptic inputs to leg MNs is not based on monosynaptical connections, but rather is submitted via intercalated premotor nonspiking interneurons. First recordings of nonspiking interneurons (NSIs) in insects were performed by Pearson and Fourtner (1975), after these local interneurons were found in other invertebrates and were shown to be involved in the pattern generation of small circuits (Mendelson, 1971). Since then, NSIs were thoroughly investigated, especially in the locust (Wilson and Phillips, 1983; Siegler, 1985; Burrows, 1996). NSIs integrate signals from the aforementioned sources and thus contribute to the control of timing and magnitude of the motor output. They receive excitatory signals from leg sense organs, inhibitory and excitatory inputs from spiking interneurons (inhibitory: midline spiking interneurons; excitatory: antero-medial spiking interneurons), and inhibitory inputs from other nonspiking interneurons (Burrows, 1979, 1996). Individual NSIs can also respond differentially to signals from the same sense organs (Büschges, 1990). Thus, there exist parallel, antagonistic pathways from leg sense organs via intercalated interneurons to the leg motoneurons (Bässler, 1993). All investigated NSIs have chemical synapses. However, not much is known about the transmitters involved in their action. Certainly, GABA is an important transmitter released by NSIs (Wildman et al., 2002). One big advantage of the nonspiking cells is that they gradually release transmitter and therefore are able to very finely control their action on MNs (Burrows and Siegler, 1978). Some NSIs are also known to tonically release transmitter which permanently affects the membrane potential of postsynaptic motoneurons (Wilson and Phillips, 1982). NSIs make output connections with motoneurons, other nonspiking interneurons, and with intersegmental interneurons. Particularly for the stick insect, NSIs involved in the control of the femur-tibia leg joint control system have been investigated to some extent (Büschges, 1990; Driesang and Büschges, 1993; Büschges et al., 1994; Sauer et al., 1996), also during walking (von Uckermann and Büschges, 2009). Interneu-

ron E4 provides excitatory synaptic drive to extensor, levator, protractor, and common inhibitor1 MNs, and inhibitory synaptic drive to retractor and depressor MNs. NSI I4 provides excitatory synaptic drive to depressor and flexor MNs and inhibitory synaptic drive to extensor MNs. These two NSIs were shown to be related to the rhythm generating network of the femur-tibia and coxa-trochanter leg-joint control system (Büschges, 1995).

Neuronal control of walking direction and walking speed Now the question arises, which parameters in the previously described leg control system have to be changed to generate adaptive forms of locomotion. How the direction of walking is changed was investigated in vertebrates (Buford et al., 1990; Buford and Smith, 1990; Islam et al., 2006; Zelenin, 2011; Zelenin et al., 2011; Musienko et al., 2012) and invertebrates. In insects, backward and curve walking was investigated in several studies concerning the kinematics (Dürr and Ebeling, 2005; Gruhn et al., 2009b), the muscle activity (Graham and Epstein, 1985; Mu and Ritzmann, 2005), the involvement of sense organs (Akay et al., 2007; Mu and Ritzmann, 2008b; Hellekes et al., 2012), and the descending control (Guo and Ritzmann, 2013). Furthermore, neuromechanical models exist in which changes in the neuronal network have been proposed which account for the change in walking direction (Toth et al., 2012; Knops et al., 2012).

The speed of locomotion in animals can be changed by different mechanisms. During swimming in the lamprey, increased tonic drive of reticulospinal neurons to spinal CPG interneurons increases the swimming frequency (Grillner et al., 1995). Also in the zebrafish and the Xenopus tadpole, studies dealt with the change in locomotion speed (McLean et al., 2008; Li and Moult, 2012). Stick insects increase their walking speed by decreasing the cycle period. Whereas the duration of the swing phase is similar during different walking speeds, the duration of the stance phase is decreased with increasing walking speed (Wendler, 1964). This has been studied at the level of the leg motoneurons. It was shown that the activity of the flexor MNs, which are active in the stance phase of the step cycle, is correlated with walking speed, whereas extensor MNs, which are active in swing, do not show such a change (Gabriel and Büschges, 2007). Furthermore, no intersegmental influences concerning the velocity of stepping front legs have been found to influence the activity of MNs in the deafferented middle leg (Gruhn et al., 2009a).

Experimental approaches The advantage of using the stick insect species *Carausius morosus* and *Cuniculina impigra* is their easy stock keeping and breeding,

and their relatively large size for an insect. This makes semi-intact preparations possible, in which one to six legs are able to walk, while muscle and nerve activity or single cells can be recorded. Compared to other well investigated insects like locusts, there is no wing musculature, which makes the thoracic ganglia easier to access for intracellular recordings.

Many different approaches have been used to investigate the neuronal circuits underlying locomotion in the stick insect. Experiments on the slippery surface have the advantage that the animal is able to freely move its legs while it is stationary above a slippery substrate. The legs are not mechanically coupled via the substrate which can be of advantage for some questions. Walking can be elicited using an optomotor stimulus, which can also induce curve walking (Gruhn et al., 2006). The slippery surface has been used to study escape responses (Camhi and Nolen, 1981), turning (Tryba and Ritzmann, 2000a,b; Gruhn et al., 2009b), backward walking (Graham and Epstein, 1985), and changes in velocity (Gruhn et al., 2009a). It also allows easy combination of intra- and extracellular recordings with kinematical analyses (Hellekes et al., 2012). The electronic measurement of tarsus ground contact on the slippery surface allows a precise measurement of step phase transitions during different walking situations and therefore an exact comparison with simultaneously recorded muscle and motoneuron activity, respectively (Gruhn et al., 2006).

The single leg-preparation allows to study the control of a single-leg without intersegmental influences from other legs. It also offers the opportunity to record intracellularly from the thoracic ganglia (Schmidt et al., 2001; Gabriel and Büschges, 2007; von Uckermann and Büschges, 2009; Berg et al., 2013). Stepping is possible on a passive, low-friction treadwheel, whereas in most cases the thorax-coxa joint is fixed and thus only leg movement in the vertical plane is possible (Fischer et al., 2001; Gabriel et al., 2003; von Uckermann and Büschges, 2009).

This thesis In this thesis, the focus lies on gaining more insights into the neural control of adaptive locomotor behaviors. This was investigated on the level of the muscles, motoneurons, and premotor nonspiking interneurons. Their activity was compared between forward and backward walking, as well as between different stepping velocities.

In the first part of this thesis, muscle recordings from the six main leg muscles were performed while the animal was walking forward, in a curve, and backward on a slippery surface. The muscle activity of each muscle was compared during these different behaviors and their exact timing with regard to the transition phases of the step cycle was determined. Data was evaluated for intact animals as well as

for reduced preparations, i.e. animals with only one or two legs.

In the second and third part of this thesis, intracellular recordings of leg muscle motoneurons and premotoric nonspiking interneurons during forward and backward walking were performed to gain a better understanding of local neuronal network activity during different behaviors. These experiments were performed in the single-leg preparation. Synaptic inputs to leg motoneurons were compared between the different walking directions, and also if MN activity and stepping velocity on the treadwheel were related. Previously described nonspiking interneurons, as well as newly described interneurons were recorded and their activity during forward and backward walking, and between different stepping speeds was compared. Stainings of local interneurons helped to identify previously described NSIs and to describe newly identified NSIs.

2 Methods

2.1 Leg muscle recordings from animals walking on a slippery surface[1]

Animals All experiments were performed on adult female stick insects (*Carausius morosus*). Animals were reared in the animal facility of the institute in a 12/12h light/dark cycle at 20-22°C and were fed with blackberry leaves (*Rubus fructiosus*) ad libitum.

Experimental setup In all experiments, animals walked on a 13.5 cm x 13.5 cm polished nickel-coated brass plate divided into two halves. In order to allow unimpeded walking under tethered conditions and remove mechanical coupling between the legs, the plate was covered with a lubricant composed of 95% glycerin, 5% saturated NaCl, and a small amount of electrode cream (Marquette Hellige, Freiburg, Germany). This created both a slippery surface and allowed recording of tarsal contact by electric current flow during ground contact (Gruhn et al., 2006). The animal was glued ventral side down on an 80 mm long and 3 mm wide balsa rod using dental cement (ProTempII, ESPE, Seefeld, Germany) so the legs and head protruded from the rod and all joints were unrestrained. Animal height above the substrate was adjustable, but was typically 10 mm. Experiments were performed in a darkened Faraday cage at room temperature.

Walking was elicited by projecting a progressive striped pattern (pattern wave length 21°) onto two 13.5 cm diameter round glass screens (Scharstein, 1989)

[1]The methods section for leg muscle recordings from animals walking on a slippery surface is already published: Rosenbaum P, Wosnitza A, Büschges A and Gruhn M. *Activity Patterns and Timing of Muscle Activity in the Forward Walking and Backward Walking Stick Insect* Carausius morosus. Journal of Neurophysiology 104: 1681-1695, 2010. The authors contributions for the paper are as followed: AB, MG, PR, and AW designed research; PR and AW performed experiments, analyzed data and prepared figures; AB, MG, PR, AW wrote the manuscript. Therefore this section is, except for minor modifications, literally taken from the paper. Descriptions for curve walking experiments were added in the appropriate sections.

placed at right angles to each other and at a 45°angle to the walking surface, approximately 6-7 cm away from the eyes of the animal. Reflections on the polished brass plate further increased the field of view. Alternatively, a single white stripe on dark background (towards which the animals orient with straight walking sequences) was placed in front of the animal. If the animal did not begin locomotion spontaneously, walking was elicited by light brush strokes to the abdomen. Backward walking was elicited by gentle pulls on the antennae (Graham and Epstein, 1985). Curved walking was elicited by moving the stripe on both glass screens in the same direction (Gruhn et al., 2011).

Electrophysiology Muscle activity (electromyogram, EMG) was recorded using two twisted, coated copper wires (57 µm or 49 µm outer diameter) cut at the tip, placed in each muscle approximately 1 mm apart and held in place with dental cement (ProTempII, ESPE) or tissue adhesive (3M Vetbond, St.Paul, MN, USA). Fig. 2.1A shows the approximate sites for the EMG wire placement in the cuticle of the leg and thorax. All recordings were differentially amplified. The EMG signal was amplified 1000 fold (preamplifier MA101 and amplifier MA102, electronics workshop, Zoological Institute, Cologne), band-pass filtered (100Hz-2000Hz) and imported into Spike2 (Version 5.05, CED, Cambridge, UK) through an AD converter (Micro 1401 II, CED, Cambridge, UK). A reference electrode was placed in the abdomen of the stick insect.

In most experiments, two antagonistic joint muscles were recorded simultaneously. Protractor coxae and retractor coxae EMGs were recorded in the thorax, depressor trochanteris and levator trochanteris in the coxa, and extensor tibiae and flexor tibiae in the femur.

Recording tarsal contact To determine the exact moment of the switch between stance and swing we used middle leg tarsal contact as a switch to open and close an electric circuit (Gruhn et al., 2006). Briefly, we used a 2-4 nA amplitude square wave signal generated with a pulse generator (Model MS501, electronics workshop, Zoological Institute, Cologne) applied to one half of the slippery surface and to a lock-in amplifier (electronics workshop, Zoological Institute, Cologne) as a reference signal. We tied a copper wire (49 µm outer diameter) with its insulation removed at the tip around the tibia of the leg being monitored, and connected it to the lock-in amplifier. The resistance between the cuticle and copper wire was reduced with a drop of electrode cream (Marquette Hellige, Freiburg, Germany) placed at the area of contact, allowing a 2-4 nA current to pass through tarsus and tibia. During stance, current flowed from the plate through tarsus and tibia

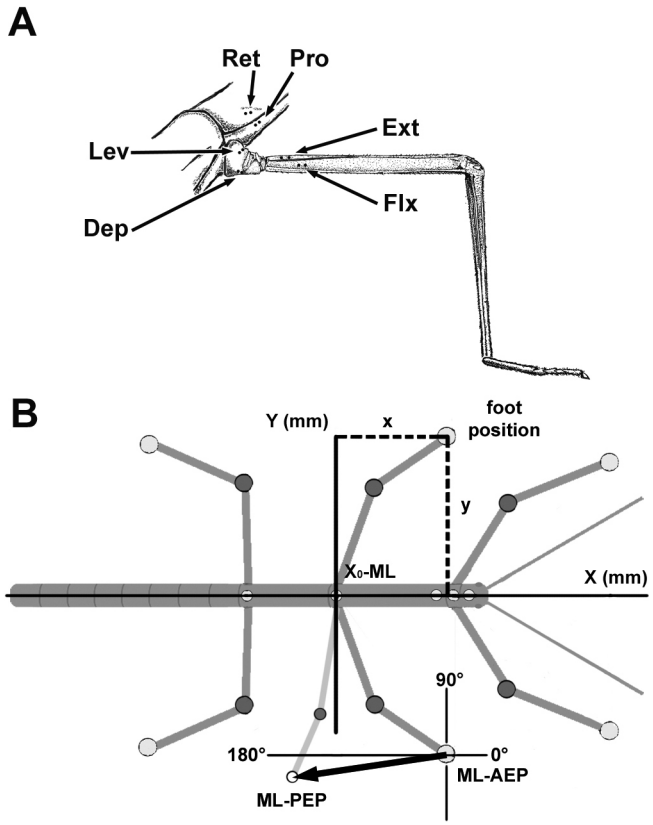

Figure 2.1 – A: drawing of the stick insect middle leg and the adjacent mesothorax with the approximate placement sites for the EMG electrodes for recordings of the main leg muscles. Pro, protractor coxae; Ret, retractor coxae; Ext, extensor tibiae; Flx, flexor tibiae; Lev, levator trochanteris; Dep, depressor trochanteris. B: schematic of the stick insect with the points tracked. X-values are always points along the length of the animal, while y-values mark points perpendicular to the animal. The x 0 value was set at the level of the middle leg coxa to give a clear reference point. As an example for the determination of the step length vector and its direction, the right middle leg is drawn at two arbitrary positions, one anterior extreme position (ML-AEP) and one posterior extreme position (ML-PEP). The vectors for all steps connecting the two positions, normalized to the origin in the AEP, gave direction in ° and step length in mm. The 0°-180° axis was always parallel to the body axis and crossed the AEP, 90° always points towards the animal perpendicularly.

into the copper wire, but during swing, when the leg was in the air, the circuit was disconnected. Amplifier output was fed into the AD converter and recorded using Spike2.

Due to the low-pass filter properties of the lock-in amplifier and the gradual lift-off/touch down of the tarsus, the signal is not exactly square. We therefore used thresholds set close to the transition point to define the timing of tarsal contact and manually checked each event. Touch downs could be determined at a resolution of less than 1 ms. Lift-off transitions were less steep and more delayed because of delayed tearing of the lubricant from the tarsus due to a capillary action and occasional upward movements of the leg during stance without complete lift-off. To have comparable lift-off times in all experiments we therefore always defined lift-off as the time point at the beginning of the steepest ascending slope.

Video recording and digital analysis of leg movements Video recordings of forward and backward walking were performed and analyzed as in Gruhn et al. (2009b). In brief, we recorded walking sequences with a high speed video camera (Marlin F-033C, Allied Visions Technologies, Germany) that was externally triggered at 100 fps. Insect head, thorax, and legs were marked with fluorescent pigments (Dr. Kremer Farbmühle, Aichstetten, Germany) mixed with dental cement. During the recording of walking sequences, the animal was illuminated with blue LED arrays (12 V AC/DC, Conrad Electronics, Germany). The video files were analyzed using motion tracking software (WINanalyze 1.9, Mikromak Service, Berlin, Germany). AEP describes the anterior extreme position of the leg at touch down, while PEP is the posterior extreme position at lift-off. In forward stepping AEP in stance is anterior to PEP, whereas in backward stepping AEP in stance is posterior to PEP. AEP and PEP values are always given in millimeters in the form xx.x; yy.y (s.d. x ; s.d. y). X-values are given with respect to the length of the animal, a virtual zero line being drawn across the animal at the level of the coxa. Positive and negative x-values indicate points anterior and posterior to the coxa, respectively. Y-values are given with respect to the axis perpendicular to the length of the animal. Larger y-values denote more distal points, smaller values more central points. Fig. 2.1B shows a schematic drawing of the stick insect with the points tracked. As an example for the step length vector determination and its direction, the right middle leg is drawn at two fictive positions, one anterior (ML-AEP) and one posterior (ML-PEP). The vectors for all steps connecting the two positions, normalized to the origin in the AEP, gave direction in ° and step length in mm. The 0°-180° axis was always parallel to the body axis and crossed the AEP, 90° always points inside perpendicularly. The simultaneous recordings of the EMG trace and the camera trigger and tarsal contact signals allowed frame by

frame correlation of filmed movement and EMG and tarsal contact traces. In calculating middle leg movement vectors all steps were transposed to reflect walking as a right leg regardless of which leg was being recorded from.

Data analysis and figure preparation Leg positions were measured with their x and y coordinates. Care was taken to choose animals of the same size and leg lengths. The number of animals used for a given condition (N) and the number of steps evaluated (n) are given in the figures. The sample size for the kinematics analysis of straight forward walks was N=5 (n=125), for backward walks N=3 (n=83).

Cycle period was calculated from touch down to touch down as determined from the tarsal contact trace. For comparisons of EMG activity of the six different muscles between intact forward, backward, and curve walking and between intact and reduced forward stepping preparations, EMG traces were rectified and smoothed (τ = 50 ms) and each single data point of each step was exported in Excel (Microsoft Corp., Seattle, USA) to allow averaging. In each step the minimum muscle activity was set to zero and the maximum to one. In several cases, weak crosstalk from the antagonist muscle was removed mathematically using the EMG trace from the antagonist: the activity of the EMG in the antagonist was triggered to the same point in time than the EMG in the agonist (i.e. lift-off or touch down of the tarsal contact trace, common for both EMGs), and exported in the same way as above. Then its minimum activity was set to 0, but its maximum to an value of 0.5, due to the smaller size of the antagonist signal in the agonist EMG. The normalized activity of the antagonistic muscle was then subtracted from the corresponding value of the muscle under investigation.

First spike latencies with respect to lift-off or touch down were calculated relative to the tarsal contact signal (see above). The absolute latency was then normalized with respect to the corresponding step cycle and averaged for the plot in Fig. 4.1C. Average swing/stance phase duration was calculated from each evaluated step from lift-off to touch down for swing and from touch down to lift-off for stance.

All angles were analyzed using the Watson-Williams test, the circular analogue of the two sample t-test (Matlab, circular statistics toolbox; Berens (2009)). Circular variance of vector angles was tested using the variance test in the same toolbox (Matlab, circular statistics toolbox; Berens, 2009). For all other statistical analyses, a non-parametric Wilcoxon-(U-) test (Matlab, Statistics toolbox; Mathworks, Inc., Natic MA, USA) was used, except for the comparison of integrals of depressor activity, where a standard student's t-test was used. Statistical significance was assumed at p-values <0.01. Figures were prepared in Origin 6.1 (Origin Lab Corp.,

Northampton, MA, USA) and Photoshop 6.0 (Adobe Systems Inc., San Jose, CA, USA).

2.2 Single leg preparation

To investigate the activity of leg motoneurons and premotor nonspiking interneurons during forward and backward walking in the mesothoracic ganglion, a single-leg preparation was used to allow stable intracellular recordings with sharp microelectrodes. For these experiments, related stick insects of the species *Cuniculina impigra* were taken, also provided by the breeding colony from the University of Cologne.

Preparation and experimental setup The single-leg preparation was firstly introduced by Bässler (1993) and improved and used in various subsequent studies (Fischer et al., 2001; Schmidt et al., 2001; Gabriel and Büschges, 2007; von Uckermann and Büschges, 2009). All legs of the animal except the left middle leg were cut at mid-coxa level and the animal was glued ventral side down on a venerit platform with dental cement (Pro TempII, ESPE, Seefeld, Germany). The animal was opened with a cut along the dorsal midline. Gut, minor trachea and fat tissue were removed in order to expose the mesothoracic ganglion. Throughout the experiment the thorax body cavity was filled with saline (pH=7.2, according to Weidler and Diecke, 1969). Protractor and retractor coxae muscles were cut at their ventral thorax insertion and the thorax-coxa joint was fixed with dental cement to allow only movements in the vertical plane. Stepping was allowed on a custom made, passive treadwheel composed of two styrofoam drums with 40 mm diameter and a center distance of 50 mm, connected via a belt of crepe paper. The two drums are each mounted on a micro DC-motor (DC 1516, Faulhaber, Schönaich, Germany) of which one measured the belt velocity and the other supported the belt movement to give a low friction (for details cf. Gabriel et al., 2003). The treadwheel height was adjusted below the middle leg of the stick insect, so that the femur of the leg was parallel to the belt when the femur-tibia joint angle was about 90°. Forward walking was elicited by gently touching the abdomen of the animal with a brush, backward walking by pulling on the antennae or stimulating the head/prothorax region with a soft brush.

Electrophysiology To monitor the walking direction, the protractor (nl2) and retractor (nl5) motor nerves were recorded extracellularly by placing the nerves on steel hooks of monopolar electrodes (modified after Schmitz et al., 1991c). The

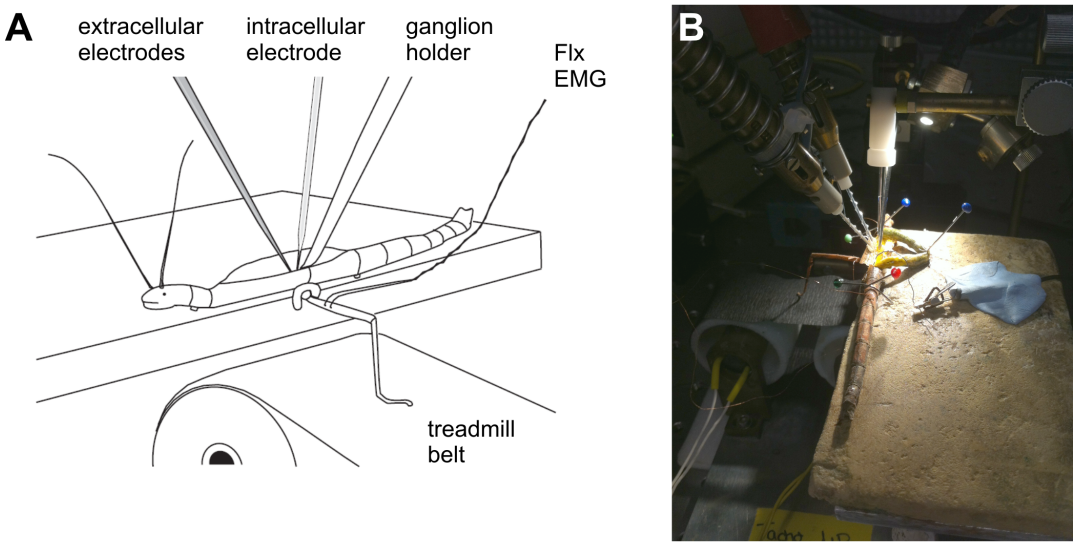

Figure 2.2 – Experimental setup of the single leg preparation. A: schematic view of the preparation. The animal is glued to a platform, only the left middle leg is intact. Stepping is possible in a vertical plane on the treadmill positioned below the leg. The ganglion holder helds the ganglion in place, so stable intracellular recordings are possible. Nerves nl2 and nl5 are recorded extracellularly. An EMG is placed in the proximal femur to record flexor muscle activity. B: photography of the experimental setup described in A. Figure A modified after von Uckermann (2008).

nerves were then crushed distally to the recording sites to abolish afferent and efferent signaling. Additionally, flexor tibiae muscle activity was recorded by inserting two twisted copper wires (49µm diameter) into holes in the cuticle of the ventral portion of the proximal femur, fixed with dental cement (electromyogram, EMG). Extracellular nerve and EMG signals were amplified 1000fold and low-pass filtered (preamplifier MA101 and amplifier MA102, electronics workshop, Institute for Zoology, University of Cologne). Then, fat tissue surrounding the ganglion was removed and the ganglion was lifted on a steel ganglion holder, coated with wax, and positioned with a micromanipulator. To stabilize the ganglion, which was necessary to achieve long lasting intracellular recordings from the mesothoracic ganglion in the walking animal, the ganglion was fixated on the holder by placing cactus spines (*Nopalea dejecta*) through the left surrounding tissue. Before recording intracellularly from the dorsal hemiganglion ipsilateral to the attached leg, the ganglion surface was treated with a proteolytic enzyme (Pronase E, Merck, Germany) to ensure an easy electrode penetration. Sharp microelectrodes with a resistance of 15-25 MΩ were pulled using a Sutter Micropuller (P-1000, Sutter Instruments, Novato, CA, USA) and filled with 3M KAc/0.1M KCl. Signals were recorded in bridge mode (intracellular amplifier SEC-10L, npi electronics, Tamm, Germany). The setup is depicted in Fig. 2.2.

Intracellular stainings For experiments in which neurons were stained intracellularly, 5% Neurobiotin tracer (Vector Laboratories Inc, Burlingame, CA, USA) were added to the electrode solution. After injecting the tracer into the neurons with depolarizing current pulses (+1.5-2.5 nA, 400ms pulse duration, 1Hz) for 3-20 minutes, 30-45 minutes were allowed for tracer diffusion. Then the ganglion was removed from the animal and treated for 20 min with 4% paraformaldehyde (PFA) in 0.1 M phosphate-buffered saline (PBS) and 5% Triton X-100 (Fluka, Buchs, Switzerland) and then fixed for 2-14h in 4% PFA. After washing 3 times with PBS, ganglia were treated with the dye-coupled Neurobiotin antibody Streptavidin-Cy3 (1:500 in PBS, Sigma-Aldrich, St. Louis, MO, USA) with 0.5% Triton X and 2-4% Normal Goat Serum (Vector Laboratories Inc, Burlingame, CA, USA) overnight on a shaker at 4ºC. After washing (3x15min in PBS) and an ascending Ethanol series (50%,70%,90%,2x100%; each 10min), the ganglia were mounted in methylsalicylate on an object slide and scanned with a confocal Laser Scanning Microscope (LSM 510; Carl Zeiss, Jena, Germany).

Identification of motoneurons and nonspiking interneurons Motoneurons (MNs) and nonspiking-interneurons (NSIs) were recorded from their neuropilar arborizations in the ganglion. Motoneurons were identified either by a 1:1 correlation of spikes in the intracellular recording and spikes in the extracellular recordings (for protractor, retractor, and flexor) or by an unambiguous movement response of the leg due to depolarizing current injection (extensor, depressor, and levator MNs). The output connections of NSIs were also identified by injecting current into the neuron and observing the response in the extracellular recordings or of a leg movement. Furthermore, the femoral chordotonal organ (fCO) of the middle leg was stimulated passively while the leg was standing on the treadwheel. A movement of the belt towards the animal led to a passive flexion of the leg and therefore an elongation of the fCO, a movement away from the animal to a passive extension/relaxation of the fCO. The responses in the membrane potential of the recorded NSIs were compared with those of previously described NSIs influencing the femur-tibia joint (Büschges, 1990; Sauer et al., 1996). Responses to an fCO-stimulation were also recorded for the other joint NSIs but since it is not known if the responses are similarly stereotyped, this was no criterion to group undescribed NSIs. In this study, newly described NSIs were grouped according to their membrane potential modulation during walking. The physiology during single-leg stepping and the morphology of recorded neurons were also compared to previously described NSIs (Schmitz et al., 1991a; Brunn, 1998; Hess and Büschges, 1997; Büschges, 1990; Sauer et al., 1996; von Uckermann and Büschges, 2009).

Neurons were considered nonspiking fulfilling the following criteria: 1) no spikes

could be evoked due to stimulation of the abdomen or antennae to elicit forward or backward walking. 2) Injection of depolarizing current caused no action potentials nor could rebound spikes after a long injection of hyperpolarizing current be observed. 3) Stimulation of sense organs did not cause spiking of the neuron. For regulations identifying NSIs further see also Burrows and Siegler (1976); Hengstenberg (1977); Burrows and Siegler (1978); Wilson (1981); Wilson and Phillips (1983); Büschges (1990). Every analyzed NSI in this work showed a clear, reproducible output on at least one pool of motoneurons, determined either by eliciting spikes in the extracellular recordings (protractor, retractor and flexor) or by an unambiguous movement response of the leg due to current injection (extensor, depressor and levator MNs). In this work, 60 recordings of MNs and 77 recordings of NSIs, of which 34 were stained, have been analyzed.

Data analysis Data was analyzed with Spike2 software using custom written scripts, Microsoft Excel 2007, and Origin 5.0. Figures were prepared with Corel DrawX4. For the statistical analysis of membrane potential and mean belt velocity regression, an ANOVA analysis, $p<0.05$, in Origin 5.0 was performed.

The mean belt velocity was determined by dividing the integral of the treadwheel trace below the ascending slope (stance phase) by the stance phase duration. By multiplying with a factor of 12.6 (treadwheel potential output x amplification x time / distance), the mean belt velocity was calculated.

Usually, the end of the stance phase was marked with events at the end of the ascending slope of the treadwheel trace. However, in some cases it was observed that at the end of stance the tarsus of the animal was clawed to the crepe paper of the treadwheel, and was pulling it towards the body. Only a few dozen milliseconds later it disengaged from the belt to start a new swing phase. In most of the cases this could be clearly traced either by an artifact in the treadwheel trace at the time point in which the tarsus disengaged and/or by the switch from retractor to protractor nerve activity during forward walking, resp. from protractor to retractor activity during backward walking, which happened just at the actual onset of swing. Steps in which the walking direction, i.e. the switching from retractor to protractor nerve activity or vice versa, could not be determined definitely were not taken into consideration.

N = number of animals, n = number of steps.

3 Results

3.1 Activity patterns and timing of muscle activity in forward, backward, and curve walking animals on a slippery surface[1]

Understanding how animals adapt their motor behavior to changing environmental conditions requires measuring limb kinematics and muscle activity in different behaviors. It has been shown previously that stick insect leg kinematics differ in straight and curve walking and the effect of reducing leg number on these changes was examined (Gruhn et al., 2009b). Here, middle leg kinematics during forward and backward in intact animals are compared, and the muscle activity in these behaviors and during curve walking in the intact and reduced preparation was examined.

3.1.1 Kinematics of straight forward vs. backward walking in the middle leg

Fig. 3.1A shows a schematic drawing of the stick insect with marked anterior and posterior extreme positions (AEP and PEP plus standard deviation, SD) of the right middle leg in forward and backward straight walking. The data for forward walking (gray) were taken from Gruhn et al. (2009b). AEP is defined as tarsus position at touch down and PEP as tarsus position at lift-off, always with respect to the direction in which the animal moves. During forward walking (FW), the leg

[1]The results for forward and backward walking animals in this section are already published: Rosenbaum P, Wosnitza A, Büschges A and Gruhn M. *Activity Patterns and Timing of Muscle Activity in the Forward Walking and Backward Walking Stick Insect* Carausius morosus. Journal of Neurophysiology 104: 1681-1695, 2010. The authors contributions for the paper are as followed: AB, MG, PR, and AW designed research; PR and AW performed experiments, analyzed data and prepared figures; AB, MG, PR, AW wrote the manuscript. Therefore this section is, except for minor modifications, literally taken from the paper. Results from curve walking experiments are added in the appropriate sections.

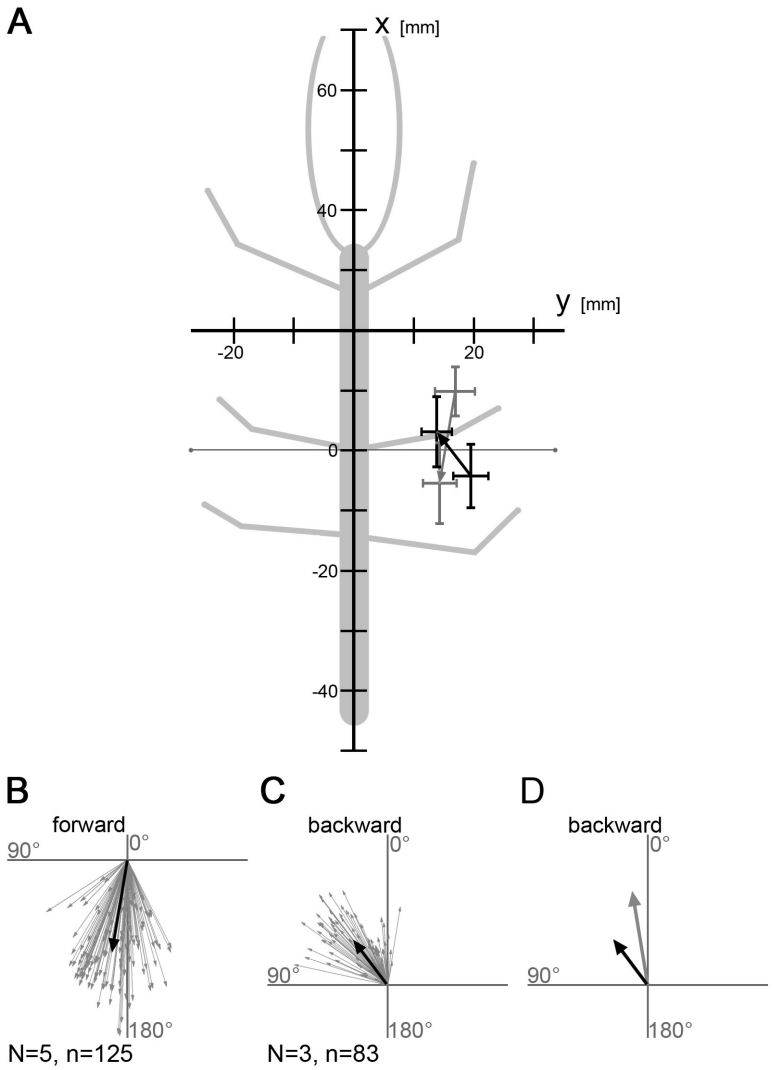

Figure 3.1 – Kinematics of a forward and backward walking stick insect middle leg on the slippery surface. A: schematic drawing of a stick insect with the mean anterior extreme position (AEP) and posterior extreme position (PEP) values (and SD error bars) of the right middle leg for forward (gray) and backward (black) walking. Note that for the backward walking animal the AEP is posterior to the PEP; the gray line marks the X_0-value for the middle leg. B and C: step-to-step variability in angle and length of stance movement of forward (B) and backward (C) steps normalized to touch down position (AEP); the average stepping vector is drawn in black in both cases. D: average stepping vectors for forward (gray) and backward (black) walking from B and C; the average vector for forward walking from figure B was mirrored across the horizontal plane for easier comparison. N = animal number, n = step number.

is moved anteriorly during swing and posteriorly during stance. This order of leg movements is reversed during backward walking (BW). In backward walking each step's AEP is therefore more caudal along the long axis of the animal than the PEP. Forward steps were significantly longer (mean step length FW: 16.2 ± 5.4 mm; BW: 9.9 ± 4.7 mm, $p<0.0001$) and their movement direction was on average more parallel to the body length axis than were backward steps (Fig. 3.1A). To compare movement vector angles, we mirror imaged the forward step movement angles in Fig. 3.1B along the horizontal axis. The resulting mean angles of forward (8.8 ± 17.3°, gray) and backward (36.1 ± 20.3°, black) steps are shown in Fig. 3.1D and differed significantly ($p<0.0001$) from each other. The variability between the movement vector angles of single steps is similar in both directions and spans angles over a range of 83° during forward walking and 88.5° during backward walking between the respective extremes. Mean touch down position along the transverse axis was significantly closer to the midline in forward versus backward walking (y-positions: AEP_{FW} 16.9 ± 3.3 mm; AEP_{BW} 19.6 ± 2.9 mm, $p<0.0001$), but mean lift-off position was not significantly different (y-positions: PEP_{FW} 14.4 ± 2.9 mm; PEP_{BW} 13.8 ± 2.6 mm, $p=0.32$). However, because during backward walking the movement is more inward directed in each step, the PEP is generally reached after a shorter step length (Fig. 3.1B-D). Taken together, these data show that in intact animals middle leg backward stepping is not simply reversed forward walking, but is instead altered to having shorter and more inward directed steps, albeit with a similar degree of variability as seen for forward stepping.

3.1.2 Stance duration alone determines cycle period

In stick insects walking on nonslippery surfaces, in which the different legs are coupled mechanically through the ground on which the animal walks, step cycle period depends on stance duration (Wendler, 1964; Graham, 1972; Graham and Epstein, 1985). It was tested if this relationship is also present in slippery surface forward, backward and curve walking, and, to test for inter-leg interactions, in animals with reduced leg numbers (only the two middle legs or only a single middle leg). In all these cases cycle period varied linearly with stance duration but did not depend on swing duration, which was essentially constant at all cycle periods (Fig. 3.2).

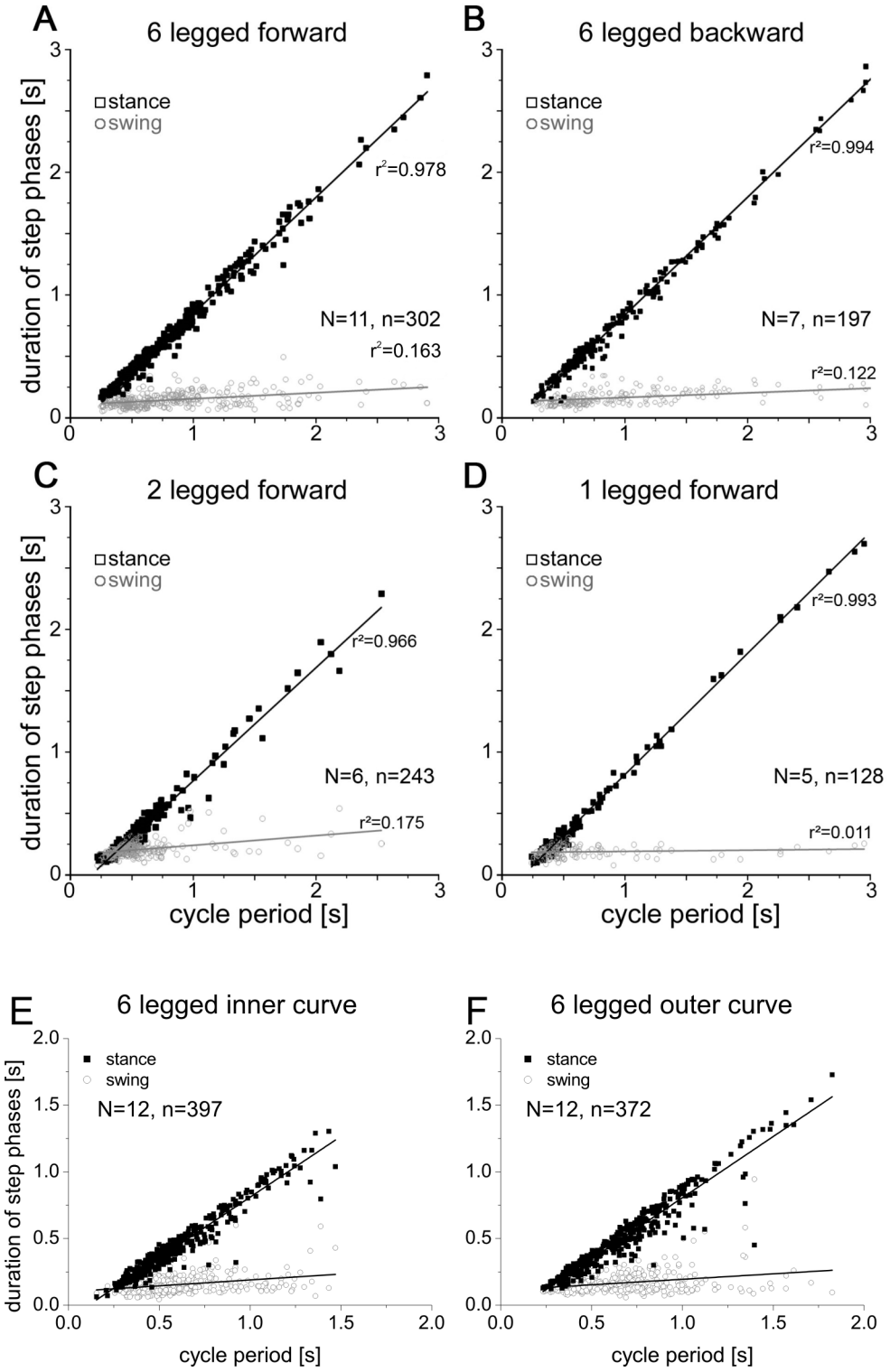

Figure 3.2 – Cycle period depends on stance, not swing duration. Gray circles represent swing phase, filled black boxes stance. A: straight forward walking, 6-legged animal. B: backward walking, 6-legged animal. C: straight forward walking, 2-legged animal (only middle legs). D: straight forward walking, 1-legged (middle) animal. E: curve inside-leg, 6-legged animal. F: curve outside-leg, 6-legged animal. N = animal number, n = step number.

3.1.3 Phasing of leg muscle activity during forward, backward, and curve walking

EMG recordings of various leg muscles during walking have been made (Graham and Epstein, 1985; Fischer et al., 2001), but with few exceptions, only the activities of single muscle pairs were recorded (Bässler, 1993; Epstein and Graham, 1983; Cruse and Pflüger, 1981). In addition, the timing reference for the beginning or end of muscle activity relative to step cycle, if present at all, was not precise. To remedy this lack we made comprehensive paired EMG recordings of all three major muscle pairs controlling leg movements, the protractor/retractor coxae, levator/depressor trochanteris, and the extensor/flexor tibiae muscles at a time during both forward and backward walking, as well as during curve walking.

Fig. 3.3 shows the activity of the muscles of the most proximal leg joint, the thorax-coxa joint, the protractor and retractor coxae muscles, which serve to protract and retract the leg, respectively. The traces in Fig. 3.3A show raw EMG activity, those in Fig. 3.3B rectified and smoothed (τ = 50 ms) activity, and those in Fig. 3.3C mean rectified activity from one stepping sequence (gray trace) and from five animals (black trace). In forward walking protractor activity began before the lift-off of the leg, reached its main activity during swing and then decreased towards the end of swing. In backward walking the protractor was barely active during swing but began at the transition between swing and stance and reached peak activity about 100 ms into stance. This activity pattern was the same for the retractor muscle except that it showed stance activity during forward walking and swing activity during backward walking.

Fig. 3.4 shows the activity of the muscles of the next most distal leg joint, the coxa-trochanter joint, the depressor trochanteris and levator trochanteris muscles, which serve to depress and lift the leg, respectively. The traces in Fig. 3.4A again show raw EMG activity, those in Fig. 3.4B rectified and smoothed (τ = 50 ms) activity, and those in Fig. 3.4C mean rectified muscle activity from one stepping sequence (gray trace) and from five animals (black trace). Depressor activity began very shortly after swing beginning, was active throughout swing, and declined shortly after stance beginning. Provided the animal was maintained at a constant height about the substrate (see below), depressor activity was the same in forward and backward walking. Moderate levator muscle activity was present at the beginning and middle of stance with a substantial peak of activity occurring just before the stance to swing transition. Levator activity decreased and reached a minimum shortly after swing beginning. As with the depressor, levator activity was the same in forward and backward walking.

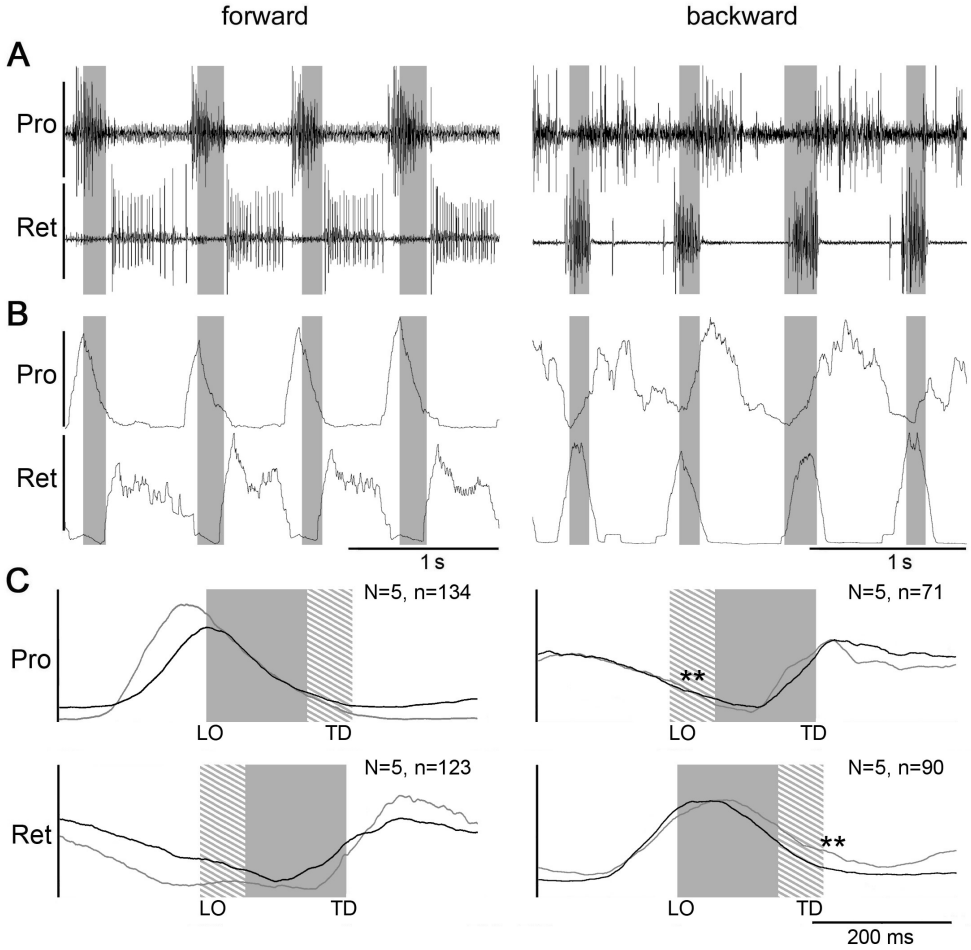

Figure 3.3 – Right middle leg protractor and retractor EMG recordings during forward (left column) and backward (right column) walking on a slippery surface. A: raw EMG recordings. B: rectified and smoothed traces of EMGs in A. C: mean rectified and smoothed traces of recordings (gray) from one and from five animals (black). Gray boxes mark the average swing duration, shaded area shows swing duration SD. Double asterisks mark where crosstalk from the retractor was removed mathematically from the protractor traces. LO= leg lift-off, TD= leg touch down. N=animal number, n=step number.

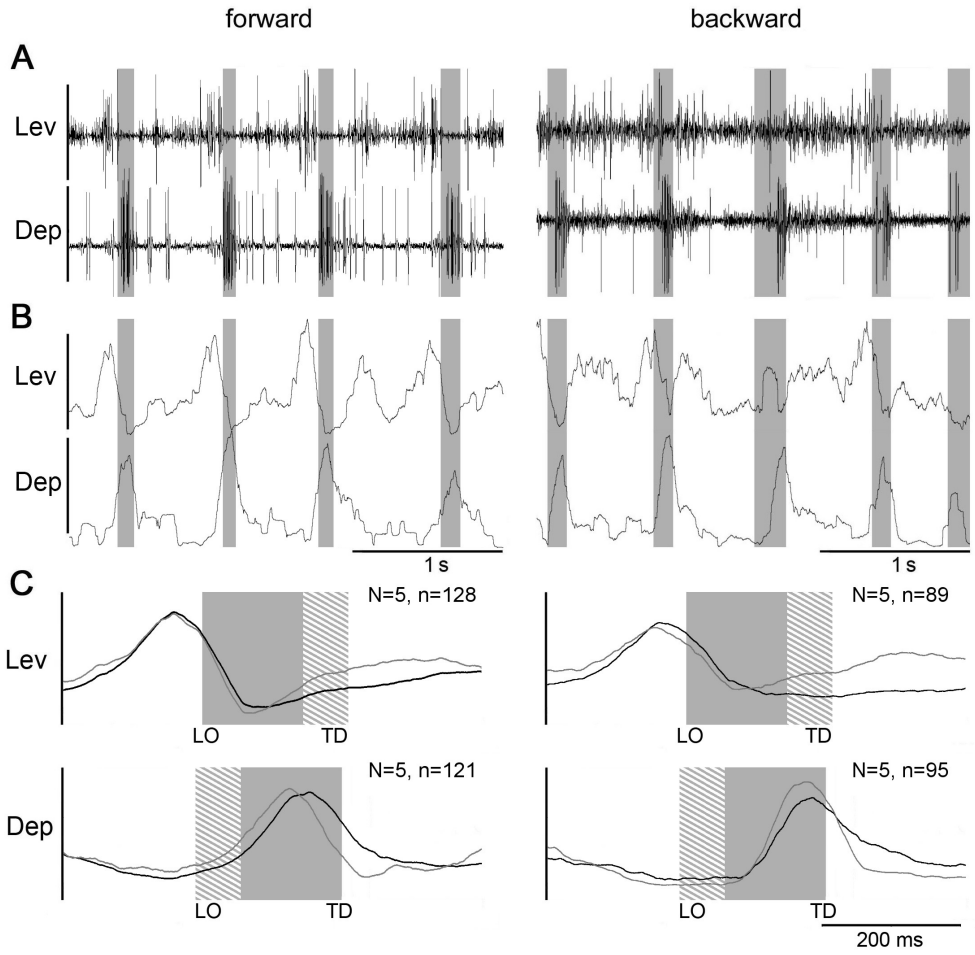

Figure 3.4 – Right middle leg levator and depressor activity during forward (left column) and backward (right column) walking on a slippery surface. A: raw EMG recordings. B: rectified and smoothed traces of EMGs in A. C: mean rectified and smoothed traces of recordings from one (gray) and from five animals (black). Gray boxes mark the average swing duration, shaded area shows swing duration SD. LO= leg lift-off, TD= leg touch down. N=animal number, n=step number.

The last muscles analyzed (Fig. 3.5) were the extensor tibiae and flexor tibiae muscles which move the femur-tibia joint and extend and flex the tibia, respectively. The traces in Fig. 3.5 A again show raw EMG activity, those in Fig. 3.5B rectified and smoothed ($\tau = 50$ ms) activity, and those in Fig. 3.5C mean rectified muscle activity from one stepping sequence (gray trace) and from five animals (black trace). Peak extensor activity occurred around lift-off in forward and in backward walking, while flexor activity peaked during the first half of stance in forward and backward walking.

Next, I looked at the leg muscle activity during curve walking, that is at the differences of muscle activity of an leg walking an outside curve or an inside curve. Fig. 3.6 shows the activity of protractor and retractor muscles, which were the only ones whose activity changed between forward and backward walking, together with a flexor EMG. Again, original EMG recordings, rectified and smoothed EMG traces, and the averaged rectified traces for all three muscles are shown. The activity of all three muscles during a curve outside leg (Fig. 3.6, left column) is very similar to the activity during forward walking. The protractor becomes active at the end of stance phase and reaches its peak activity during swing phase. The retractor is mostly active during stance but becomes active shortly before touch down of the leg. The flexor is activated at the onset of stance and quickly reaches its peak activity. In the flexor muscle, this activity is not altered when active during an inner curve, but the protractor and retractor activity changes (Fig. 3.6, right column). The protractor is only slightly active at the stance-swing phase transition and the retractor peak activity is shifted to the swing phase. This can be explained by the kinematics of the leg movement during curve walking. Gruhn et al. (2009b) already showed that the outside middle leg during a curve has similar kinematics to the forward walking middle leg, thus the EMG activity is largely unchanged. However, a middle leg stepping an inner curve has a shorter step length. Steps are also more laterally directed, compared to the movement from anterior to posterior during swing phase in forward walking (Gruhn et al. (2009b)). Furthermore, inner curve steps can be directed anteriorly, which means protractor activity occurs in the swing phase, in laterally directed steps there is a reduced protractor activity, and backward directed steps, when the animal is walking a very steep curve, showed protractor EMG activity during stance and retractor activity during swing (like in Fig. 3.3). All these differently directed steps were averaged in Fig. 3.6, but looked at independently in Fig. 3.7. There, it becomes apparent that the muscle activity depends on the direction the inside curve leg is stepping, and fits the previously described protractor and retractor muscle activity during forward and backward walking on the slippery surface.

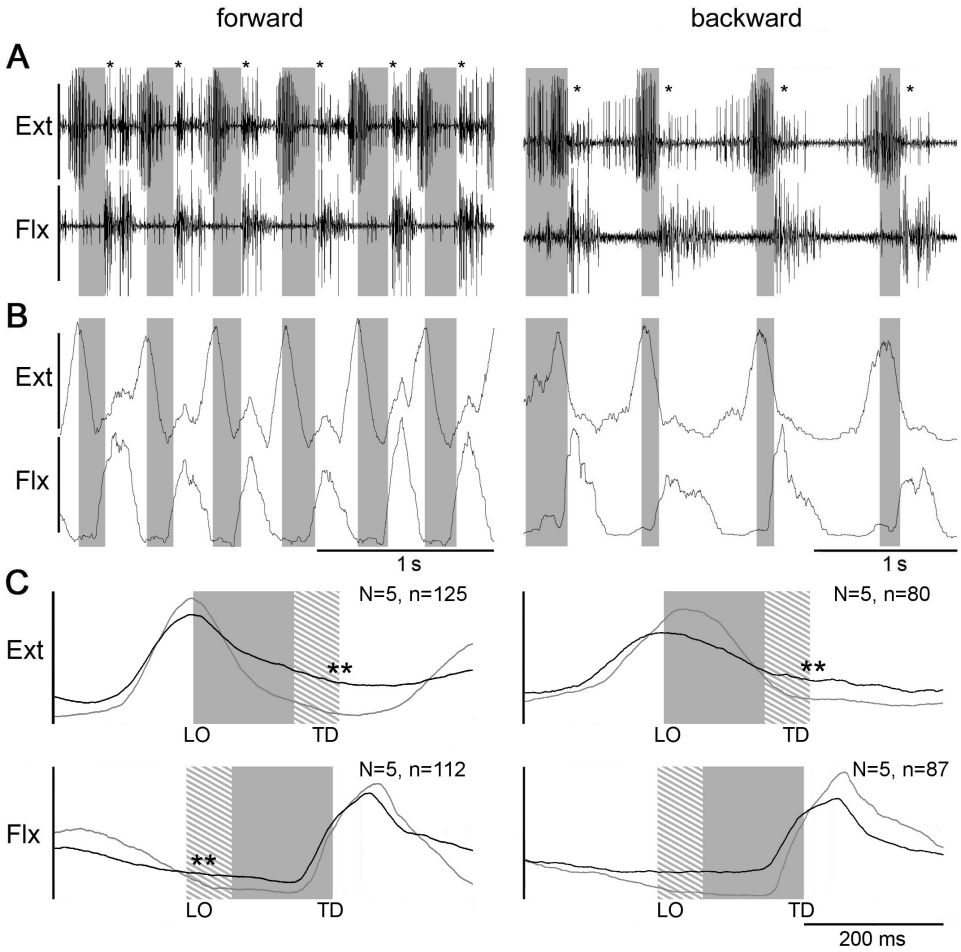

Figure 3.5 – Right middle leg extensor and flexor activity during forward (left column) and backward (right column) walking on a slippery surface. A: raw EMG recordings, asterisks mark crosstalk from the flexor in the extensor trace. B: rectified and smoothed traces of EMGs in A. C: mean rectified and smoothed traces of recordings from one (gray) and from five animals (black). Gray boxes mark the average swing duration, shaded area shows swing duration SD. Double asterisks mark where crosstalk from the flexor muscle was removed mathematically from the extensor trace. LO= leg lift-off, TD= leg touch down. N=animal number, n=step number.

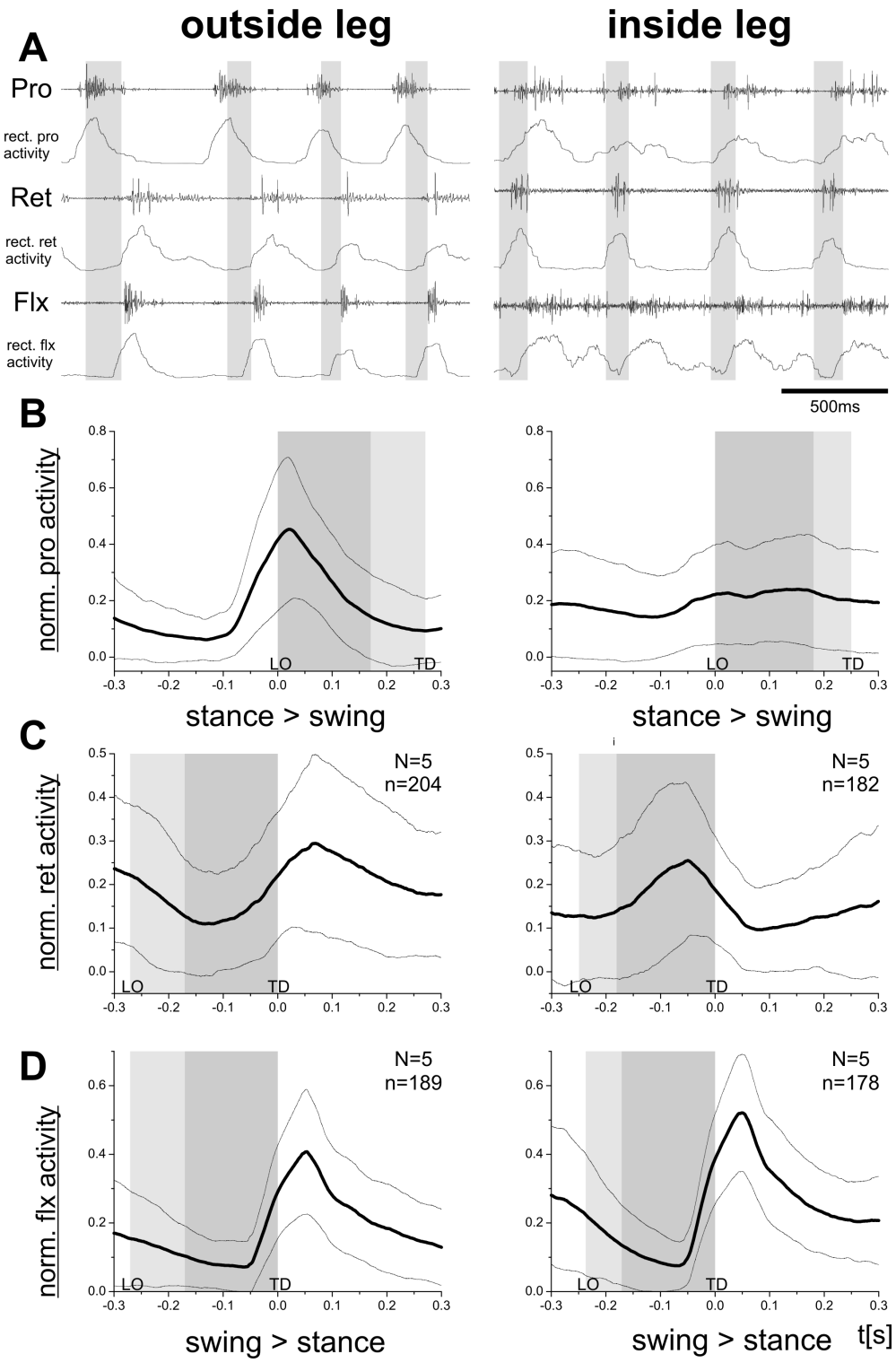

Figure 3.6 – Right middle leg protractor, retractor and flexor EMG recordings of a curve walking outside (left column) and inside leg (right column). A: raw EMG recordings of the three muscles and the corresponding rectified and smoothed EMG traces. B: mean rectified and smoothed traces of protractor activity of 5 animals (black trace) and its standard deviation (lighter gray traces), which indicates the range in which the muscle activity could occur. C: mean rectified and smoothed traces of retractor activity of 5 animals. D: mean rectified and smoothed traces of flexor activity of 5 animals. Gray boxes mark the average swing duration, lighter gray areas show swing duration SD. LO= leg lift-off, TD= leg touch down. N=animal number, n=step number.

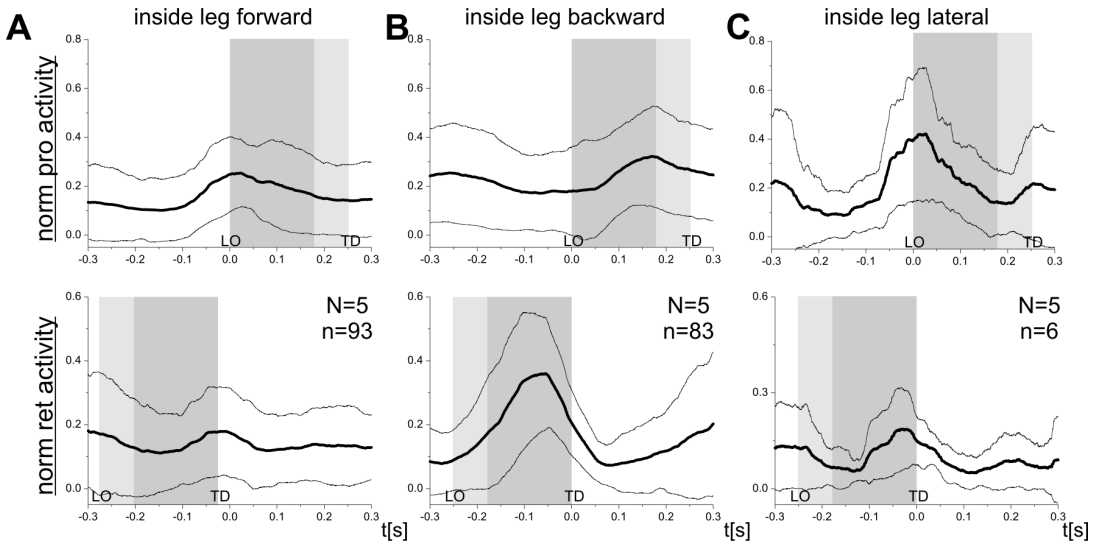

Figure 3.7 – Right middle leg protractor and retractor EMG recordings averaged and rectified during inner curve stepping with different directions. A: mean rectified and smoothed protractor and retractor activity for forward directed steps of an leg walking an inside curve. B: mean rectified and smoothed protractor and retractor activity for backward directed steps of an leg walking an inside curve. C: mean rectified and smoothed protractor and retractor activity for laterally directed steps of an leg walking an inside curve. Thick black traces mark the averaged activity, thinner gray traces the SD. Gray boxes mark the average swing duration, lighter gray areas show swing duration SD. LO= leg lift-off, TD= leg touch down. N=animal number, n=step number.

Finally, the muscle activity of depressor, levator and extensor muscles were compared during curve walking (Fig. 3.8). In analogy to the comparison between forward and backward walking, also the muscle activity of the levator and extensor does not change when walking an outside or an inside curve (Fig. 3.8B and C). In both cases the muscles are activated before the leg lift-off, and are mainly active during swing phase. The depressor muscle shows during both an outside and inside curve an activation at the start of swing and a maximum activity during the second half of swing. However, in the outside curve depressor activity is prolonged during stance phase (Fig. 3.8A).

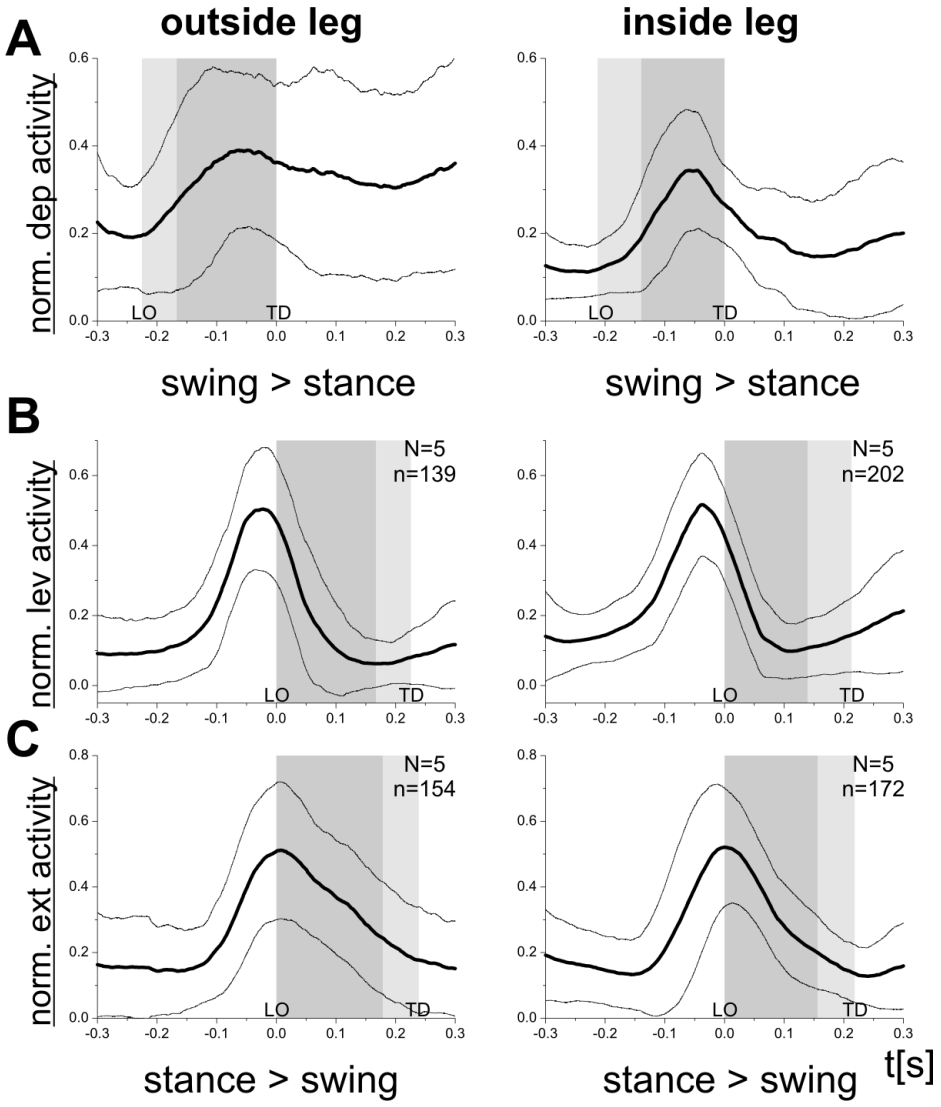

Figure 3.8 – Right middle leg depressor, levator and extensor EMG recordings during curve walking outside (left column) and inside legs (right column). A: mean rectified and smoothed traces of the depressor activity of 5 animals (black trace) and its standard deviation (lighter gray traces), which indicates the range in which the muscle activity could occur. C: mean rectified and smoothed traces of the levator activity of 5 animals. D: mean rectified and smoothed traces of the extensor activity of 5 animals. Gray boxes mark the average swing duration, lighter gray areas show swing duration SD. LO= leg lift off, TD= leg touch down. N=animal number, n=step number.

3.1.4 Latency of muscle timing during forward, backward, and curve walking

Reliably comparing muscle activity in different walking directions and across preparations requires determining the exact timing of muscle activity within the step cycle. Swing to stance and stance to swing transitions are two such points. Fig. 3.9 and Fig. 3.10 show first spike latencies relative to these points for all six muscles in forward and backward walking, respectively, from 5 animals each.

The gray areas mark mean swing duration averaged across all steps and animals.

The protractor, levator and extensor muscles move the middle leg forward, up, and extend the femur-tibia joint. During forward walking these movements occur during swing. We therefore measured the first spikes in these muscles relative to lift-off (Fig. 3.9A, C, E). Activity occurred earliest in the levator (mean first muscle potential 99.9 ± 64.2 ms before lift-off), followed by the extensor (66.9 ± 47.3 ms) and then the protractor (36.5 ± 36.3 ms). The retractor, depressor and flexor muscles move the leg backwards, down, and flex the femur-tibia joint. During forward walking these movements occur during stance. We therefore measured the first spikes in these muscles relative to touch down (Fig. 3.9B, D, F). Activity occurred earliest in the depressor with the mean first muscle potential 93.1 ± 33.9 ms before touch down, 21% into the swing phase. The first flexor activity occurred next with mean first muscle potential 9.0 ± 13.3 ms after touch down. Single first spikes occurred just before touch down, confirming previous findings for the timing of this muscle (Gruhn et al., 2006). First retractor activity was more variable, with mean first muscle potential 34.6 ± 33.6 ms after touch down and first activity occurring up to 50 ms before touch down. The joint activation sequence in swing is thus the same as that for stance, i.e., first coxa-trochanter, then femur-tibia, and finally thorax-coxa. The high standard deviations result from the high variability in the stepping of the stick insect on the slippery surface. Walking sequences with many consecutive straight forward steps do not occur often and every step has a slightly different direction and stance duration.

As was shown above in the kinematics and EMG data, in backward walking protractor and retractor timing is the reverse of that in forward walking. To continue to compare the timing of functional swing and stance muscles in the two walking directions, in backward walking sequences we therefore referenced retractor activity to lift-off and protractor activity to touch down but continued to reference the activity of the other muscles as before (Fig. 3.10A-F). Sequence of levator and extensor activation as well as the latencies for the first muscle potential (100.2 ± 60.5 ms, Fig. 3.10C; 56.8 ± 48.0 ms, Fig. 3.10E, respectively) were the same as in

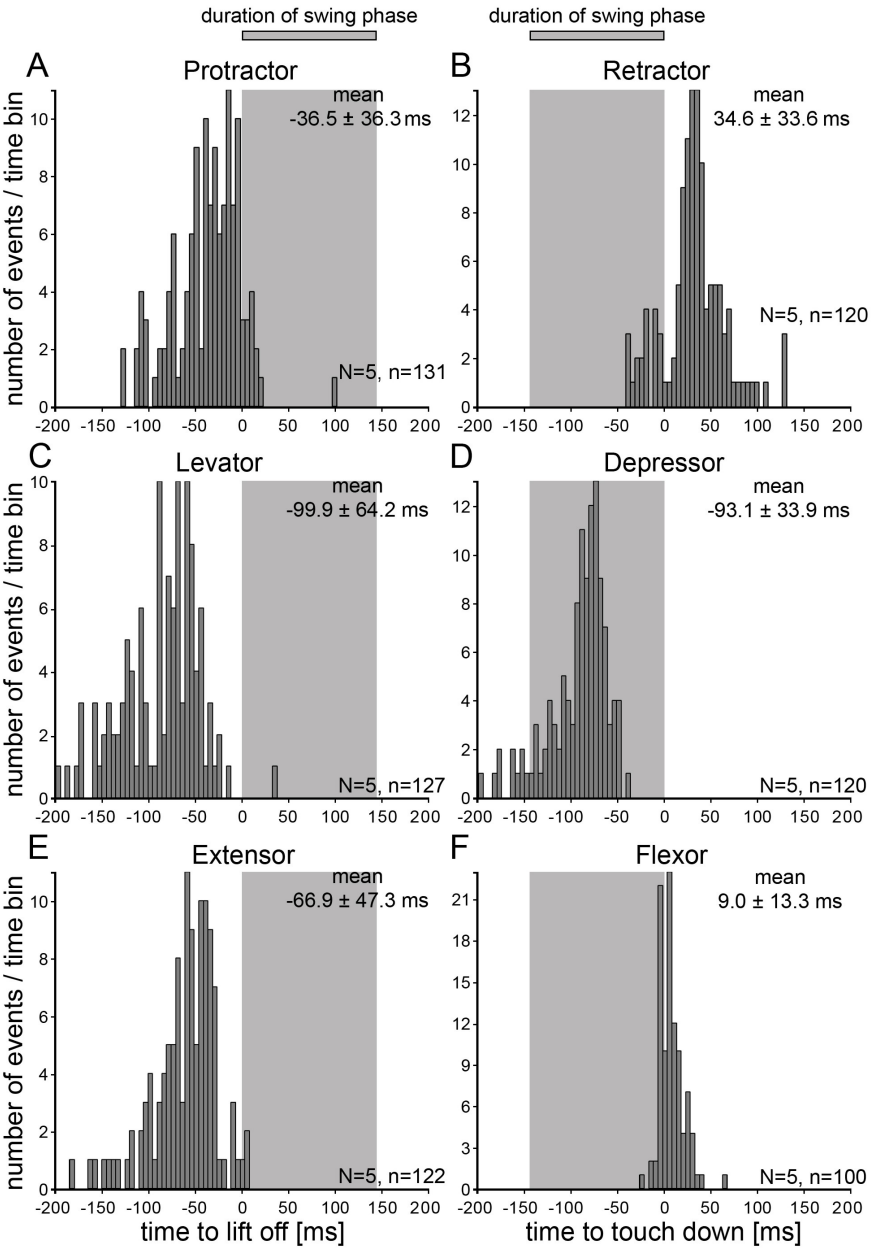

Figure 3.9 – Histograms of the latency distribution of the first muscle potentials in the EMG traces of the six analyzed leg muscles during forward walking. The timing of the first spikes in protractor, levator and extensor were measured with respect to the time of lift-off. Retractor, depressor and flexor activity spikes were measured with respect to leg touch down. Gray boxes mark the average swing phase length. Average latency of the first spike is given with SD. N=animal number, n=step number.

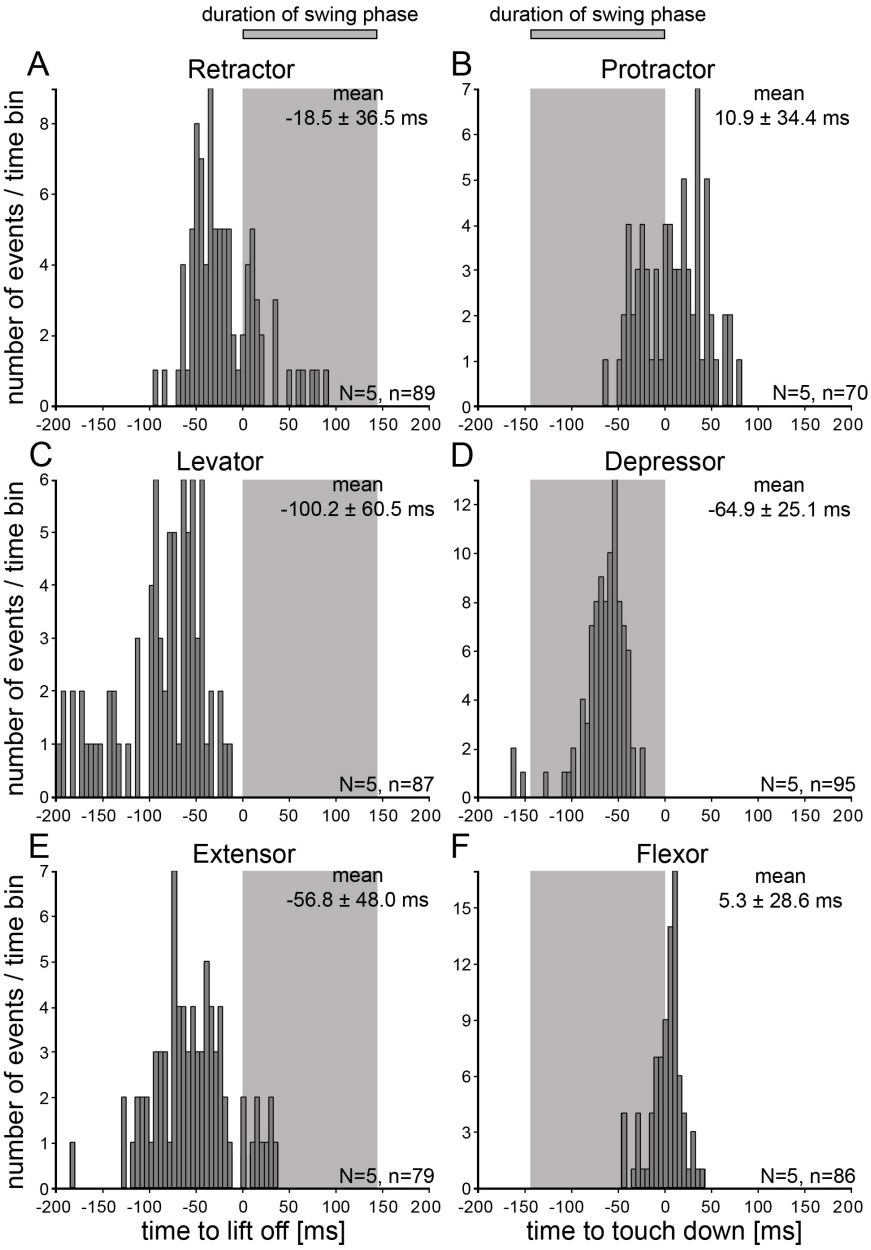

Figure 3.10 – Histograms of the latency distribution of the first muscle potentials in the EMG traces of the six analyzed leg muscles during backward walking. The timing of the first spikes in retractor, levator and extensor were measured with respect to the time of lift-off. Protractor, depressor and flexor activity spikes were measured with respect to leg touch down. Gray boxes mark the average swing phase length. Average latency of the first spike is given with SD. N=animal number, n=step number.

forward walking (p Lev =0.98; p Ext =0.31). During backward walking the retractor activated 18.5 ± 36.5 ms before lift-off (Fig. 3.10A), dramatically different from this muscle's activation in forward walking (Fig. 3.9B), but barely not significantly different from the timing of the functionally analogous protractor during forward walking (p=0.012, Fig. 3.9A).

Except for the difference mentioned above that the protractor is a stance phase muscle in backward walks, the timing and activation sequence of the functional stance phase muscles were also similar in forward and backward walking. The depressor again activated first (Fig. 3.10D), however, only half way through swing at 64.9 ± 25.1 ms before touch down, significantly later than in forward walking (p<0.0001). The protractor and flexor activated next at almost the same time, 10.9 ± 34.4 ms and 5.3 ± 28.6 ms after touch down (Fig. 3.10B, F). Flexor timing did not differ significantly from that in forward walking (p=0.12). Despite their large standard deviations, protractor timing in backward walking (10.9 ± 34.4 ms) and retractor timing in forward walking (34.6 ± 33.6 ms) did differ significantly (p<0.0001).

The latencies for the coxa-trochanter and femur-tibia joint muscles activation during curve walking are shown in Fig. 3.11. Firstly, comparing the activation of these muscles between the curve walking outside and inside leg shows similar latencies between step cycle transitions and muscle activation. The levator is activated on average 75.9 ± 29.9 ms in the outer curve leg and 85.3 ± 45.3 ms in the inside leg before a lift-off of the leg, and the depressor 115.1 ± 50.7 ms outside and 89.5 ± 26.7 ms inside the curve before leg touch down. In the femur-tibia joint, the extensor activity starts at similar times both during outside and inside curve walking before the start of the swing phase (outside: 51.5 ± 32.3 ms; inside: 47.5 ± 41.6 ms). Similarly, the flexor muscle, like during forward and backward walking, is activated shortly after the onset of stance phase (outside: 10.6 ± 10.2 ms; inside: 6.1 ± 16.8 ms). Except for the depressor, these values are statistically not significantly different between the outside and inside curve walking leg. However, when comparing the latencies of muscle activation during curve walking with those during forward walking, there is a statistically significant difference between all outside and inside levator, extensor, and flexor muscles and depressor outside leg latencies, but not for depressor inside leg latencies. Protractor and retractor latencies are not shown here, because often steps with different walking directions occur directly one after another and so protractor and retractor muscle activity can occur at any time during the step cycle, which makes determining the start of an enduring activity very difficult.

In summary, these data show that 1) only the muscles controlling the thorax-coxa

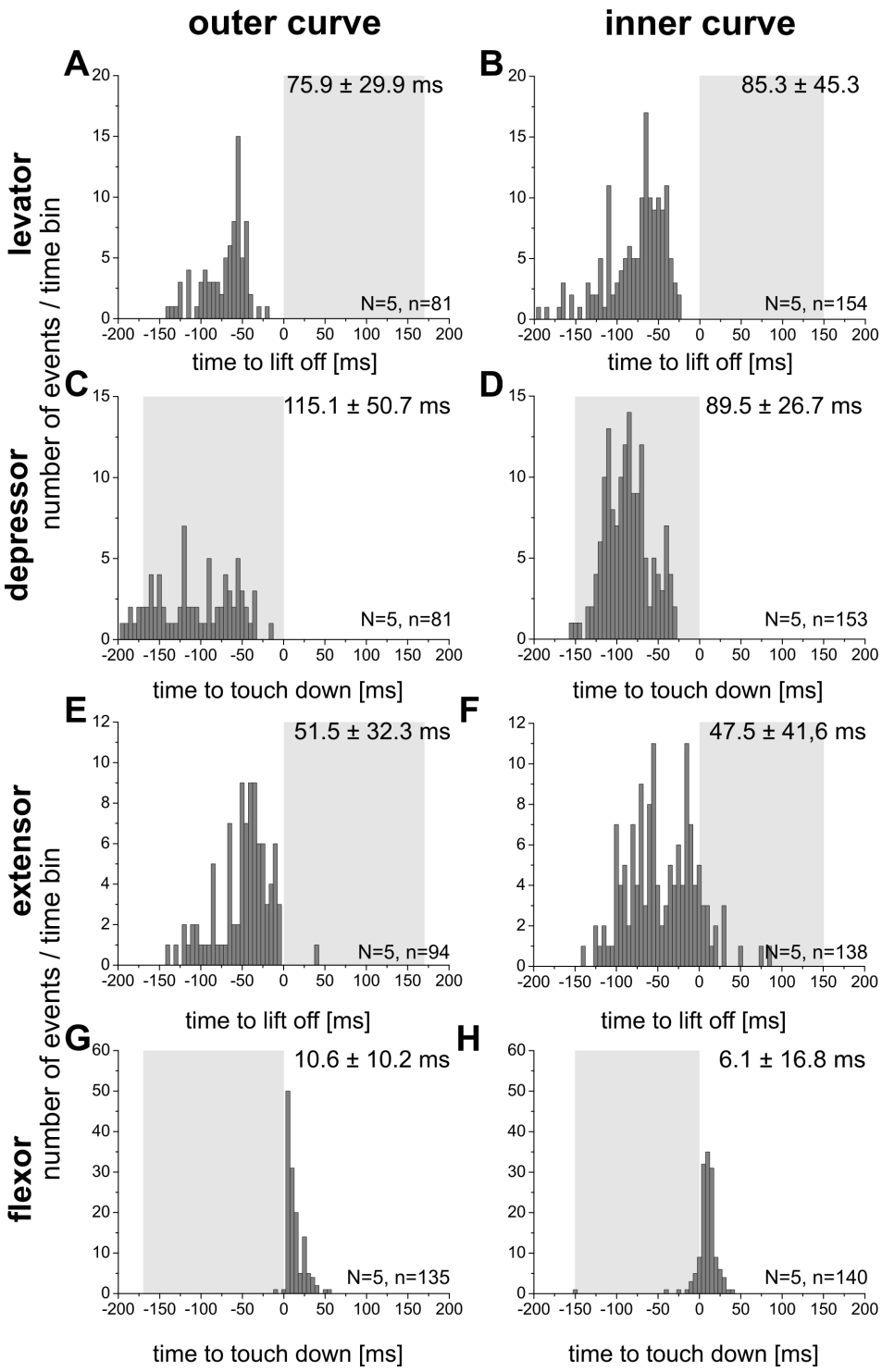

Figure 3.11 – Histograms of the latency distribution of the first muscle potentials in the EMG traces of CTr- and FTi-joint muscles during curve outside (left column) and inside (right column) leg walking. The timing of the first muscle potentials in levator and extensor were measured with respect to the time of lift-off. Depressor and flexor activity potentials were measured with respect to leg touch down. Gray boxes mark the average swing phase length (outside leg: 170±80ms; inside leg 153±70ms). Average latency of the first muscle potential is given with SD. N=animal number, n=step number.

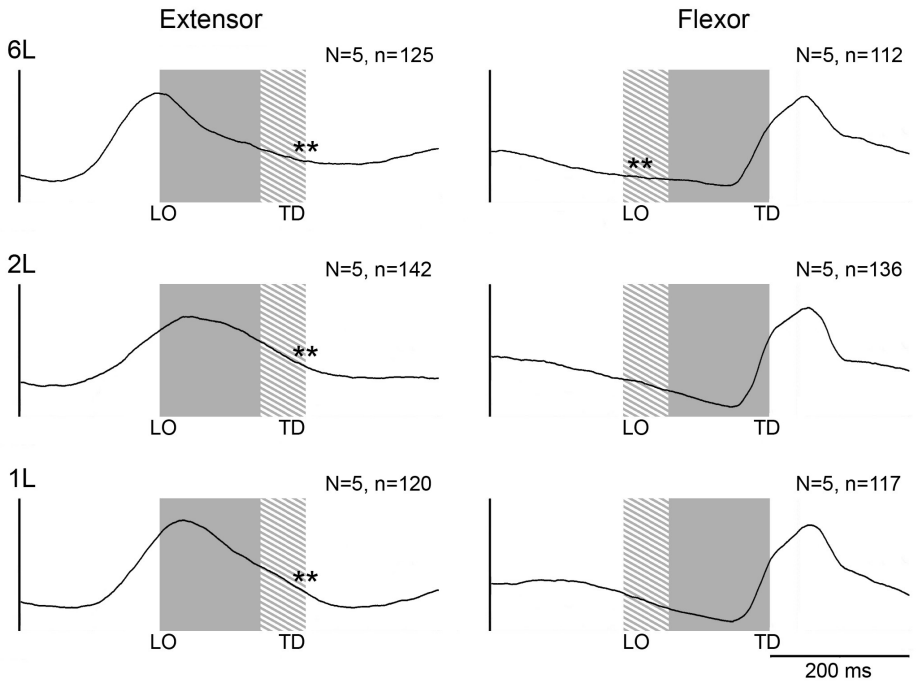

Figure 3.12 – Averaged, rectified, smoothed, and normalized middle leg extensor and flexor EMGs in intact, 2-legged, and single-leg preparations during forward walking. Double asterisks mark traces where crosstalk from antagonist muscle was removed mathematically. Gray boxes show mean swing duration, shaded areas swing duration SD. N=animal number, n=step number. LO = lift-off, TD = touch down.

joint showed large changes when walking direction changed, and 2) with respect to lift-off and touch down, the timing of functionally analogous muscles in swing and stance is very similar in forward, backward, and curve walking.

3.1.5 Muscle activity in reduced preparations

Many studies on stick insect walking have been conducted in preparations with reduced leg number (e.g. Akay et al., 2001, 2004; Fischer et al., 2001; Gabriel et al., 2003; Gabriel and Büschges, 2007; von Uckermann and Büschges, 2009). Because these preparations lack inter-leg sensory interactions, it is important to test if data from such experiments are applicable to intact animals. Leg kinematics in straight forward walking and turning change only little in reduced preparations (Gruhn et al., 2009b), but muscle activity in reduced preparations has not been measured. We therefore next compared forward walking muscle activity in intact and two-legged (2L) and one-legged (1L) animals.

Fig. 3.12 shows mean rectified and smoothed extensor and flexor EMGs from 112 to 142 steps from five different animals for each leg number condition. Extensor activ-

ity began about 100 ms before the stance-swing-phase transition, peaked between the stance-swing-transition and the first third of swing, and lasted throughout swing. Flexor activity was also similar in all leg number conditions. It started at the beginning of stance and largest activity occurred during the first 100 ms of stance. Similar data were found for the levator/depressor and protractor/retractor. In no case were major differences in EMG activity of the three antagonistic muscle pairs found between the intact, 2L, or 1L preparations (data not shown).

Removal of four or five legs to produce 2- or 1-middle legged preparations, did, however, alter the timing of first muscle activity in all three muscle pairs, at least under some reduced leg number conditions. The first swing phase muscle to be activated, the levator, was on average activated 92.8 ± 99.4 ms before lift-off in the 2L preparation and 88.4 ± 37 ms before lift-off in the 1L preparation. For both preparations this time was not significantly ($p_{2L}=0.15$, $p_{1L}=0.61$) later than in intact animals, neither were the values for the 1L and 2L-preparations significantly different from each other ($p=0.38$). The second muscle to be activated in swing, the extensor, activated significantly later in both reduced preparations than in intact animals, with first activity occurring on average 29.7 ± 38.9 ms (2L) and 33.2 ± 27.9 ms (1L) before lift-off ($p<0.0001$). The latencies of the first extensor spike in the two reduced preparations, on the other hand, did not differ significantly from each other ($p=0.47$). The third muscle activated in swing, the protractor, activated 19.9 ± 32.5 ms before lift-off in the 2L-preparation, significantly later than in intact animals ($p=0.0005$, 1L preparations were not investigated in this muscle).

All stance muscles showed small changes in activation timing. The depressor activated slightly but significantly earlier than in intact animals in both the 2L (99.6 ± 24 ms, $p<0.0001$) and 1L (123.7 ± 32.5 ms, $p<0.0001$) preparations. The flexor activated at statistically equivalent times in both reduced preparations (2L, 16 ± 12.5 ms; 1L, 15.9 ± 9.5 ms, $p=0.9$) with both preparations also differing significantly from intact animals ($p<0.0001$). In the 2L-preparation the retractor showed a large and significant change in the timing of first activity (10.2 ± 34.5 ms after touch down, $p<0.0001$) compared to intact animals (1L preparations were not investigated in this muscle).

The data show that middle leg muscle activity changes only slightly in reduced preparations and thus intersegmental influences are certainly not required for determining the sequence of muscle activity and overall phasing. Nonetheless, the presence of clear changes in the latencies of most muscles indicates that inter-leg sensory input does contribute to the timing of middle leg swing and stance muscle activation.

3.1.6 Depressor muscle activity depends on animal height

Depressor activity is strongly influenced by movement, strain, and load related inputs from the trochanteral hair plate (Schmitz, 1986b,a; Cruse et al., 1993; Berg et al., 2013), campaniform sensilla (Borgmann et al., 2007, 2012; Zill et al., 2012) and from the femoral chordotonal organ (Hess and Büschges, 1997, 1999; Bucher et al., 2003). In our experimental setup the animals were attached to a small wooden dowel held at a fixed height above the slippery surface. The animals therefore could not regulate their height and hence did not experience the changes in leg loading that would occur in completely free walking. We therefore tested the effect of decreased and increased load by lifting or lowering the tethered animal during walking sequences and comparing the depressor activity under these conditions. Fig. 3.13A-C shows middle leg depressor trochanteris and levator trochanteris recordings from a single stick insect while the animal walked at 10 (the physiological walking height and height of all other experiments shown here), 13, and 7 mm above the slippery surface. The normalized rectified and smoothed depressor activities from all recorded steps of all animals under the different conditions are shown in Fig. 3.13D. Increasing walking height from 10 to 13 mm (Fig. 3.13B) had little effect on the depressor activity (Fig. 3.13A). At both heights the depressor was mainly active during the second half of swing, although in 3 out of 6 animals, as in this example, slightly fewer depressor spikes occurred in stance at a height of 13 mm. Levator activity showed no detectable changes in activity. At a height of 7 mm the depressor was active not only in the second half of swing but also throughout two thirds of stance, continuing until levator activity began. Since the depressor activity was very similar during swing, we compared the integrals under the rectified and smoothed EMG traces after touch down from 6 animals at 7 mm, and 5 animals at 10 and 13 mm. 4 out of 6 animals showed higher mean depressor activity during stance at 7 mm compared to the other two conditions. Even with all animals at this condition pooled together, average depressor activity was significantly greater at 7 mm than in the other two situations ($p<0.0001$), while the activity was the same in the animals at 10 and 13 mm height ($p=0.49$). These differences in depressor activity at different animal heights made it very important to measure depressor activity in freely walking animals that could control their own body height. We therefore dismounted the stick insect from the wood dowel after first recording depressor and levator activity under tethered conditions at different heights. The glycerin was then wiped from the slippery surface and the still completely wired animal was allowed to walk freely on the surface while continuing to record stepping tarsal contact (Fig. 3.13E). Under these conditions, depressor EMG activity did not start at a different time from the

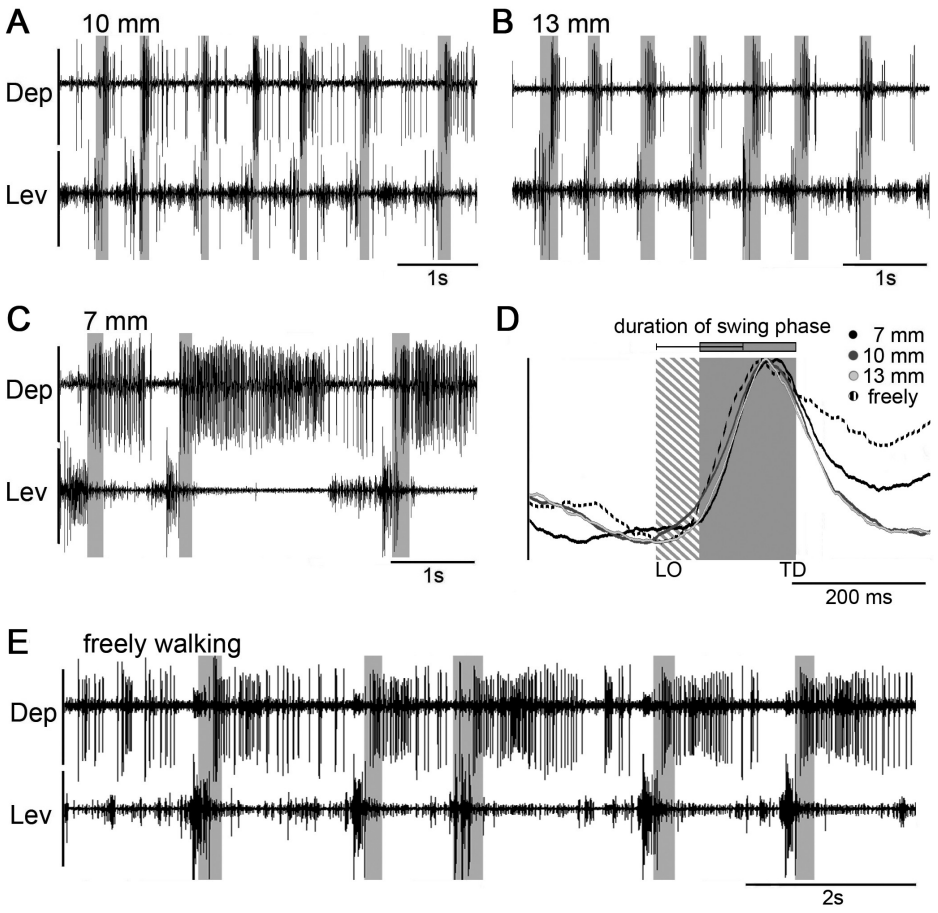

Figure 3.13 – Middle leg depressor and levator in forward walking, intact animals fixed at different walking heights. A: 10 mm. B: 13 mm. C: 7 mm. D: averaged, rectified, and smoothed depressor EMG traces at 7 (black, N=6), 10 (dark gray, N=6) and 13 (light gray, N=6) mm and from a freely walking animal (stippled, N=1). E: middle leg depressor and levator EMG activity in forward free walking. Gray boxes mark swing duration.

values at all heights seen in the tethered animal. The stippled trace in Fig. 3.13D shows the similarity in mean rectified activity for the freely walking animal and the 6 animals fixed at 7 mm. The time course of depressor activity pattern, however, was very similar to that seen in tethered walking at 7 mm height (Fig. 3.13C), i.e., depressor activity lasted long into stance. This suggests that, when the animal has to control its own height during walking, the depressor acts not only to lower the leg to the ground (swing activity), but also acts during stance to help carry the animal's weight and keep it at a specific height above the ground.

3.2 Patterning of leg motoneuron activity during single-leg forward and backward stepping on a treadwheel

3.2.1 Synaptic drive to motoneurons

The previously described changes in muscle activity during forward and backward walking led to the question of how the activity during the change of walking direction is altered on the level of the leg motoneurons. It is known that during walking, leg muscle motoneurons are tonically depolarized by descending input, they receive alternating phasic excitatory and inhibitory inputs from leg sense organs, and phasic inhibitory input from leg central pattern generating networks (Ludwar et al., 2005b; Büschges et al., 2004; Schmidt et al., 2001). The goal of this set of experiments was to investigate if backward walking is relying on similar inputs to motoneurons as was shown for forward walking.

Therefore, we used an experimental setup in which intracellular recordings of neurons in the mesothorax can be steadily performed. In the single leg preparation (see Methods), only the investigated middle leg was left intact whereas all other legs were cut at mid-coxa level to eliminate intersegmental information, i.e. sensory feedback from other legs. Furthermore, the thorax-coxa joint was fixed such that stepping on a treadwheel was only possible in a vertical plane. In contrast to the experiments on the slippery surface, the kinematics of the leg movement while walking on the treadwheel are very different. As previously described by von Uckermann and Büschges (2009), the leg is moved towards the body during stance phase. Thereby the flexion constitutes the majority of the movement. During swing phase the leg is lifted and extended, i.e. the tarsus is moved away from the body. Von Uckermann & Büschges also described the change in the joint angles during single leg stepping. They observed a two fold increase in FTi-joint angle as in the CTr-joint during swing, and even a multiple-fold increased angular change during stance phase (von Uckermann and Büschges, 2009). This supports the notion that the flexion constitutes the main movement during stance phase. Furthermore, stance phase is shorter than swing phase in the single-leg preparation and there is no fixed correlation between stance and swing observable like on the slippery surface, where stance phase is longer and more variable compared to the relatively constant swing phase (Fig. 3.2).

As described in the Methods section, forward walking can be elicited by touching the animal with a brush at the abdomen, and backward walking by pulling on the antennae or stimulating the antennae/head region with a brush. The walk-

ing direction could be identified by extracellularly recording the motor activity of nerves nl2 and nl5, through which the axons of the protractor coxae (nl2) and retractor coxae motoneurons (nl5) run. A recording of those nerves' activity plus a muscle recording of the flexor tibiae as an stance phase indicator is shown in Fig. 3.14A. The treadwheel signal in the lowermost trace helps to determine swing and stance phase of the step cycle. During stance phase, the treadwheel is pulled towards the animal, which is represented as the ascending slope of the trace, the descending slope and the default signal belong to the swing phase, whose activity can thus only be determined indirectly. In Fig. 3.14 and all subsequent figures, stance phase is indicated by a gray bar. Like the investigation of muscle activity of freely walking stick insects on the slippery surface showed (sec. 3.1.3), the protractor is active in swing and the retractor is active in stance in the forward walking animal. In the right panel, during backward walking, the phase of the nerve activity is reversed: protractor activity occurs during stance phase and retractor activity in swing phase. Thus, during forward walking retractor and flexor are active in phase, and during backward walking protractor and flexor are active in phase. In Fig. 3.14B the nerve activity in respect to the walking direction is quantified. This shows that fictive forward and backward walking can be elicited in the single leg preparation in which the ThC-joint is fixed and the protractor and the retractor nerve are crushed distally to the recording site. The reliability of the stimulation is shown in Fig. 3.14C: in 97% of the 7 animals tested here, an abdominal stimulation led to nerve activity that would occur during forward walking, whereas the remainder were uncoordinated steps. Antennal stimulation led to 86% 'fictive' backward directed steps, 12.5% uncoordinated steps and even in 1.5% of the cases to forward directed steps. This tendency can be confirmed for the rest of the experiments, where the proportions were not tested explicitly. Thus, fictive forward and backward walking in the single leg preparation can be reliably elicited. Consequently, every time when forward and backward walking during single-leg stepping on the treadwheel is mentioned, the extracellularly recorded nerve activity of the deafferented motor nerves nl2 and nl5 during 'fictive' forward and backward walking is meant.

In the following I will describe the activity of motoneurons from all three main leg joints during single-leg stepping on a treadwheel during forward and backward walking, and the synaptic inputs they receive.

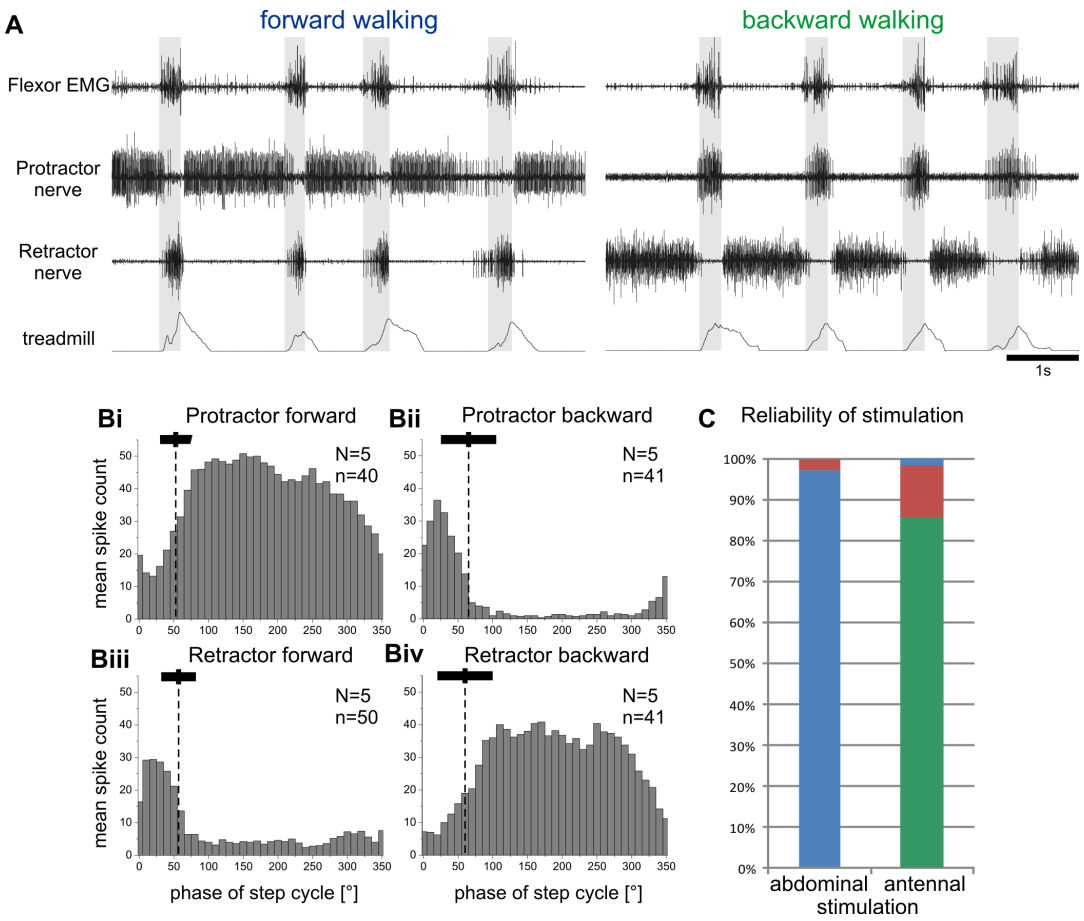

Figure 3.14 – Fictive forward and backward walking can reliably be elicited in the single leg preparation. A: extracellular recordings from the retractor (nl5) and protractor coxae (nl2) motor nerves during forward and backward walking. An electromyogram (EMG) of the flexor muscle is performed as an additional stance phase indicator. The lower trace shows the treadmill movement, the ascending slope of the signal marks stance phase, indicated by gray boxes, the remaining signal swing phase. Note the clear inversion of the nerve activity during the two walking directions. B: analysis of protractor and retractor nerve activity during forward and backward walking. Peri-stimulus time histograms of motor nerve activities during one step cycle are shown. The horizontal dashed lines mark the transition from stance to swing phase, the black bar above the standard deviation. C: percentage of evoked responses due to abdominal or antennal stimulation. In blue forward, in green backward directed steps, red=uncoordinated steps. N=7 animals, n steps abdominal stimulation=112, n antennal stimulation=116.

3.2.1.1 Retractor motoneurons

The retractor coxae muscle is innervated by 16-17 motoneurons and the common inhibitor 1 (CI1), whose axons run through the nervus lateralis 5 (nl5) as revealed by dye backfills (Goldammer et al., 2012). The motor nerve activity shows, ideally, the activity of all axons of the retractor motoneurons (and CI1) running through the recorded nerve. Here, retractor motoneurons are recorded intracellularly from their neuropilar arborizations in the hemiganglion ipsilateral to the walking leg. Motoneurons could be identified by a one to one correlation from intracellularly and extracellularly recorded spikes. Fig. 3.15 shows an example of a recording from a retractor motoneuron. In Fig. 3.15A a forward and a backward walking sequence is shown. As the extracellular recordings indicate, the intracellular recorded motoneuron also changes its phase of activity from stance phase activity during forward walking to swing phase activity during backward walking. There is a shift in the resting membrane potential (RMP) in this recording, which is negligible because the potential stayed constant during both walking episodes.

To reveal the synaptic inputs the motoneuron receives during stepping, its membrane potential is altered via current injection. When positive/depolarizing current is injected into the retractor MN until it is tonically firing action potentials and walking is elicited, a distinct hyperpolarization during the activity of the antagonist is revealed (Fig. 3.15Bi and Ci). This means that the retractor MN receives inhibitory synaptic inputs during this phase of the step cycle, which could be mediated by potassium (K^+)-ion outflow of the cell or chloride (Cl^-) ion inflow into the cell. When the membrane potential is farther away from the reversal potential of these ions (K^+: -90 mV, Cl^-: -92 mV; Eckert, 2000) by injecting positive current, the electrochemical driving force for these ions gets larger and therefore the hyperpolarization is increased in amplitude. On the other hand, the depolarization is decreased in amplitude, because sodium (Na^+) and calcium (Ca^+) ions are closer to their reversal potential (Na^+: +65 mV, Ca^{2+}: +120 mV). For the same reasons an injection of negative current leads to a better visualization of the excitatory inputs to the retractor MN (Fig. 3.15Bii, Cii). A large tonic depolarization is clearly visible throughout the stepping sequence with smaller phasic depolarizations on top of the tonic depolarization during stance in forward stepping and in swing during backward stepping. Furthermore, overdraws of the membrane potential during single steps are shown to illustrate the course of the membrane potential during the transition from stance to swing phase in more detail (Fig. 3.15Biii, Ciii). Spikes were eliminated by substituting the fast portion with a vertical line maximally 3 ms before and after the spike, using a custom written Spike2 script. Here, a stereotypical course of the membrane potential is shown with a depolarization

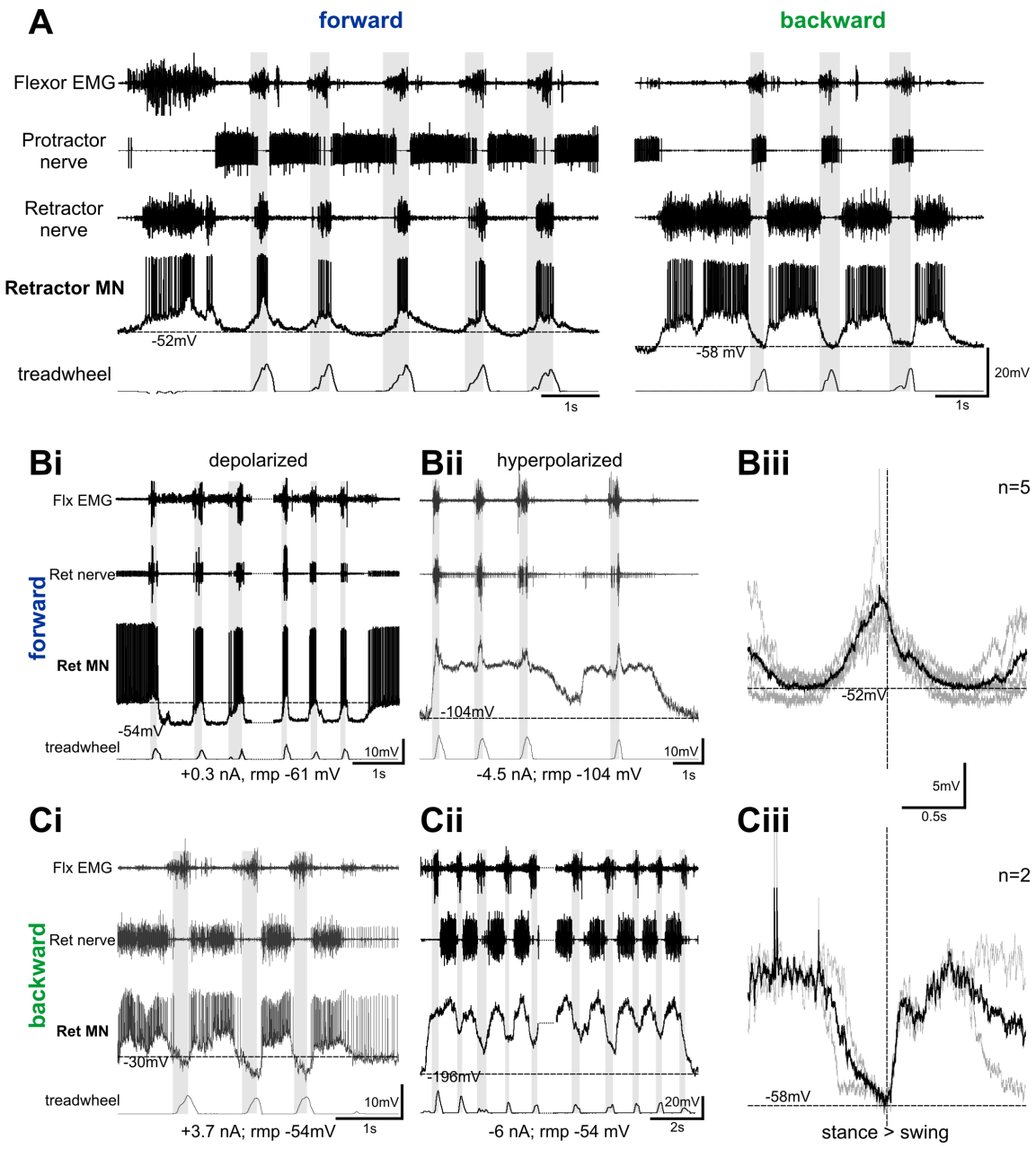

Figure 3.15 – Intracellular recording of a retractor motoneuron during walking. A: stepping sequence during forward (left side) and backward walking (right side). The topmost trace shows the flexor EMG, followed by protractor and retractor nerve activity recorded extracellularly, which indicate the walking direction. The 4th trace shows the intracellular recording of a retractor MN. The lowermost trace shows the treadwheel activity, stance phases are marked with gray bars. Note the change of retractor MN activity from stance activity during forward walking to swing activity during backward walking. B: injecting depolarizing current during forward walking reveals an inhibition of the MN in swing (Bi), injection of hyperpolarizing current demasks the tonic depolarization underlying stepping activity and phasic depolarizing inputs on top of it in stance (Bii). Biii: overdraws of the membrane potential of single steps (gray) at the stance-swing transition (black: average, gray: single steps). Spikes were eliminated. C: backward stepping sequences while injecting depolarizing (Ci) and hyperpolarizing current (Cii). Ciii: overdraw of the MP at the stance-swing transition. The dashed black lines in the intracellular recording traces indicate the RMP, resp. the adjusted RMP via current injection, in those cases original RMP and amount of current injected are stated below the figures.

of the retractor MNs during stance phase in the forward walking animal and in swing phase in the backward walking animal.

A total of 22 Retractor MNs were recorded in 21 animals. In every recording forward walking could be elicited, and in 14 animals backward walking. The above described pattern of activity, in which the activity was reversed during backward walking, could be observed in all of the recorded MNs.

In conclusion, retractor MNs receive a tonic depolarizing synaptic input during walking and phasic excitation/inhibition during forward and backward walking, whereas in backward walking the phase of the step cycle during which the phasic synaptic inputs occur is reversed.

3.2.1.2 Protractor motoneurons

The protractor coxae muscle is innervated by 6-9 motoneurons and the common inhibitor 1 (CI1). Their axons process through the nervus lateralis 2 (nl2) branch C (Goldammer et al., 2012). Six protractor MNs were recorded in six animals, all of which showed forward and backward stepping. During forward walking, the protractor muscle is active during swing phase and moves the leg from a posterior to an anterior position (Rosenbaum et al., 2010). An intracellular recording of a protractor MN during forward walking shows a quick depolarization of the membrane potential at the onset of swing and spiking throughout swing phase. During backward walking the MN is active during stance (Fig. 3.16A). A tonic depolarization of $>$ 10 mV throughout the stepping sequences and phasic excitation and inhibition of the neuron during stepping is clearly visible. In Fig. 3.16B overdraws depict the course of the membrane potential modulation at the transition from stance to swing phase for single steps (gray) and the averaged potential (black, spikes were eliminated). At the onset of swing, during forward walking the protractor MN is rapidly depolarized, and quickly hyperpolarized during backward walking. In Fig. 3.16C a stepping sequence from another animal during backward walking is shown, in which the resting membrane potential was more depolarized (-48 mV) and therefore an inhibition during swing phase is apparent. Together, these observations show for protractor MNs, similar to retractor MNs, tonic synaptic inputs during both walking directions and phasic synaptic inputs which change their phase of occurrence. The origin of these synaptic inputs and how the change in activity arises will be discussed later.

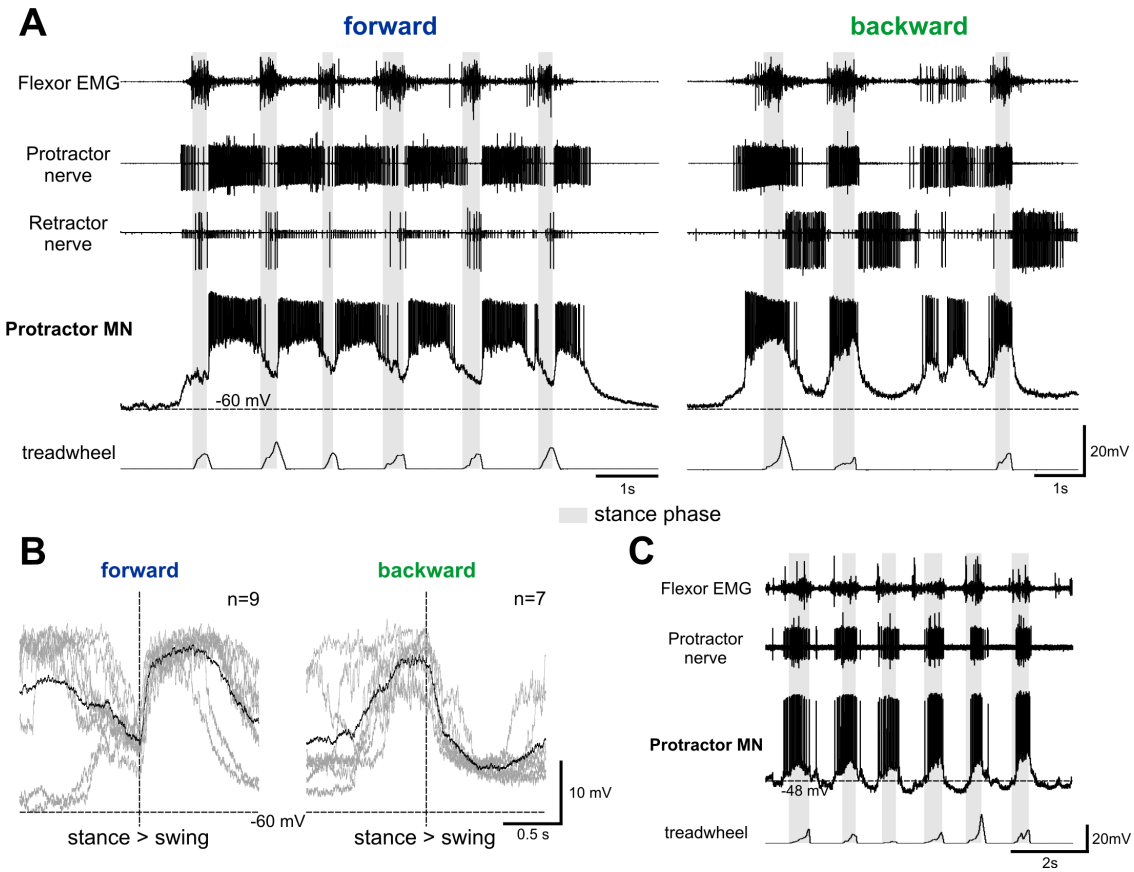

Figure 3.16 – Intracellular recording of a protractor motoneuron during forward and backward walking. A: forward and backward walking sequences of a protractor MN, together with a flexor EMG as stance phase indicator. Protractor and retractor nerve recordings indicate the walking direction. Gray bars mark the stance phase as determined by the treadwheel trace. Note the change from swing phase activity during forward walking to stance phase activity during backward walking. In both stepping sequences a tonic depolarization is apparent. B: overdraws of the membrane potential modulation during forward (left side) and backward walking (right side) illustrate the course of the membrane potential at the stance-swing transition. C: backward stepping sequence while recording from another protractor MN. Note the inhibition during swing phase.

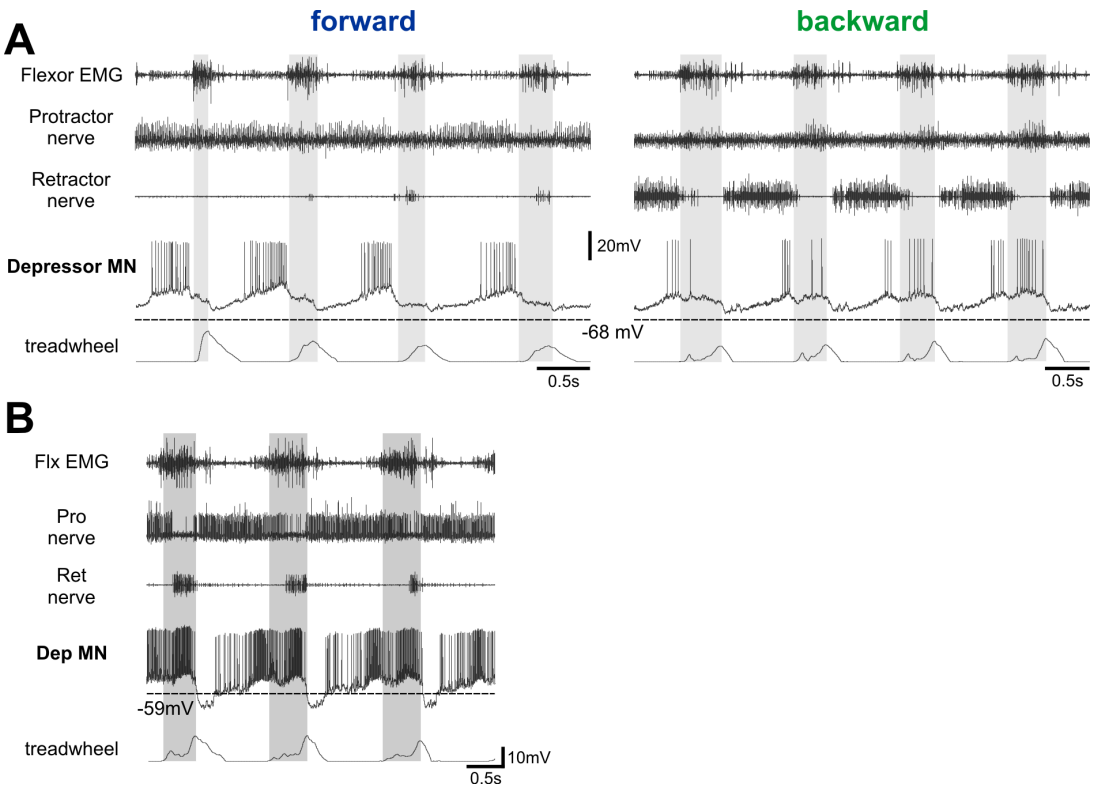

Figure 3.17 – Depressor motoneurons activity during forward and backward walking. A: an intracellular recording of a depressor MN (3rd trace) during forward and backward walking. Additionally, flexor muscle activity and treadwheel mark stance phase, protractor and retractor nerve recordings indicate walking direction. Depressor spikes occur at the end of swing phase during both walking directions and in stance phase during backward walking (see text). B: recording from a depressor MN during forward stepping. It is tonically spiking throughout the step cycle and only inhibited at the onset of swing.

3.2.1.3 Depressor motoneurons

Nerve C2 innervates the depressor trochanteris muscle. It contains axons of two excitatory motoneurons, the fast depressor trochanteris MN (FDTr) and the slow depressor trochanteris MN (SDTr), plus three inhibitory MNs: CI1,CI2 and CI3 (Goldammer et al., 2012). The depressor muscle is activated at the end of the swing phase to move the leg downwards (Rosenbaum et al., 2010). In sec. 3.1.6 it was shown that depressor muscle activity depends on the preparation. If the animal is glued to a stick/platform and therefore does not have to carry its own weight, the muscle activity of the depressor does not last long into stance phase. In contrast, muscle recordings of the depressor in a freely moving animal showed depressor activity starting during swing and throughout stance phase (cf. Fig. 3.13). In Fig. 3.17A an intracellular recording of a depressor MN is shown during forward and backward walking. During both walking directions depressor spikes occur during the second half of swing phase and during backward stepping in the

stance phase of the step cycle. In this particular recording no depressor spikes occur during stance phase, which is atypical. In Fig. 3.17B another depressor MN recording is shown, in which the MN is tonically active throughout the step cycle and only inhibited during the start of swing phase. This is similar to the muscle recordings in Fig. 3.13, in which muscle activity in swing and throughout stance could be observed. The leg has to be actively depressed at the end of swing phase and remains active during stance phase to support the body weight. Only at the start of swing phase, at which the leg has to be lifted off the ground, the MN is inhibited. Why this occurs, although the animal does not have to support its own body weight, has to be discussed. The same activity patterns as described above have been observed in eight depressor MN recordings in eight animals, of which seven showed forward walking and six backward walking.

3.2.1.4 Levator motoneurons

The levator trochanteris muscle is innervated by nerve C1, through which axons of 9-11 motoneurons and of CI1 process (Goldammer et al., 2012). The levator muscle is active at the transition from stance to swing phase to lift the leg before the start of swing. As can be seen in the intracellular recording of a levator MN, the neuron is only depolarized at the beginning of the swing phase and then repolarized to resting membrane potential. This indicates that once the leg has been lifted, no further levator activity is necessary (Fig. 3.18 A). This is true for forward and backward walking, during backward walking the leg is lifted at an anterior position compared to a posterior position during forward walking (see also Fig. 3.1). Fig. 3.18B shows one step of a stepping sequence during which the levator MN was constantly depolarized. Here, an inhibition of the MN can be clearly seen in stance phase. Overdraws of the levator membrane potential for several steps during forward and backward walking emphasize the similar course of the membrane potential modulation (Fig. 3.18C).

Seven levator MNs were recorded of which all showed forward walking but only three backward walking.

3.2.1.5 Flexor motoneurons

The flexor tibiae muscle is innervated by several branches of the nervus cruris (ncr) through which 8-25 flexor motoneurons plus CI2 and CI3 process, as identified by dye backfills. The large variety in the MN number is probably due to difficulties in backfilling all of the small flexor branches of ncr (Goldammer et al., 2012).

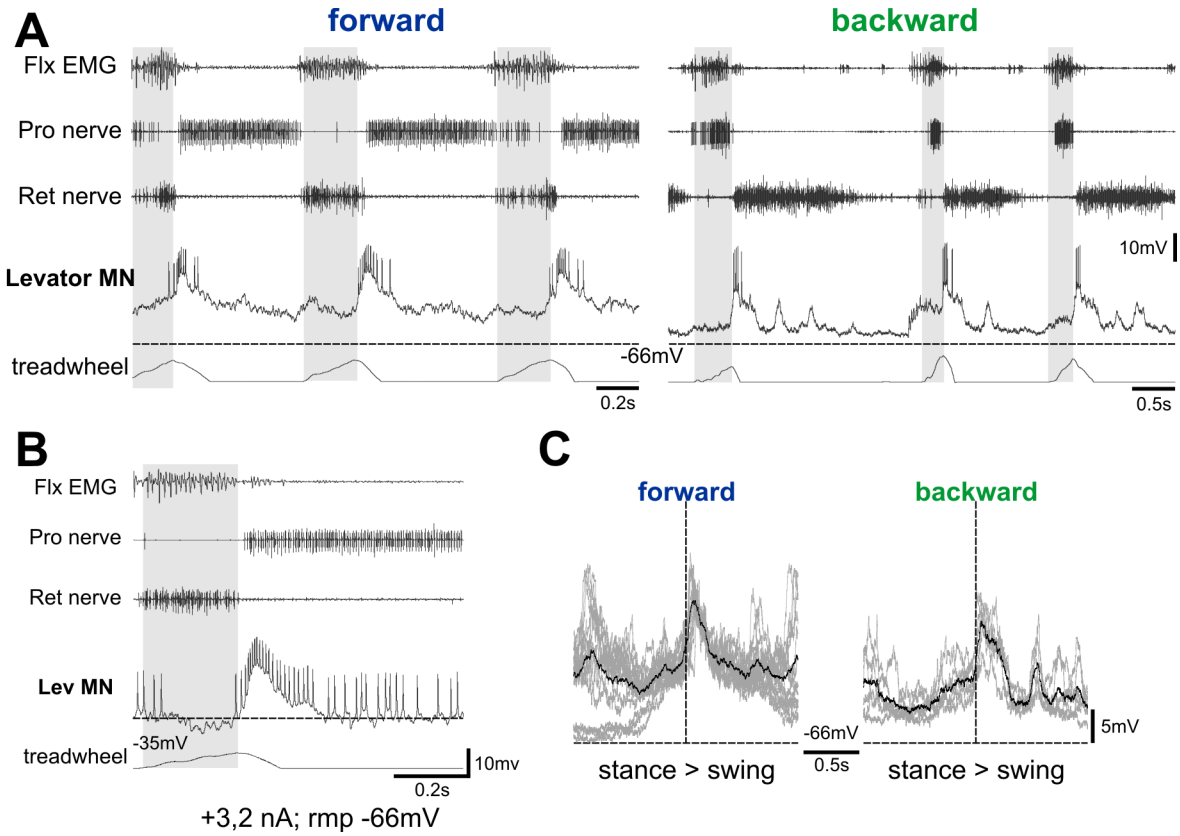

Figure 3.18 – Forward and backward single-leg stepping on a treadwheel while recording a levator motoneuron. A: the third trace shows the intracellular recording of the levator MN which has an unaltered activity during forward and backward walking. Flexor EMG and treadwheel trace serve as stance phase indicator, which is marked by gray bars. Extracellular protractor and retractor recordings indicate the walking direction. B: one forward directed step while the MN is held depolarized: an inhibition at the end of stance phase becomes apparent. C: overdraws of the membrane potential during forward and backward walking with single steps (gray) and the averaged course of the MP (black). Note the similar, quick depolarization at the start of swing phase.

The flexor is a stance phase muscle which is shortly activated after the start of stance phase, i.e. the touch down of the leg, both during forward and backward walking (Fig. 3.5, Fig. 3.9F, Fig. 3.10F). Intracellularly recordings of flexor MNs were already thoroughly described by Gabriel and Büschges (2007) during forward walking. In Fig. 3.19A a flexor MN recording is shown during forward and backward walking. Flexor MN activity occurs only in stance phase in both walking directions. In the forward walking sequence, two different stepping velocities and different depolarization amplitudes of the flexor membrane potential are highlighted by dashed lines. This shows that the stepping velocity on the treadwheel is correlated to flexor MN activity, which will be further analyzed in the next chapter. As was already shown by Gabriel (2005), the flexor MN is inhibited during swing phase, which becomes apparent by injecting depolarizing current (Fig. 3.3Bi). A large tonic depolarization during walking is revealed by the injection of hyperpolarizing current. In addition, the phasic excitation during stance phase is visible with an increased amplitude compared to the the normal stepping sequence (Fig. 3.19Bii). The course of the membrane potential modulation during several overlayed steps for forward and backward stepping is shown in Fig. 3.19C and shows a very similar activity of the flexor MN during both walking directions.

Flexor MNs were recorded in 14 animals, backward walking could be elicited in 8 animals.

In summary, MNs of all three main leg joints were recorded intracellularly and their activity was described during single-leg forward and backward stepping on a treadwheel. Similar to the description of muscle activity in the first section of the results, only the activity of the thorax-coxa joint MNs, protractor and retractor MNs, was changed during backward walking. The retractor MNs are active during stance phase and the protractor MNs during swing phase in forward stepping, during backward stepping the retractor is active in swing and the protractor in stance. All other intracellularly investigated MNs showed no change in activity between different walking directions. Furthermore, synaptic inputs modulating the MN activity during walking, i.e. the tonic depolarization underlying stepping, and phasic excitatory and inhibitory synaptic inputs, are similar during both walking directions. Only the phase of the step cycle in which they occur is reversed in MNs of the thorax-coxa joint. The origin of the changed synaptic inputs to these MNs will be described in the third main section of the results.

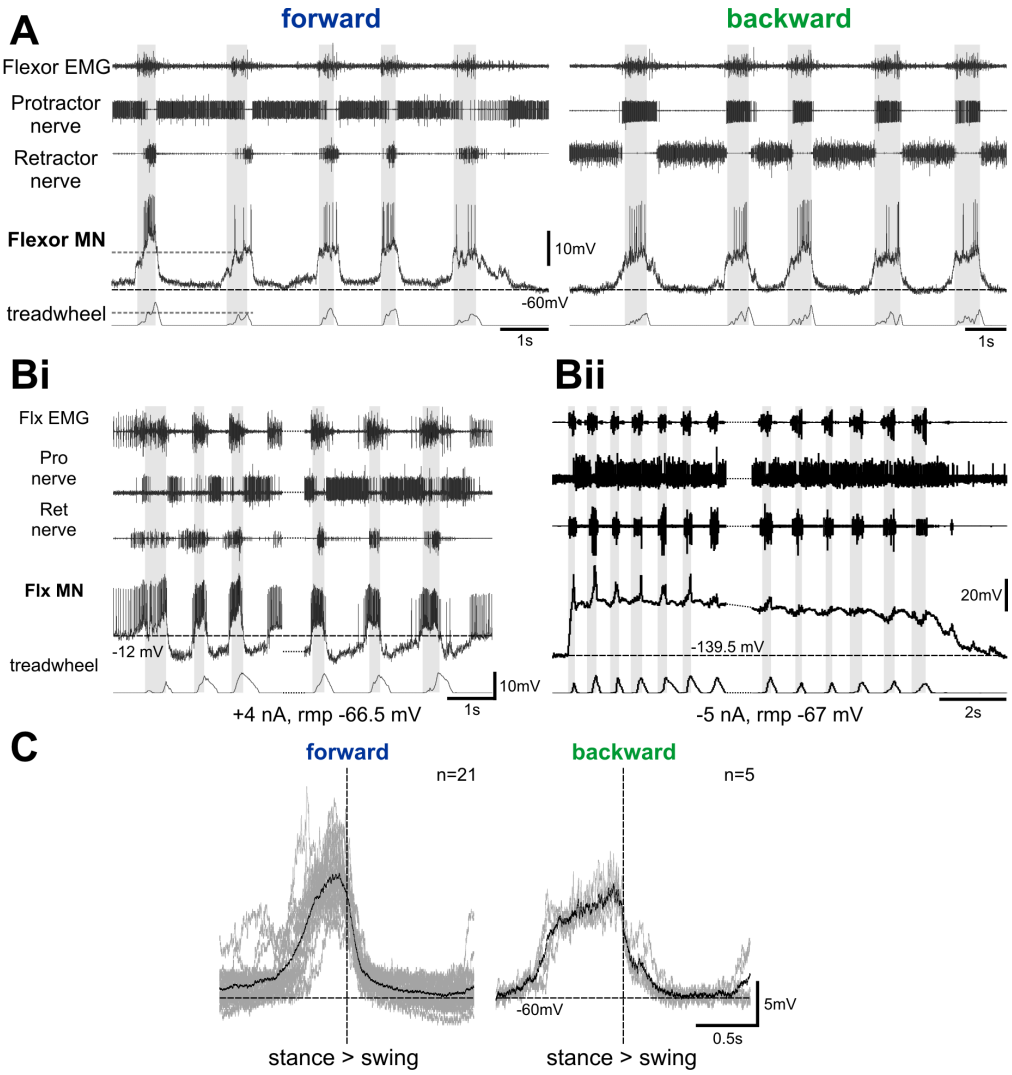

Figure 3.19 – Intracellular recording of a flexor motoneuron during forward and backward walking. A: flexor EMG and treadwheel mark the stance phase (gray bars). Protractor and retractor nerve recordings indicate the walking direction. The intracellular recording of a flexor MN (4th trace) shows a similar modulation with a depolarization during stance phase in forward and backward walking. The dashed line in the lower two traces on the left side help to distinguish the different amplitudes of the flexor MP and the treadwheel trace during the first two steps. B: lowering the MP by injection of hyperpolarizing current reveals an inhibition of flexor MNs during swing phase (Bi) while injection of depolarizing current shows a strong tonic depolarization during the stepping sequence with phasic excitatory potentials in stance phase. Both forward stepping sequences. C: overdraws from single steps (gray) and the average potential (black) show the course of the MP (spikes eliminated) during the stance-swing transition (forward n=21, backward n=5).

3.2.2 Velocity dependence of motoneuron activity during forward and backward walking

Another form of motor adaptation, besides the change of walking direction, is the change of locomotion speed. Stick insects increase their walking speed by decreasing cycle period. This is accomplished by an decrease in stance phase duration, whereas swing duration stays rather constant (Wendler, 1964). In sec. 3.1.2 this was shown during walking on a slippery surface. The neuronal control of walking speed has been investigated on the neuronal level in the stick insect to some extent, especially for motoneurons of the FTi-joint: flexor and extensor MNs (Gabriel and Büschges, 2007; Gruhn et al., 2009a). It was shown that only stance phase MN activity (flexor MNs) and not swing phase MN activity (extensor MNs) is correlated with the stepping velocity on the treadwheel (Gabriel and Büschges, 2007). Furthermore, no velocity dependent intersegmental influence of a stepping front leg on MNs in the deafferented mesothoracic ganglion (neither ipsi- nor contralateral) was found (Gruhn et al., 2009a).

Here, the activity of MNs described in the previous chapter was analyzed with regard to walking speed. It was investigated if other MNs than flexor MNs, especially other stance phase MNs, also show a correlation between their membrane potential modulation and stepping velocity during forward and backward walking. Thereby it is of particular interest, if the activity of subcoxal MNs shows a correlation to walking speed and if this is changed during different walking directions. Thus, it was analyzed if there is a correlation between stepping velocity and retractor MN activity during forward walking and/or between protractor MN activity and stepping velocity during backward walking. Therefore, I analyzed stepping sequences and measured peaks and troughs of the membrane potential modulation of single steps. Additionally, the peak-to-peak amplitude of the membrane potential change was calculated, and also the MN spike frequency during stance or swing phase. This was plotted against the mean belt velocity (see methods), which describes the velocity during stance phase in which the belt was pulled towards the animal.

It was already pointed out in the last section (cf. Fig. 3.19A) that in flexor MNs different depolarization amplitudes are associated with different belt velocities. Fig. 3.20 shows the correlation between flexor MN activity and stepping velocity. It was previously shown by Gabriel and Büschges (2007), that stepping velocity and peak activity of flexor MNs during forward walking on the treadwheel are correlated. Here, in 2 of 5 stepping sequences during forward walking (Fig. 3.20A) and 1 of 4 during backward walking (Fig. 3.20B), peak potentials of flexor MNs during different stance phase velocities are significantly correlated ($p<0.05$, ANOVA), but no trough potentials. The distance between resting membrane potential and

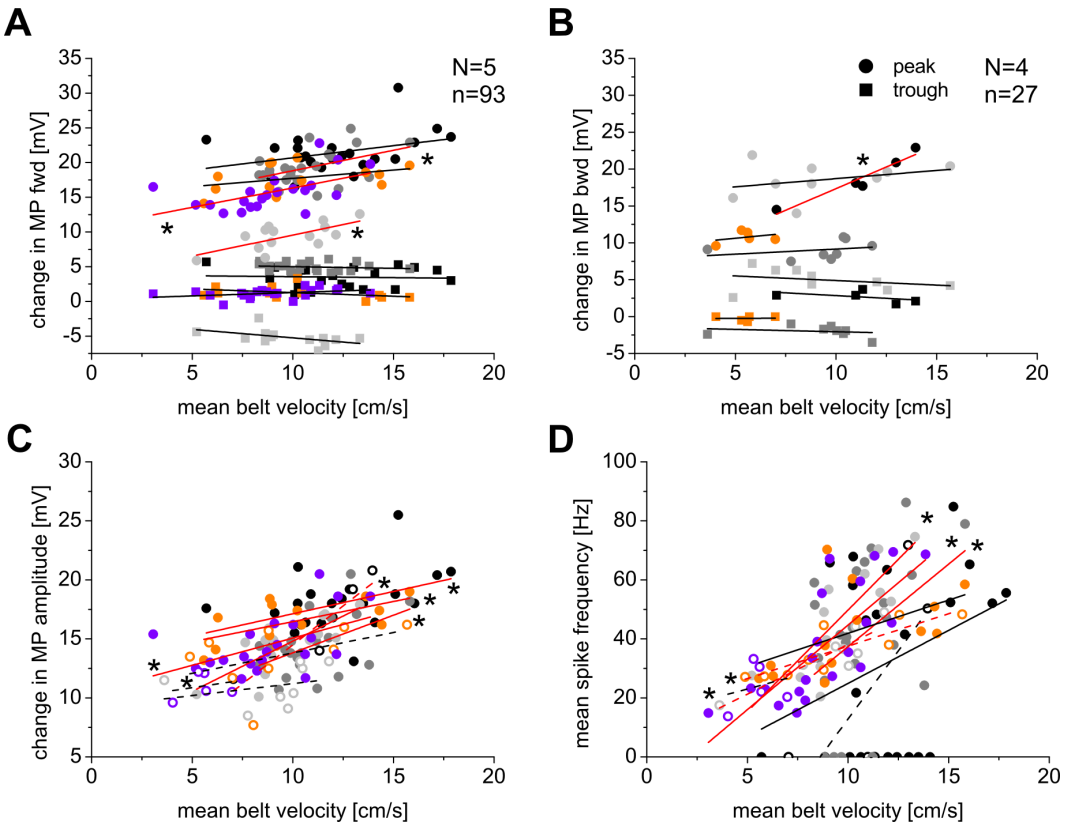

Figure 3.20 – Velocity dependence of flexor MN activity. A: peak and trough membrane potentials during steps with different mean velocities for forward directed steps (RMP subtracted from measured potentials). B: peak and trough membrane potentials vs. mean belt velocity for backward walking. Filled circles mark peak potentials, filled rectangles trough potentials. Same colors are from the same animal. Red regression lines, also marked with asterisks, mark significance ($p<0.05$, ANOVA). C: Maximal change in amplitude (peak+trough) for forward and backward steps vs. mean belt velocity. Forward steps: filled circles, continuous lines; backward steps: open circles, dashed lines; same colors=same animals. D: Mean spike frequency vs. mean belt velocity. Data points at the zero line are from steps where no spikes occurred.

peaks/troughs was measured. The correlation becomes clearer when looking at the peak-to-peak amplitude of the membrane potential modulation during stepping: here, in all (5 of 5) forward stepping sequences flexor MN activity is significantly correlated with stepping velocity (filled circles with continuous red lines) and in 1 of 4 backward stepping sequences (open circles with dashed red line, Fig. 3.20C). I also determined the mean spike frequency of flexor MN activity during stance phase, and found a significant correlation in 3 of 5 forward sequences and 2 of 4 backward walking sequences. This trend is in agreement with the results of Gabriel and Büschges (2007), and suggests that the control of stepping velocity depends on flexor activity also during backward walking.

Next, the activity of the coxa-trochanter joint MNs was compared with stepping velocity. The levator muscle is mostly active during swing. Its activity during

walking is shown in Fig. 3.18. An analysis of the peak and trough potential amplitude during forward and backward walking is shown in Fig. 3.21. Both, during

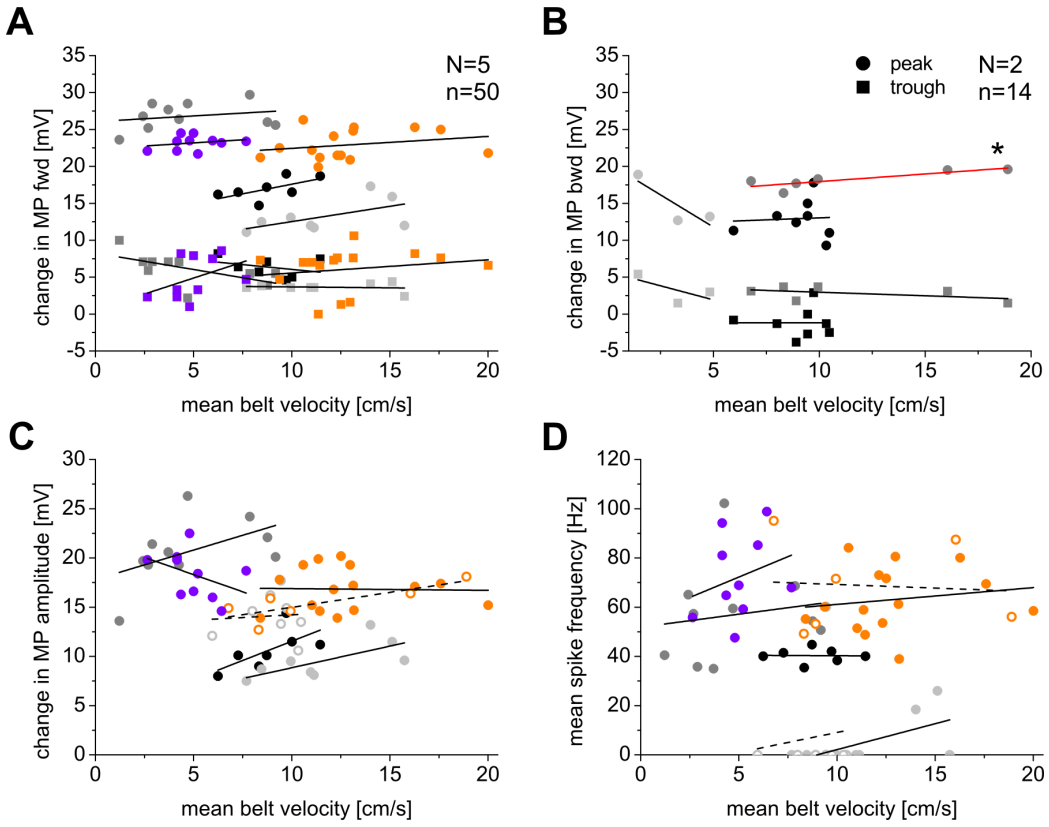

Figure 3.21 – Velocity dependence of levator MNs. A: peak and trough membrane potentials of levator MNs during forward walking, plotted against the mean belt velocity. Circles represent peak potentials, squares trough potentials, same color=same animal. B: peak and trough membrane potentials during backward walking. Peak potentials in one animal are significantly correlated to the mean belt velocity. C: amplitude (peak-trough) of membrane potential modulations during forward and backward walking vs. mean belt velocity. Filled circles and continuous lines from forward walking steps, open circles and dashed lines for backward stepping. D: mean spike frequency during forward and backward walking plotted against belt velocity. No significant correlation was found. N=number of animals, n= number of steps.

forward and backward walking (Fig. 3.21A and B) the majority of the stepping sequences shows similar peak and trough amplitudes during different walking speeds. Only in one backward stepping sequence, a significant correlation between mean belt velocity and peak potentials was observed. A comparison between the peak-to-peak amplitude change in the membrane potential and the mean belt velocity (forward N=5, backward N=2) shows no significant correlation to the walking speed for both walking directions, too. Also the mean levator spike frequency is not significantly correlated to the stepping velocity.

Depressor MNs are active during stance and parts of swing phase in the single leg preparation (cf. Fig. 3.17). In Fig. 3.22A and B the amplitudes of peak and

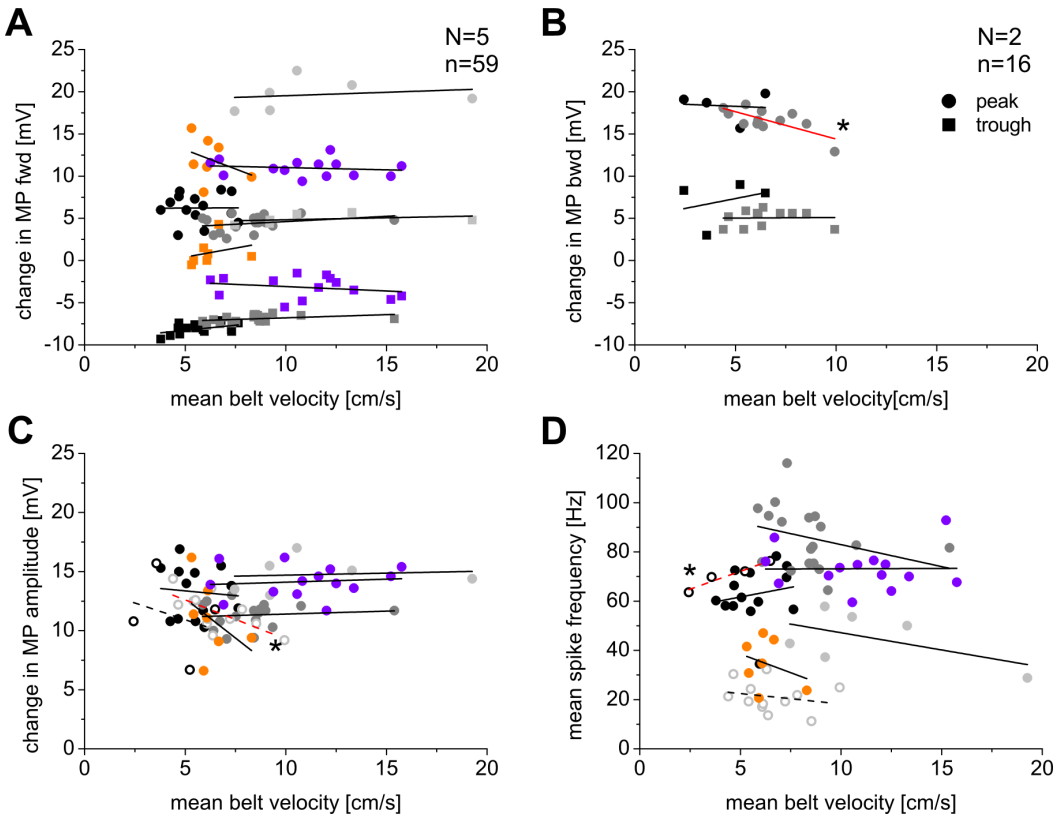

Figure 3.22 – Dependence of depressor MN MP on stepping velocity. A: peak and trough potentials during forward stepping compared with mean belt velocity. No significant correlation could be found (N=5, n=59). B: peak and trough membrane potentials during backward stepping. Peak membrane potentials from one animal are negatively correlated with the stance phase velocity (N=2, n=16). C: change in overall membrane potential amplitude during forward and backward stepping plotted vs. the mean belt velocity. In the same backward stepping sequence as in B, MP amplitude and belt velocity are negatively correlated. D: mean spike frequency of depressor MNs during forward and backward walking plotted versus the mean belt velocity. Only one sequence (backward) of seven is correlated to stepping velocity.

trough membrane potentials are plotted against the mean belt velocity for five forward stepping and two backward stepping sequences. In one sequence during backward walking a negative significant correlation of peak potentials to walking speed was found. The peak-to-trough amplitude change of the membrane potential modulation during both walking directions did not change significantly during all five forward walking and the single backward walking episodes. Only in one backward stepping sequence a significantly negative correlation with walking speed was found. An analysis of the mean spike frequency during single steps also showed in only one case a correlation to stepping speed. The other plots show a rather constant relationship.

The MNs which innervate the muscles of the most proximal leg joint, the thorax-coxa joint, are of particular interest with regard to a connection to walking speed. Because the retractor muscle is the functional stance phase muscle during forward

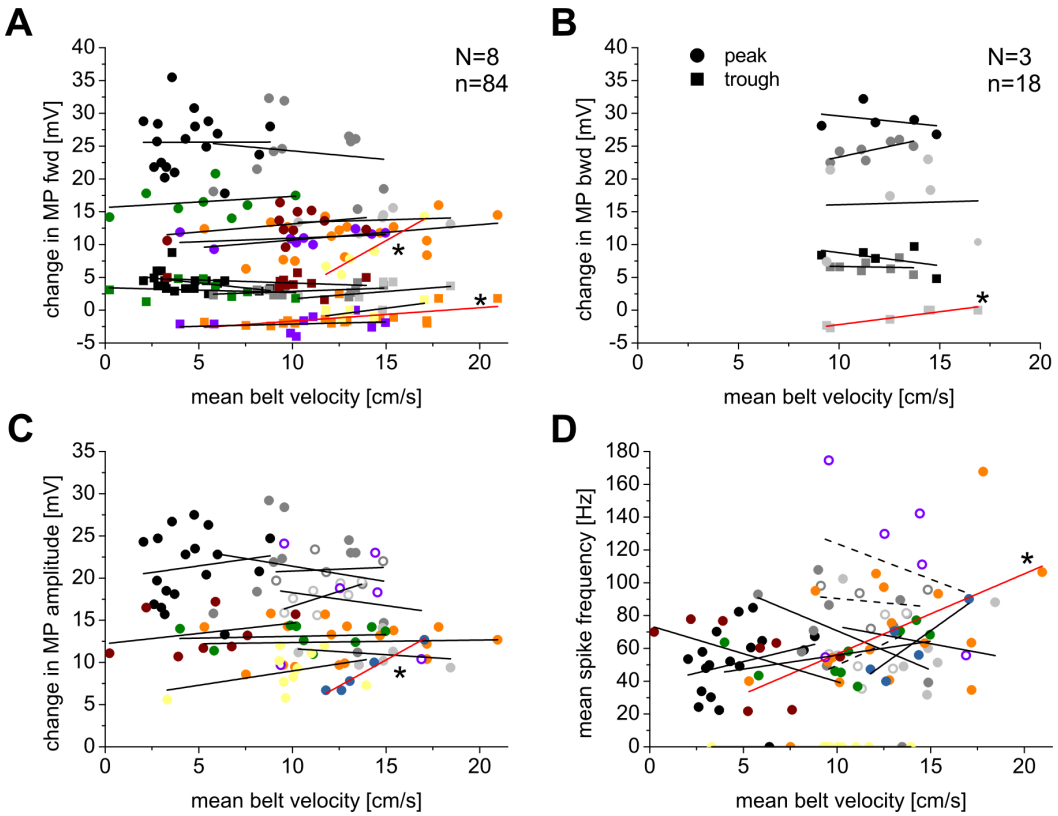

Figure 3.23 – Velocity dependence of retractor MN membrane potential modulation. A: peak and trough membrane potentials, subtracted of RMP, during forward walking. In only 1 of 8 animals peak membrane potentials are significantly correlated with mean belt velocity, in one animal trough membrane potentials (N=8,n=84). B: peak and trough membrane potentials of retractor MNs during backward walking. In one animal trough potentials are significantly correlated with mean belt velocity (N=3, n=18). C: comparison of the overall amplitude of membrane potential modulations during forward and backward walking. Only 1 out of 11 sequences is significantly correlated to mean belt velocity (same as peaks during forward stepping). D: mean spike frequency of retractor MNs plotted vs mean belt velocity, 1of 11 is significantly correlated.

walking, whereas during backward walking the protractor muscle takes this part, it is interesting to see if there is a correlation of walking speed and motoneuron activity during the change of walking direction. The results for the retractor MNs are shown in Fig. 3.23. The majority of steps of analyzed animals shows an equal distribution of belt velocities with little variations in the membrane potential peak and trough amplitudes. In one case, even different peak amplitudes of the membrane potential at similar belt velocities during forward walking were found (the values marked with black filled circles in Fig. 3.23A). One walking episode during both forward walking and backward walking showed a significant correlation of peak potentials with walking speed. In one case trough potentials during backward stepping are correlated to the belt velocity. Furthermore, when comparing the peak-to-tough amplitudes and mean spike frequencies with mean belt velocity,

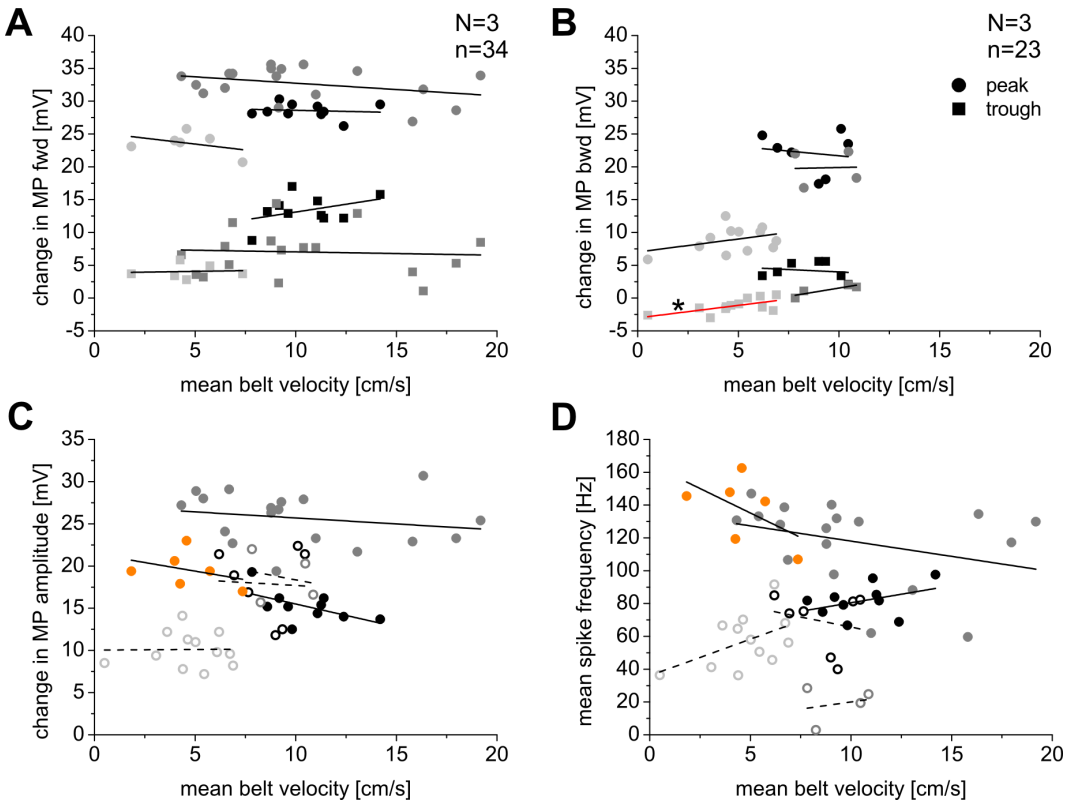

Figure 3.24 – Velocity dependence of protractor MN membrane potential. A: during forward walking, neither peak nor trough membrane potentials are significantly correlated to the mean belt velocity (N=3, n=34). B: peak and trough membrane potentials of protractor MNs during backward walking plotted against mean belt velocity. The trough potentials from the stepping sequence of one animal is significantly correlated with stepping velocity (N=3, n=23). C: change in MP amplitude during forward and backward walking. No correlation with mean belt velocity could be stated. D: mean protractor MN spike frequency vs. mean belt velocity. No significant correlation was found. Circles mark peak potentials, squares trough potentials, stars overall peak-to-peak MP amplitude during a step. Filled symbols and continuous regression lines for forward, open symbols and dashed regression lines for backward stepping. Red regression lines mark significance ($p<0.05$, ANOVA).

no overall correlation with walking speed was found, neither during forward nor during backward walking. Therefore, retractor MNs do not seem not be involved in the control of walking speed in the single leg preparation.

Protractor MNs are active in stance during backward walking, but when comparing backward directed steps with forward directed ones (Fig. 3.24A and B), no dependency on walking speed could be observed in either walking direction. In one case, however, trough membrane potentials during stepping showed a correlation with belt velocity. Plotting the amplitude of the membrane potential change and the spike frequency of protractor MNs versus the mean belt velocity also showed no correlation.

In conclusion, only a close correlation between stepping velocity on the treadwheel and flexor MN activity was found. Stance phase velocity showed no systematic correlation to the activity of all other MNs investigated here. That might mainly be due to the kinematics of stepping on the treadwheel with only two main leg joints free to move, in which the main movement of the leg takes place in the femur-tibia-joint (cf. von Uckermann and Büschges, 2009). However, an interesting point is that although the leg is moved at different speeds, no influence of the activity of other stance phase MNs, depressor and retractor during forward walking, depressor and protractor during backward walking, on the stepping velocity was found. Thus, no inter-joint signals between the femur-tibia joint and the other two more proximal joints seem to be necessary for the control of walking speed on the treadwheel. This is further evidence for the joint specific generation of motor output in the stick insect leg and its weak coupling.

3.3 Patterning of premotor nonspiking interneuron activity during single-leg forward and backward stepping on a treadwheel

To find out more about the inputs to leg motoneurons during walking, one group of their presynaptic neurons was investigated, the premotor nonspiking interneurons (NSIs). These local neurons are known to integrate signals from sense organs, intersegmental and central information, to contribute to the control of timing and magnitude of the motor output (e.g. Burrows, 1987; Laurent and Burrows, 1988; Burrows, 1989; Laurent and Burrows, 1989; Büschges, 1990; Büschges et al., 1995). In the stick insect exists only for the femur-tibia joint a comprehensive overview of NSIs involved in the leg muscle control network (Büschges, 1990; Büschges et al., 1994; Büschges, 1995). Furthermore, only few studies dealt with NSI activity during walking (e.g. Schmitz et al., 1991a; von Uckermann and Büschges, 2009). Von Uckermann and Büschges (2009) gave an overview of FTi-joint NSI membrane potential modulations during single leg stepping on a treadwheel. Here, previously identified NSIs providing synaptic drive to femur-tibia joint MNs, as well as newly identified NSIs controlling the coxa-trochanter and the thorax-coxa joint activity, were recorded during forward and backward stepping on a treadwheel.

Newly identified NSIs were labeled in the following way, according to Hess (1998); Hess and Büschges (1997): the first letter stands for the motoneuron pool whose activity is changed upon current injection to the NSI. If the neuron is described physiologically and morphologically, this letter is a capital, if only the physiology is described, the letter is small. The second character denotes if the influence of the NSI to that pool of MNs is excitatory or inhibitory. A number is given in ascending succession, beginning with the neuron with the most recordings. One example is Pe1. It provides excitatory input to protractor motoneurons, its physiology and morphology is described, and it is the first one described here in that fashion. If also a MN pool of another leg joint is influenced by that NSI, another two letters, divided by a point to the first two letters, are added.

3.3.1 Nonspiking interneurons influencing the thorax-coxa joint

Only some studies described local nonspiking interneurons which are presynaptic to protractor and retractor MNs (Schmitz et al., 1991a; Brunn, 1998; Brunn and Heuer, 1998). Schmitz et al. (1991a) recorded ThC-joint NSIs during walking, but input and output properties of the four investigated neurons weren't described in detail.

Nonspiking interneurons providing synaptic drive to retractor motoneurons
One type of nonspiking interneuron which provided excitatory synaptic drive to retractor MNs was recorded five times and is labeled re1. The output was revealed by an increase in activity in the extracellular nl5 (retractor nerve) recording while injecting depolarizing current into this neuron (Fig. 3.25A, right panel). During forward walking, re1 is depolarized above resting membrane potential during stance phase with the peak amplitude occurring shortly before the stance-swing transition. At the onset of swing, re1 is quickly hyperpolarized below resting membrane potential and stays there until the end of swing, upon which it is again depolarized (Fig. 3.25A, left side). In three of the five recordings, coordinated backward stepping sequences could be elicited, whereupon re1 shows a reversion of its activity. re1 stays active in phase with retractor activity and thus is depolarized in the swing phase but only slightly hyperpolarized in stance during backward walking (Fig. 3.25A, right side). In other recordings, the hyperpolarization amplitude during the stance was larger (not shown). The membrane potential modulation of re1 at the transition from stance to swing phase during forward and backward stepping is illustrated by overdraws of the membrane potential course during single steps and the averaged potential in Fig. 3.25B; gray traces: single steps, black trace: averaged potential. The average peak-to-peak amplitude of the membrane potential in all five animals was 13.6 ± 3.2 mV (N=5, n=43) during forward walking, and 16.9 ± 4.5 mV (N=3, n=12) during backward walking. The average resting membrane potential of all NSIs was -47.1 ± 4.8 mV (see also Tab. 3.1). In two of the five recorded re1 neurons, also an inhibition of protractor MNs could be observed. In another animal, stepping was elicited while the neuron was hyperpolarized by injecting negative current (Fig. 3.25D). In this case a tonic depolarization of the membrane potential of re1 throughout stepping could be observed on top of which the membrane potential was modulated in phase with retractor MN activity during stance. The phasic depolarizations in stance had higher amplitudes than during uninfluenced stepping, whereas the hyperpolarizing portion during swing phase disappeared. As described for the motoneurons (sec. 3.2.1.1), this is due to the hyperpolarized level of the membrane potential close to the reversal potential of K^+ and Cl^- Ions, which are most likely responsible for the inhibition. During a walking sequence at an artificially more depolarized membrane potential, a modulation including depolarizing and hyperpolarizing portions in accordance with retractor MN activity could be observed. The amplitude of the hyperpolarization increased compared to a stepping sequence in which no current was injected into re1 (Fig. 3.25E).

Furthermore, it was analyzed if re1 activity is related to the stepping velocity on the belt. In Fig. 3.25C the peak, trough and peak-to-trough amplitude membrane

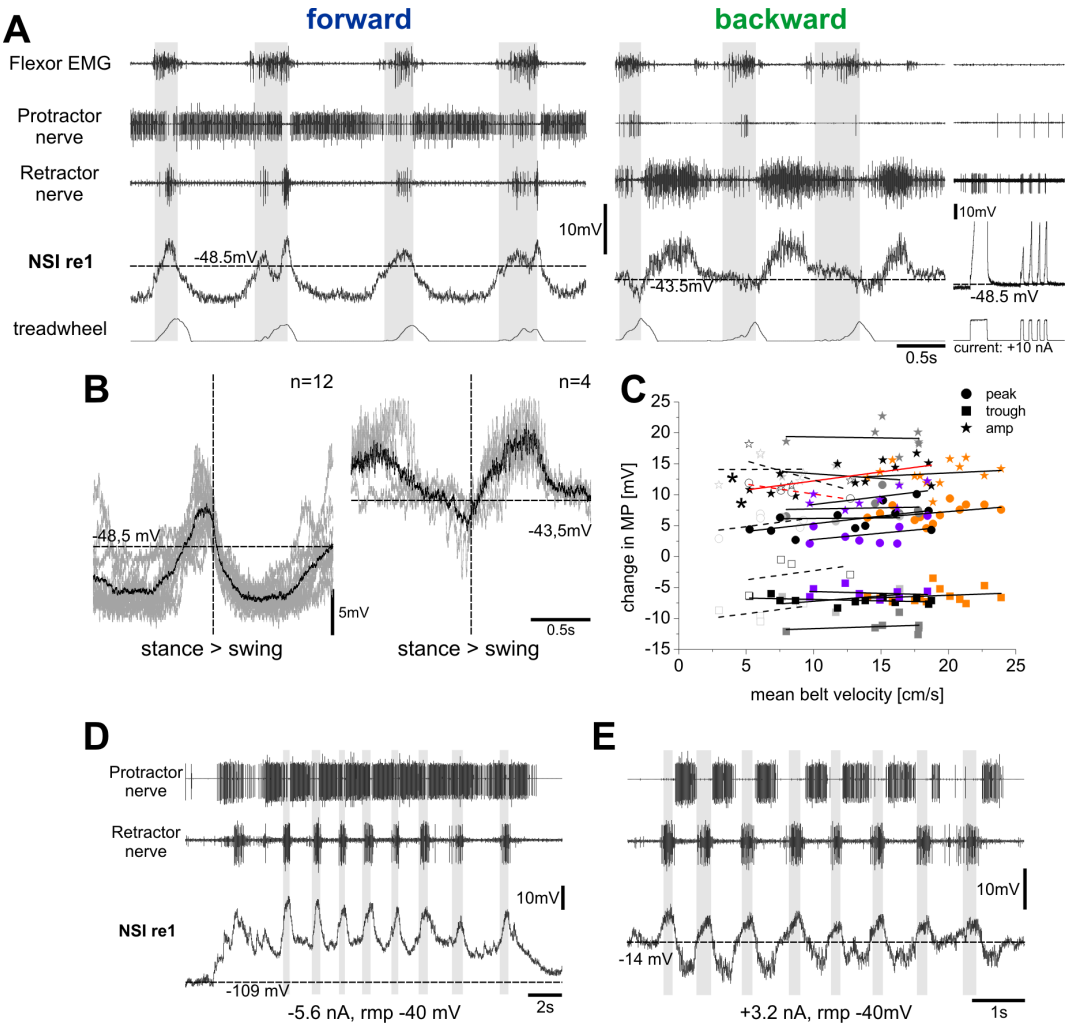

Figure 3.25 – Activity of NSI re1. A: during forward stepping, re1 is depolarized above resting membrane potential (-48.5 mV) in stance phase and hyperpolarized in swing phase. During backward walking, re1 is depolarized during swing and just slightly hyperpolarized during stance phase. The resting membrane potential drifted to -43.4 mV before this stepping sequence. Injecting depolarizing current into re1 evokes retractor MN activity. Gray bars mark the stance phase. B: overdraws of the membrane potential modulation during forward and backward stepping illustrate the activity at the transition from stance to swing phase. C: correlation of the membrane potential change during stepping with the mean belt velocity. Circles mark peak potentials, squares trough potentials, stars peak-to-trough amplitudes during a step. Filled symbols and continuous regression lines for forward, open symbols and dashed regression lines for backward stepping. Red regression lines mark significance ($p<0.05$, ANOVA). Only in one animal, forward stepping amplitudes of re1 were significantly correlated to mean belt velocity, and backward stepping peak potentials were negatively correlated to the belt velocity. D: forward stepping sequence with a re1 recording during injection of hyperpolarizing current (-5.6 nA). A tonic depolarization underlying walking activity becomes apparent, also the amplitudes of the phasic depolarization become larger. E: forward stepping sequence while re1 is held depolarized (+3.2 nA), a larger hyperpolarization during the swing phase is visible.

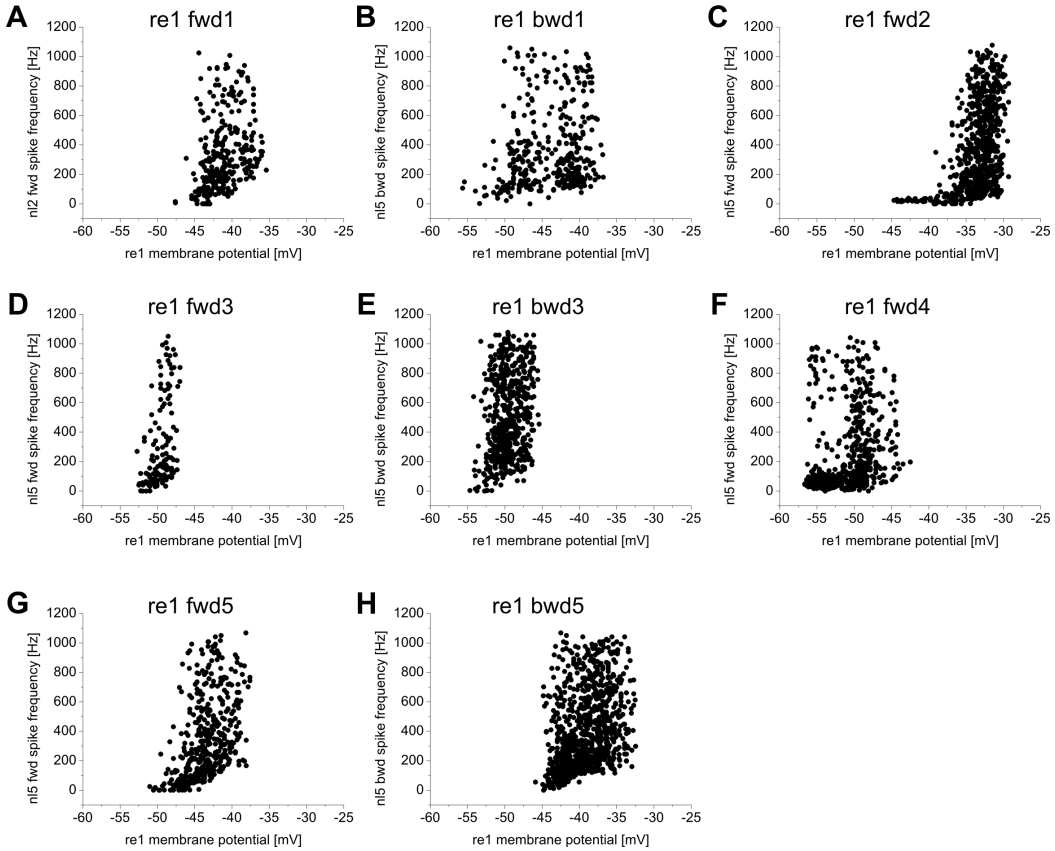

Figure 3.26 – Correlation between the membrane potential of re1 and retractor MN activity. A (fwd n=7) and B (bwd n=2); C (fwd n=13); D (fwd n=3) and E (bwd n=6); F (fwd n=8); G (fwd n=12) and H (bwd n=4) each are from one animal. The membrane potential of NSI re1 was plotted against the instantaneous spike frequency of the retractor MNs in motor nerve nl5.

potential changes during walking are plotted versus the mean belt velocity. Except the peak amplitudes from one animal, no significant correlation between the membrane potential modulation of NSI re1 and the stepping velocity on the treadwheel could be observed.

A passive stimulation of the femoral chordotonal organ (fCO) yielded in three of the five recorded NSIs re1 to hyperpolarizing responses to elongation and relaxation, in one case to hyperpolarization to elongation stimuli and very weak depolarizing responses due to relaxation. In one recording depolarizing responses to both stimuli were found.

To see how much retractor MN activity is correlated to the membrane potential modulation of NSI re1, the instantaneous spike frequency of motor nerve nl5 was determined (which includes all recorded units), and was plotted against the membrane potential of re1 (Fig. 3.26). In all cases the membrane potential of re1 was correlated to retractor MN activity during both forward and backward walking, which suggests a strong influence of re1 on retractor MN activity.

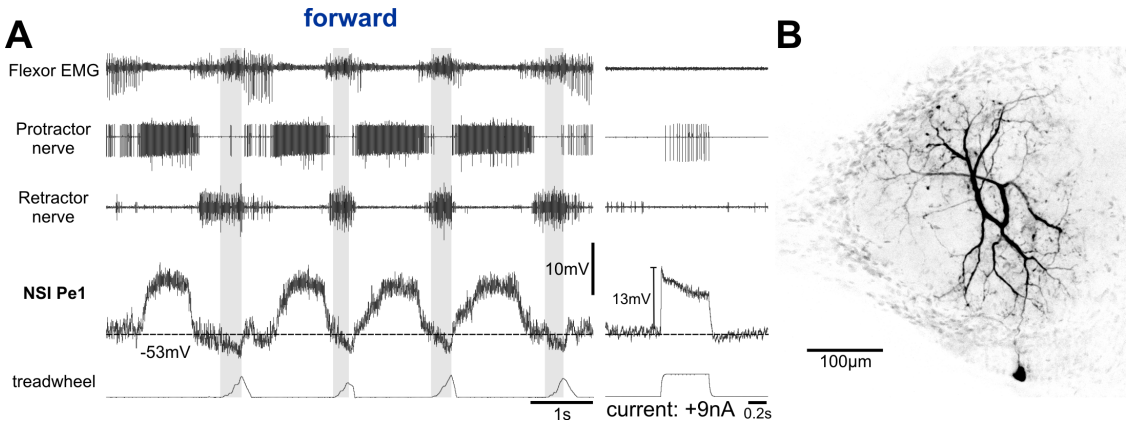

Figure 3.27 – Membrane potential modulation of NSI Pe1 during forward stepping. A: Pe1 activity during forward walking. It is active in phase with protractor MNs during swing phase. In some steps, a slight hyperpolarization below RMP (-53 mV) during stance can be seen. Injecting of depolarizing current (+9 nA) into Pe1 evokes protractor MN activity. B: morphology of Pe1. The soma is located at the posterior margin of the hemiganglion ipsilateral to the walking leg. Neurites arborize in the anterior and posterior part of the hemiganglion with a prominent bifurcation of two thick neurites in the middle of the hemiganglion.

Nonspiking interneurons providing synaptic drive to protractor motoneurons

The first type of NSIs providing excitatory drive to protractor MNs described here was recorded twice and labeled Pe1. Its effect on protractor MNs upon positive current injection is shown in the right panel of Fig. 3.27A. In the left panel, a forward walking sequence is shown in which Pe1 is active in phase with protractor nerve activity during swing phase. Pe1 is depolarized at the begin of swing and stays at this level (about 11.5 mV above RMP) until the end of swing. Than, it is rapidly repolarized below resting potential during stance. Because in this case no coordinated backward sequences could be recorded, it remains unclear how Pe1 is active during a change in walking direction. The responses of Pe1 to a passive stimulation of the fCO were depolarizing both for elongation as well as relaxation. The morphology of this type of interneuron has not been described before. The soma is positioned at the posterior margin in the ipsilateral hemiganglion of the recording site, the main neurites process in anterior direction where two thick, prominent neurites bifurcate in the middle portion of the hemiganglion and run in anterior direction (Fig. 3.27B). Both recorded neurons of this type have been stained and are thus clearly the same NSI.

Another NSI which excites protractor MNs, labeled pe2, was recorded once and is shown in Fig. 3.28. pe2 is active in phase with protractor MN activity during both walking directions. It stays at resting membrane potential during swing phase and is hyperpolarized in stance phase during forward stepping. In contrary, during backward walking the phase of activity is reversed so it is hyperpolarized

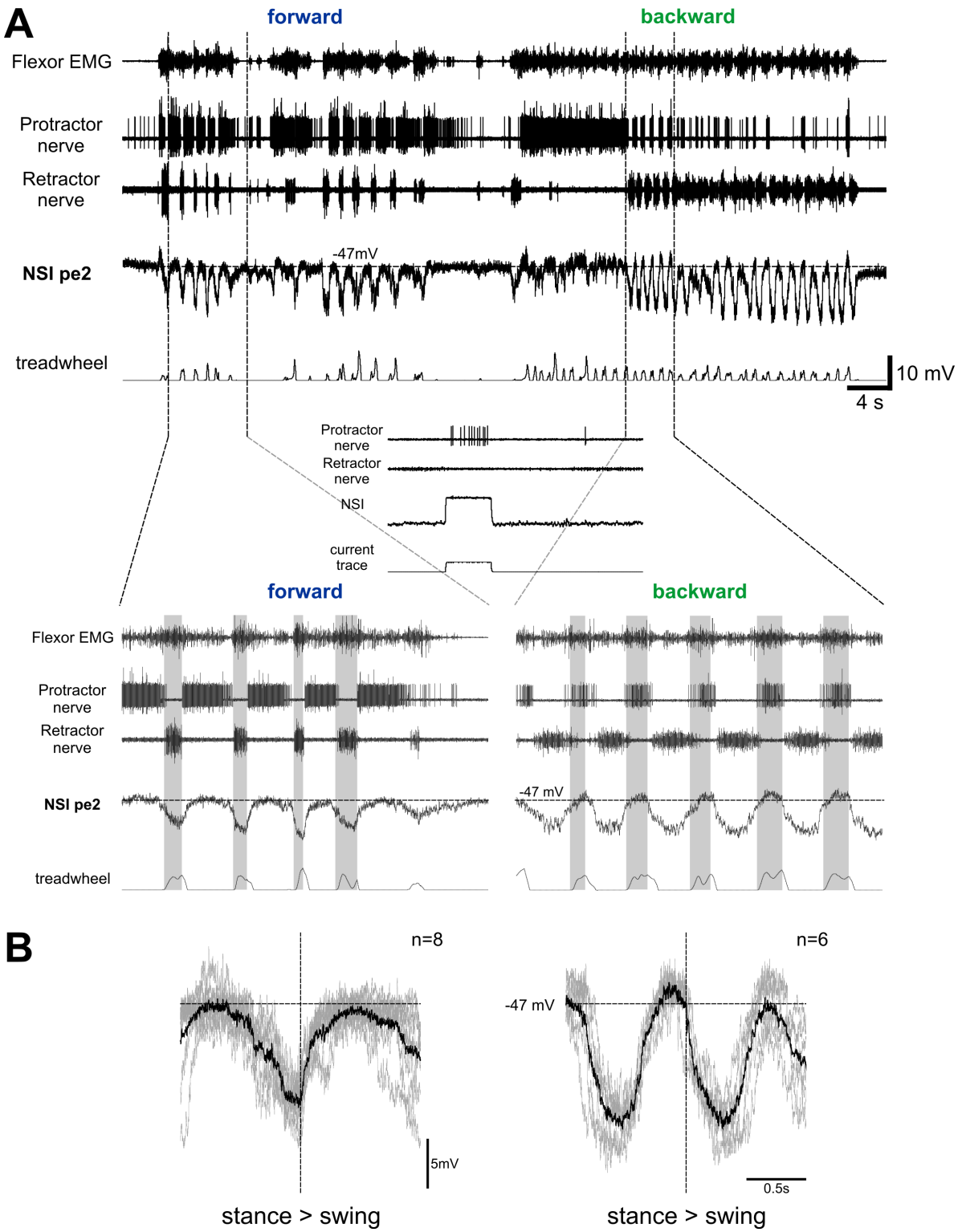

Figure 3.28 – The activity phase of NSI pe2 switches with the change of walking direction. A: the top portion shows a long stepping sequence with forward stepping on the left and than, after touching the antennae, a subsequent backward stepping sequence on the right side. Enlarged sections are marked with dashed lines. During forward walking, pe2 is hyperpolarized during stance phase and remains at resting membrane potential (-47 mV) in swing phase. During backward stepping this pattern is reversed. The inset shows the influence of depolarizing pe2 on protractor MNs. B: overdraws emphasize the course of the membrane potential modulation at the transition from stance to swing phase (forward n=8, backward n=6 steps).

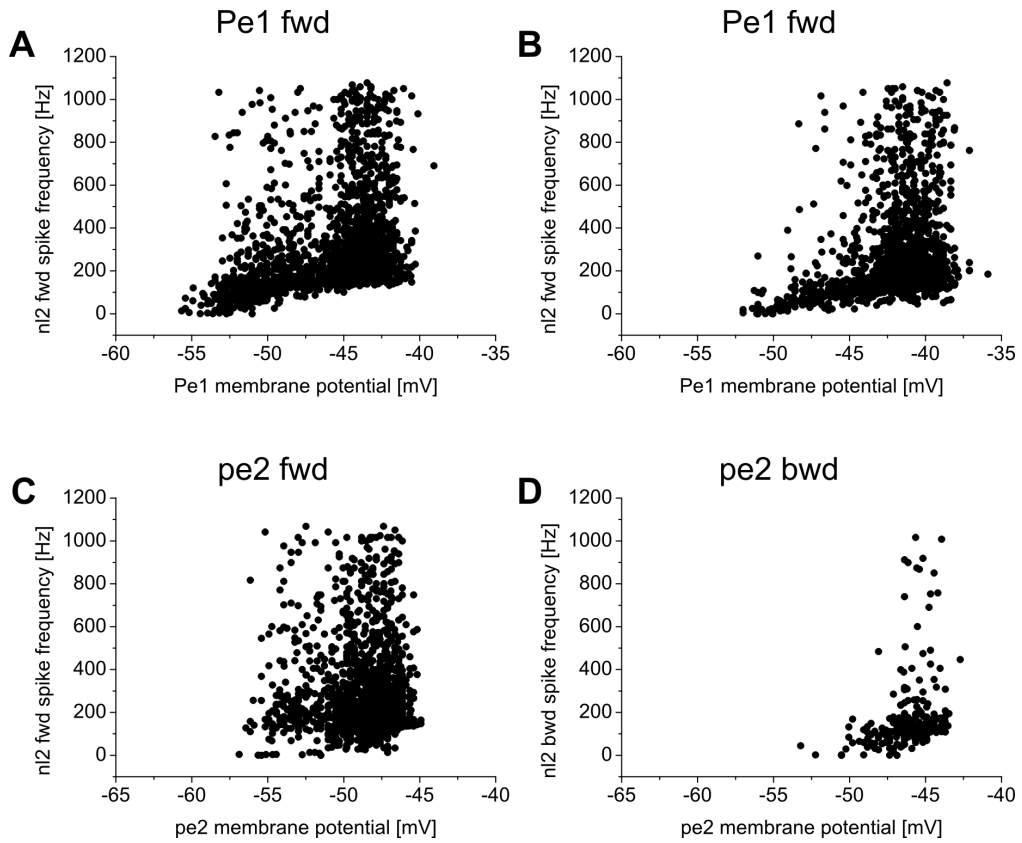

Figure 3.29 – Correlation between the membrane potential of Pe1 and pe2 and nl2 activity. A and B: correlation of the instantaneous nl2 spike frequency with the membrane potential from each one forward walking sequence of Pe1 (A: n=6; B: n=3). C and D: data sets of pe2 during forward (n=8) and backward stepping (n=6).

during swing and stays at resting potential during stance. The activity of pe2 at the transition from stance to swing phase is pointed out in the overdraws of the membrane potential modulations during single steps (Fig. 3.28B).

To see how much influence NSIs Pe1 and pe2 exert on protractor MNs, their membrane potential was plotted as a function of the nl2 instantaneous spike frequency (Fig. 3.29). The protractor MN activity is correlated to the membrane potential modulation of both NSI types .

Nonspiking interneurons providing synaptic drive to protractor and retractor motoneurons One nonspiking interneuron was recorded (N=2), which excited protractor as well as retractor MNs upon current injection (Fig. 3.30A and B). It was labeled pe.re1, and shows a rapid depolarization at the onset of swing and a slow repolarization back to resting membrane potential until the start of stance. There, it stays at resting level, in some steps it is slightly hyperpolarized (Fig. 3.30A, first step in the forward walking sequence). The activity is the same during both forward and backward stepping. Which function this neuron could

fulfill has to be discussed. When injecting hyperpolarizing current into pe.re1, a tonic depolarization underlying stepping with additional phasic depolarizing inputs during the swing phase becomes apparent (Fig. 3.30D).

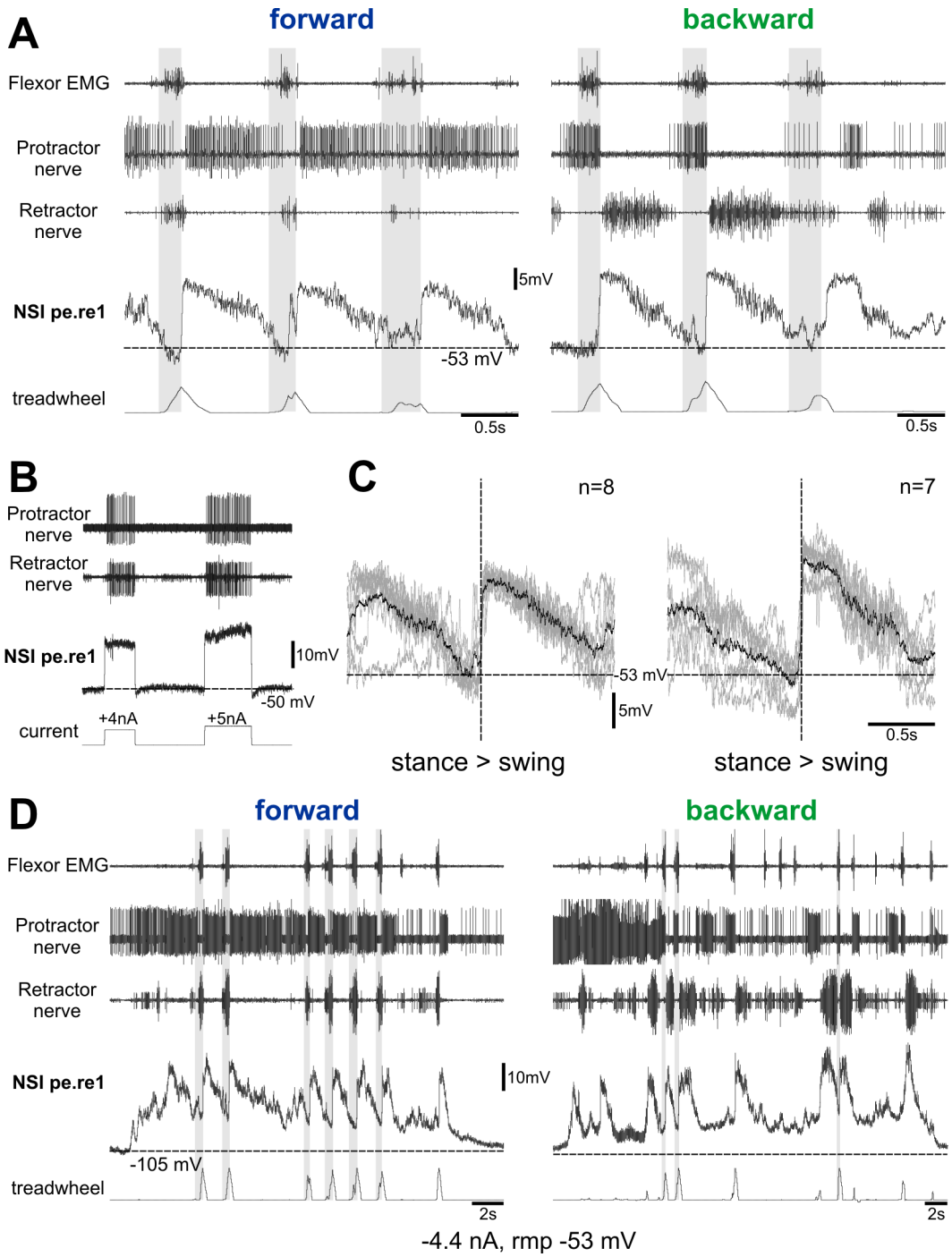

Figure 3.30 – Membrane potential modulation of NSI pe.re1 during forward and backward stepping. A: during both forward and backward walking, pe.re1 is quickly depolarized at the start of swing phase and slowly repolarizes to the resting membrane potential (-53 mV) until the start of stance. Gray bars mark the stance phase. B: upon injecting depolarizing current, spikes in the extracellular protractor and retractor nerve recordings are elicited. C: overdraws of the membrane potential changes of single steps during forward and backward stepping. The course of the membrane potential stays the same (gray: single steps, black: averaged potential). D: stepping sequences while injecting hyperpolarizing current (-4.4 nA) reveal a tonic depolarization during forward and backward walking underlying the phasic modulation of the membrane potential.

3.3.2 Nonspiking interneurons influencing the coxa-trochanter joint

Hess (1998) and Hess and Büschges (1997) described the activity of nonspiking interneurons which are involved in the control of coxa-trochanter joint movements, and how they participate in interjoint reflex actions. They labeled those NSIs, amongst others, De1 and Le1 to le4. Here, newly described NSIs for the CTr-joint are thus labeled subsequently De2-de5 and le5-le8. In the following, NSIs premotoric to depressor and levator motoneurons are physiologically described during forward and backward stepping on a treadwheel, and it was analyzed if they are involved in the control of stepping velocity.

Nonspiking interneurons providing synaptic drive to depressor motoneurons
Intracellularly recorded NSIs providing excitatory synaptic drive to depressor MNs were classified into four groups, according to their membrane potential modulation during walking. They were named De2 to de4. Fig. 3.34 shows the physiology of NSI De2, which was recorded in five animals and provided excitatory synaptic drive to depressor MNs, as revealed by a clear downward movement of the leg due to positive current injection. In one of the De2 recordings, also an inhibition of levator MNs could be observed. During stance phase, De2 remained at resting membrane potential (average for all 5 animals: -44.9 ± 3.3 mV) or at a slightly depolarized level. Upon start of swing phase it rapidly hyperpolarized and slowly repolarized continuously to resting membrane potential until start of next stance (Fig. 3.31A, left side). During backward walking, the same pattern could be observed although here a small depolarization in the stance phase occurs more often than during forward walking. This can be clearly seen when aligning the membrane potential to the transition from stance to swing phase (Fig. 3.31B). The mean peak-to-peak amplitude for all 5 animals was 14 ± 1.8 mV in forward stepping and 17.4 mV, 12.4 mV in backward stepping (N=2). In another recorded De2, forward walking was elicited while hyperpolarizing current was injected (Fig. 3.31C). Here, at first a tonic depolarization of the NSI was revealed. But different to normal conditions, now the peak depolarization occurs before the start of stance, whereas the quick hyperpolarization at the start of swing phase remains but with a more rapid hyperpolarization. In the remainder of the swing phase and in the stance phase, the membrane potential stays on a similar level. De2 could be stained twice (neurobiotin/streptavidin-Cy3). In both stainings the morphology is very similar with the cell body located posteriorly and a primary neurite which processes first in anterior direction and than bends to the periphery with many small arborizations (Fig. 3.32). These stainings show a strong similarity to Li2 described by Hess and

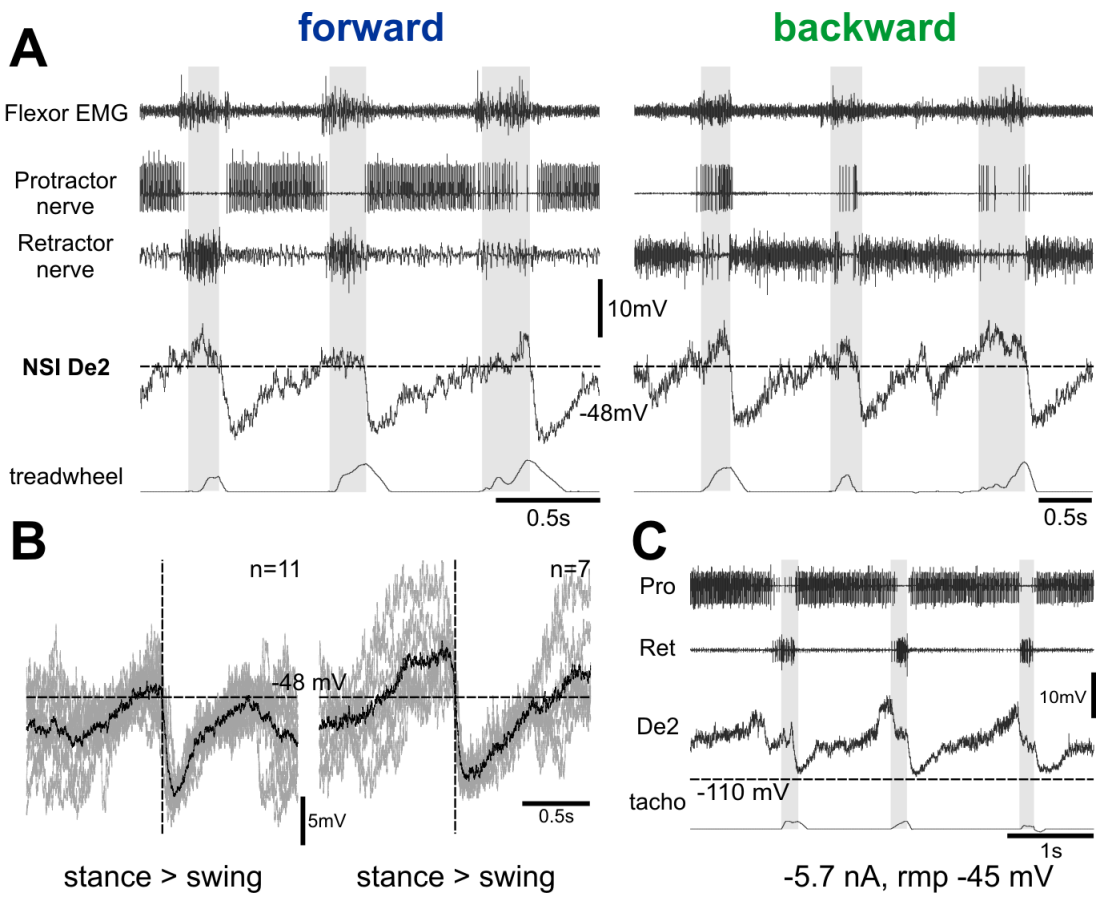

Figure 3.31 – Membrane potential modulation of NSI De2 during forward and backward walking. A: De2 stays at resting membrane potential (-48 mV) or slightly depolarized during stance phase, quickly hyperpolarizes at the begin of swing and slowly repolarizes till the start of stance. Treadwheel trace and flexor EMG activity mark stance phase (gray bars), protractor and retractor nerve recordings indicate walking direction. B: overdraws of the MP modulation for forward (left, n=11) and backward (right, n=7) stepping at the transition from stance to swing phase, RMP: -48 mV. C: activity of De2 during stepping whilst hyperpolarized (-5.7 nA). Note that in this case the peak potential occurs before the start of the stance phase.

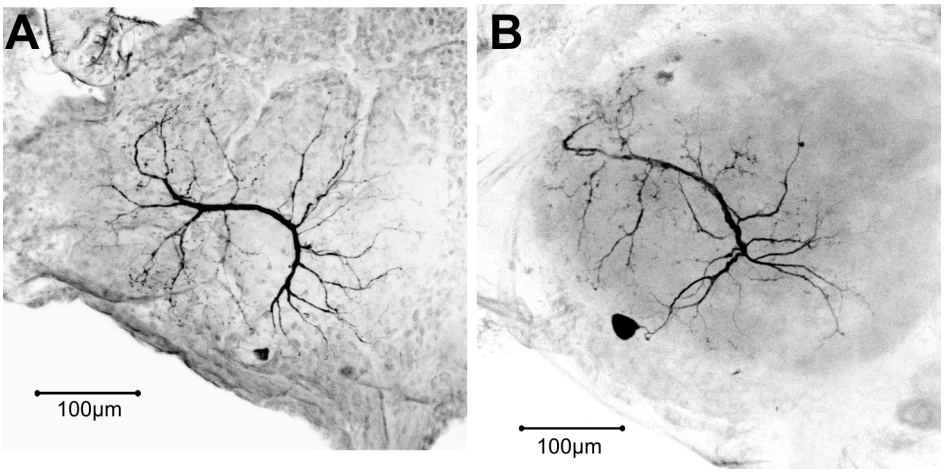

Figure 3.32 – Morphology of two neurobiotin stainings of NSI De2. Both neurons have a posteriorly located cell body, the main neurite processes from posterior to anterior and makes a prominent bend to the lateral margin of the ganglion.

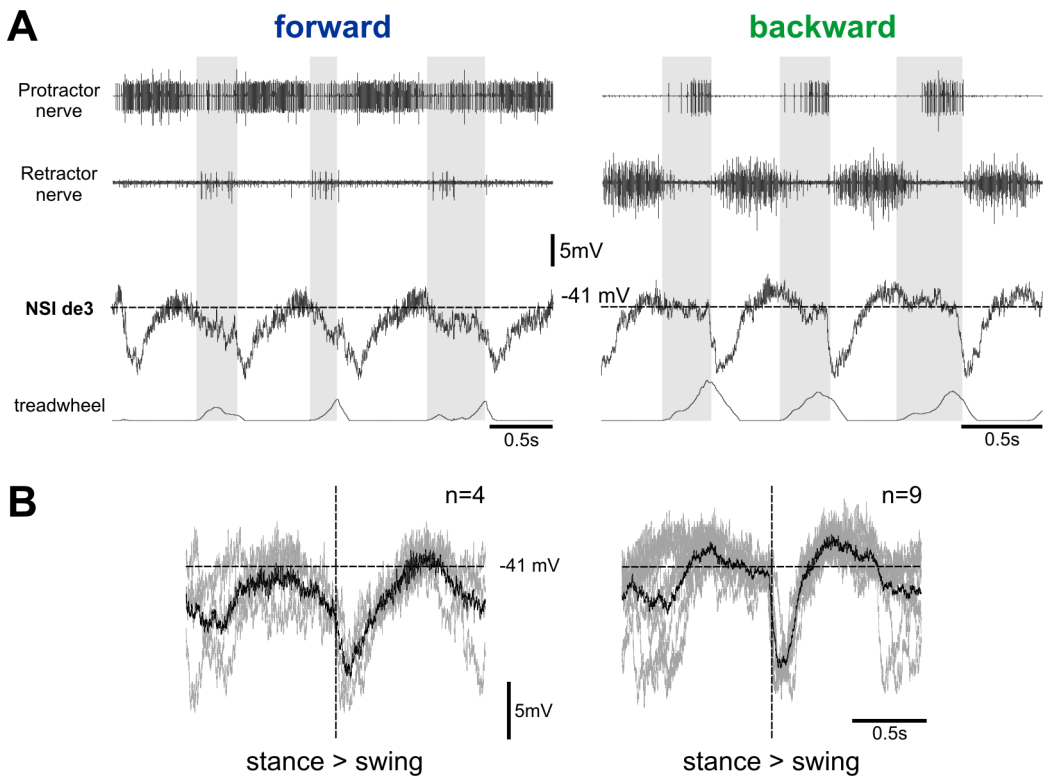

Figure 3.33 – Membrane potential modulation of NSI de3 during forward and backward stepping. A: intracellular recording of de3. Gray bars mark the stance phase, protractor and retractor nerve recordings indicate the walking direction. B: overdraws of the activity of de3 at the transition from stance to swing phase with single steps (gray) and the mean potential (black) during forward (n=4) and backward (n=9) stepping.

Büschges (1997), in which only inhibitory drive to levator MNs was described. Here, such an influence on levator MNs could only be shown in 1 of 5 recordings. A passive stimulation of the femoral chordotonal organ led to diverse responses in De2 (see Tab. 3.1). However, this still leaves the possibility that De2 and Li2 are the same interneurons.

The physiology of the second group of NSIs providing excitatory drive to depressor MNs, de3, is shown in Fig. 3.33 during walking. The peak amplitude of the membrane potential of this type of neuron occurs at the end of the swing phase. From there, the membrane potential slowly and continuously hyperpolarizes, throughout stance, to a peak hyperpolarization shortly after the onset of the next swing phase and than, similarly slowly and continuously, repolarizes until the end of swing. This is the case during forward and backward stepping. The average peak-to-peak amplitude during forward walking was 14.2 ± 1.8 mV (N=4) and during backward walking 13.7 ± 0.6 mV (N=3).

The third group of nonspiking interneurons displaying an excitatory influence to depressor neurons, de4, is shown in Fig. 3.34. de4 is depolarized shortly before

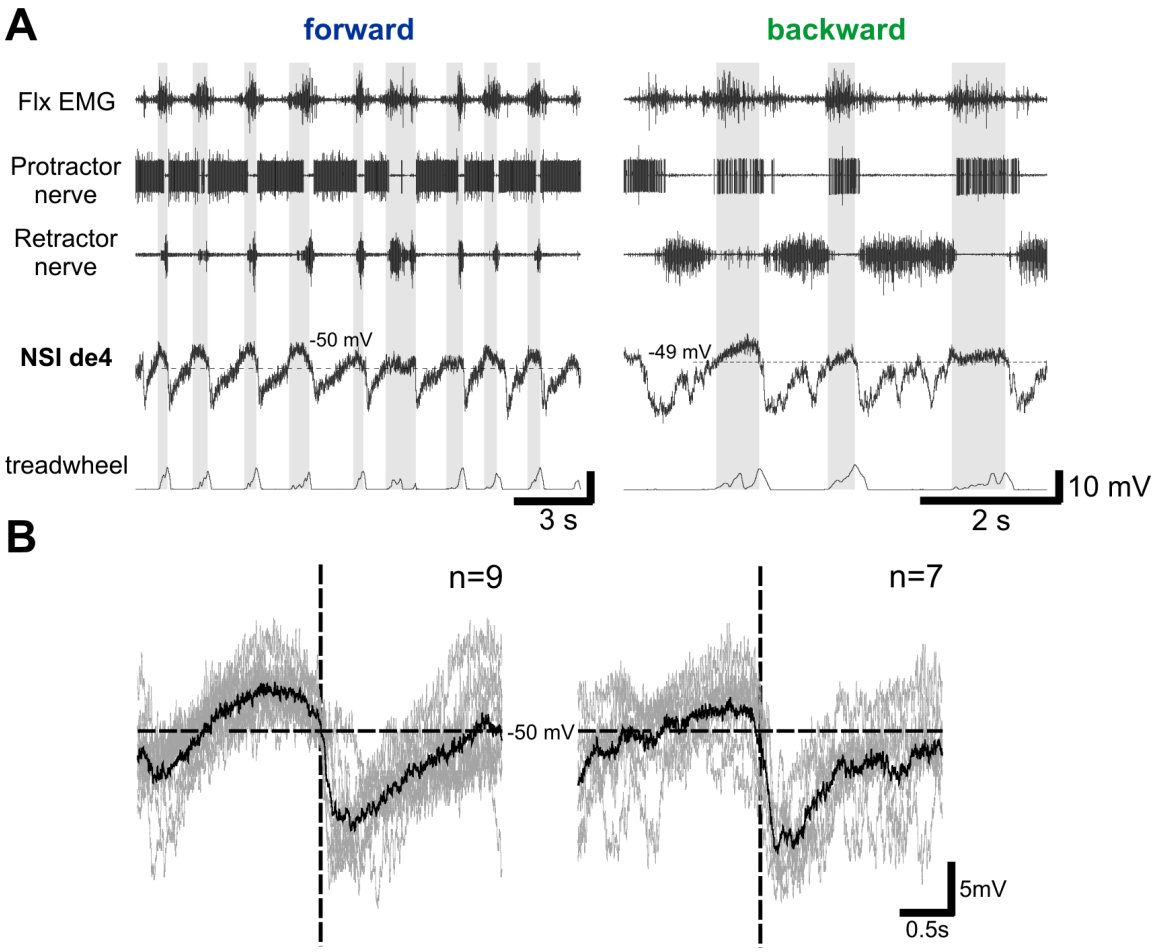

Figure 3.34 – Activity profile of NSI de4 during forward and backward walking. A: intracellular recording of NSI de4 during forward and backward walking, extracellular recordings indicate the walking direction (protractor and retractor nerve) and the stance phase (flexor EMG). Note the similar activity during both walking directions. B: overdraws of the membrane potential modulation during forward (n=9) and backward walking (n=7). Single steps are shown in gray, the averaged potential in black.

the beginning of stance phase. Compared to De2, this depolarization has a higher amplitude during stance. Similarly to De2, at the onset of swing a quick hyperpolarization occurs and de4 slowly repolarizes till the end of swing phase. The average peak-to-peak membrane potential modulation of de4 in the two recorded animals was 13.6 and 20 mV, which is in the same range as the average amplitude of De2.

Premotor interneurons providing excitatory synaptic drive to depressor MNs of the fourth group, de5, show the following modulation during forward and backward walking: the membrane potential is depolarized above resting potential at the end of swing phase and repolarizes to resting potential during stance. Upon the onset of swing, the potential quickly hyperpolarizes and is than quickly depolarized again. This pattern looks somewhat similar to the pattern shown for hyperpolarized De2

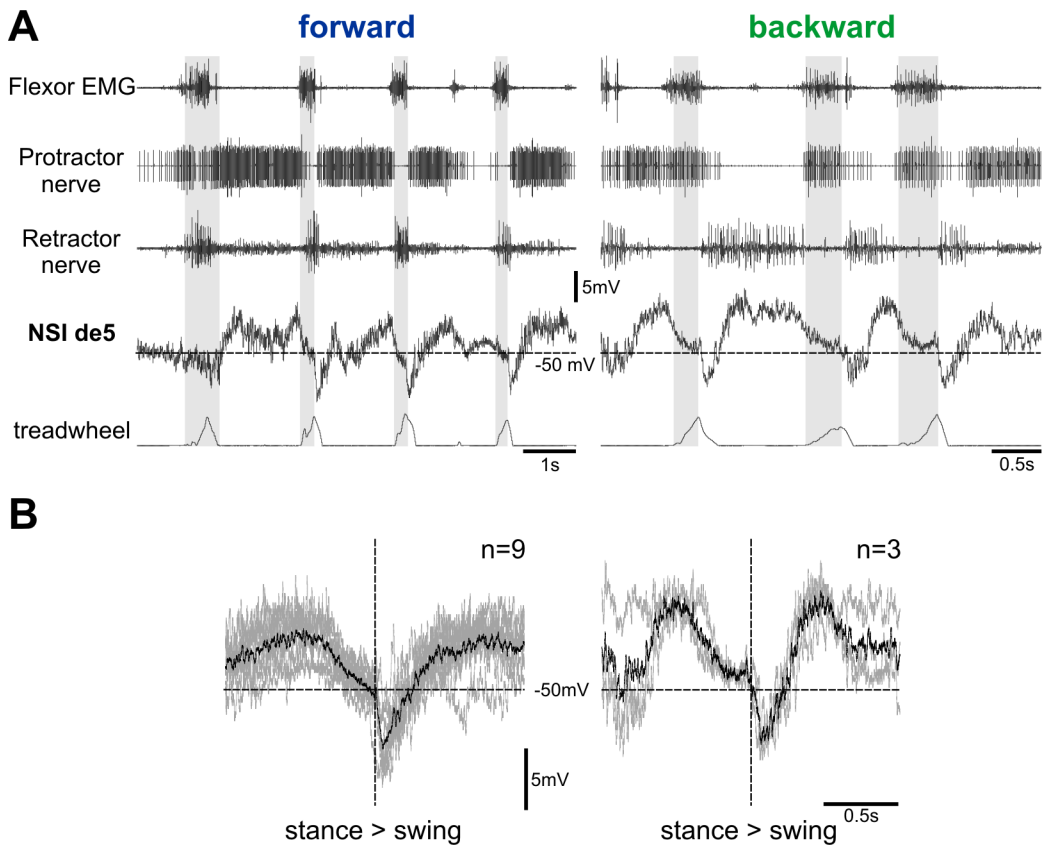

Figure 3.35 – Membrane potential modulation of NSI de5 during forward and backward stepping. A: example of two stepping sequences with an intracellular recording of de5. Note the same activity during forward and backward walking. B: overdraws of the membrane potential modulation during forward (N=9) and backward stepping (n=3) with single modulations in gray and the averaged MP modulation in black. RMP: -50 mV.

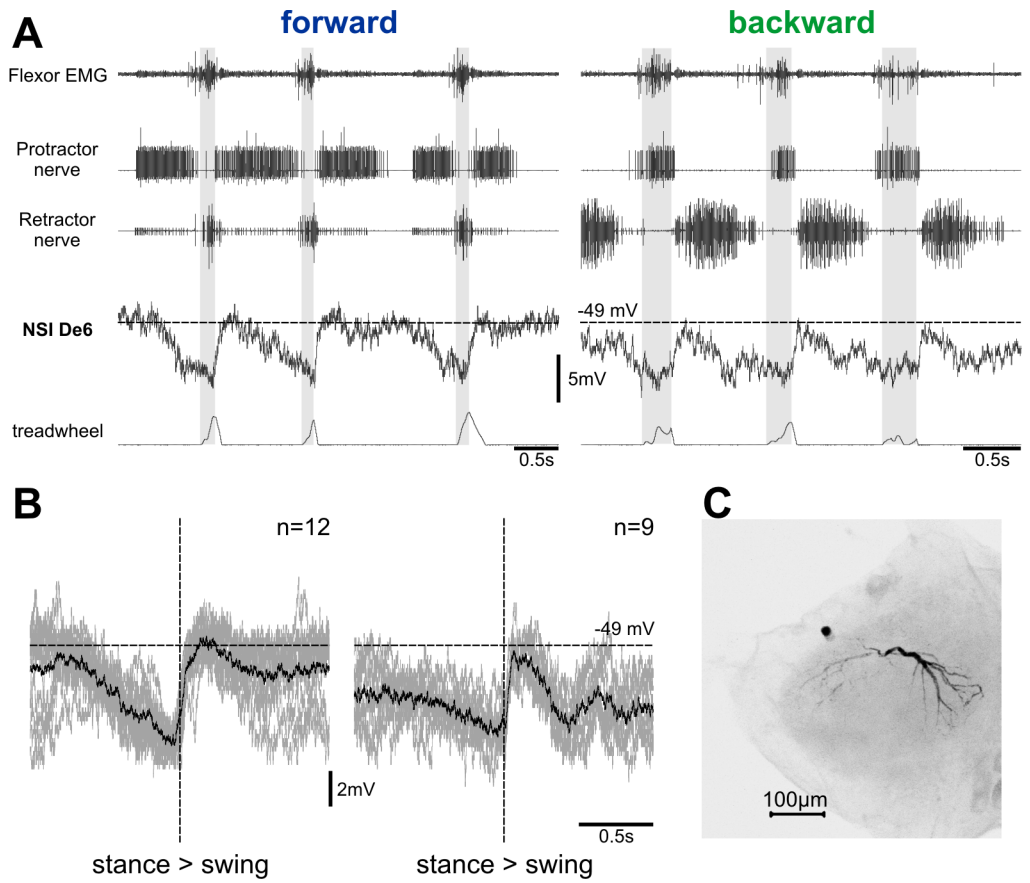

Figure 3.36 – Intracellular recording of NSI De6. A: during forward and backward walking, NSI De6 is at RMP at the start of swing phase and slowly hyperpolarizes until the end of stance. B: overdraws of single steps emphasize the course of the membrane potential modulation at the transition from stance to swing phase. C: morphology of De6. The cell body is located anteriorly lateral.

NSIs during forward walking (Fig. 3.31C). de5 was recorded twice.

For NSIs controlling the FT-joint, it has been shown that the sign of polarization during one phase of the step cycle does not necessarily correlate to the synaptic drive exerted by this neuron (e.g. NSI E6, cf. von Uckermann and Büschges, 2009). In this study, three single recordings from physiologically different neurons providing excitatory synaptic drive to depressor MNs were made, which are active during swing. One example is given in Fig. 3.36. This neuron, labeled De6, is hyperpolarized during stance phase and rapidly depolarizes to the resting membrane potential at the onset of swing phase. During the first half of swing it stays at the resting level and than slowly hyperpolarizes to a minimum membrane potential during the stance phase. This neuron was also stained, its cell body is located at the anterior-lateral margin of the hemiganglion ipsilateral to the walking leg. Neurites arborize extensively in the anterior half of the hemiganglion (Fig. 3.36C).

Since the depressor is a stance phase muscle, it is also interesting to look if NSIs providing excitatory synaptic drive to depressor MNs have an influence on stepping

velocity. Thus, peak and trough potentials, and the overall peak-to-peak amplitudes of De2, de3, de4 and de5 were plotted against the mean belt velocity for each step. This is shown in Fig. 3.37. Like in the previous figures, significant correlations are marked by a red regression line and asterisks next to them. Only sporadically, significant correlations between the membrane potential of depressor NSIs and the mean belt velocity were found. Recordings of de3 showed in 2 of 4 cases a significant correlation between peak potentials and peak-to-peak amplitudes to the stepping velocity during forward walking. Only one significant correlation of the trough potential with belt velocity was found in backward stepping. In de5, in one of three animals, peak and peak-to-peak potentials were significantly correlated to the mean belt velocity in forward stepping. In De2 in one animal (n=3), peak potentials were significantly correlated to mean belt velocity. In de4 no significant correlations could be found. Also for NSI De6, no significant correlations of peak, trough and peak-to-peak membrane potential amplitudes could be found (not shown). Thus, there does not seem to be a systematic influence of depressor NSI activity on the stepping velocity.

Nonspiking interneurons providing synaptic drive to levator motoneurons In this section, recorded nonspiking interneurons which had excitatory influence on levator MNs are described. They were divided into four groups due to their physiology during walking. Fig. 3.38 shows the membrane potential modulation during walking of the first type, le5 (N=3). The membrane potential of le5 is at resting level during stance phase, rapidly depolarizes at the start of swing and slowly repolarizes to resting potential until start of next stance, both during forward and backward stepping. The average membrane potential peak-to-peak amplitude was 12.1 $\pm$ 4.4 mV during forward walking (N=3), and 11.6mV during backward walking (N=1, see Tab. 3.1).

NSI le6 was recorded twice, no coordinating backward stepping sequences could be elicited. The physiology of le6 is shown in Fig. 3.39A and B. Like le5, le6 is quickly depolarized at the onset of swing, but at a more hyperpolarized membrane potential during stance. A slow repolarization of the membrane potential to resting potential stops at mid-swing, than le6 depolarizes again, not as high as before, until the end of swing. Than it is quickly hyperpolarized at the swing-stance phase transition.

The membrane potential of Le7 during forward walking looks similar to that of le5, except that the membrane potential is more negative. During stance phase, Le7 is hyperpolarized and than quickly depolarizes to resting potential at the start of swing. Then it slowly repolarizes to the stance phase potential (Fig. 3.39C and

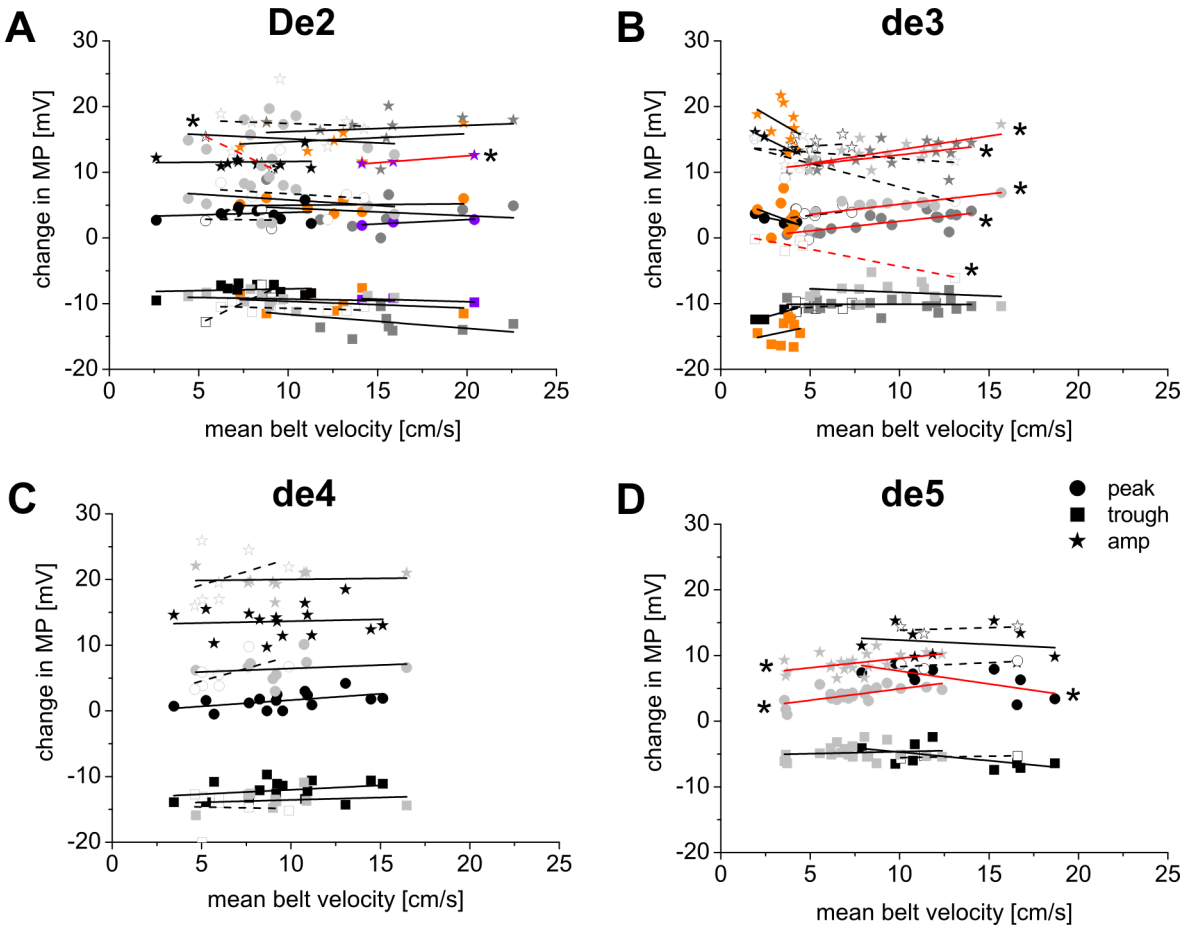

Figure 3.37 – Velocity dependency of depressor NSIs. A: correlation of NSI De2 peak, trough and peak-to-peak potentials during forward and backward stepping to mean belt velocity (fwd N=5, n=40; bwd N=2, n=10). In one experiment, the peak-to-peak amplitude was significantly correlated to mean belt velocity, in another experiment it was significantly negative correlated. B: de3 peak and peak-to-peak potentials from 2 of 4 animals forward stepping sequences are significantly correlated to the mean belt velocity. In one case trough potentials during backward walking show a significant negative correlation (fwd N=4, n=41; bwd N=3, n=18). C: for de4, no significant correlation between activity and belt velocity was found (fwd N=2, n=24; bwd N=1, n=7). D: de5 activity vs. mean belt velocity. In one animal forward peak potentials are significantly negative and a in second animal peak and peak-to-peak potentials are significantly positive correlated (fwd N=2, n=30; bwd N=1, n=3). Circles mark peak potentials, squares trough potentials, stars peak-to-peak MP amplitude during a step. Filled symbols and continuous regression lines denote forward, open symbols and dashed regression lines denote backward stepping. Red regression lines mark significance ($p<0.05$, ANOVA).

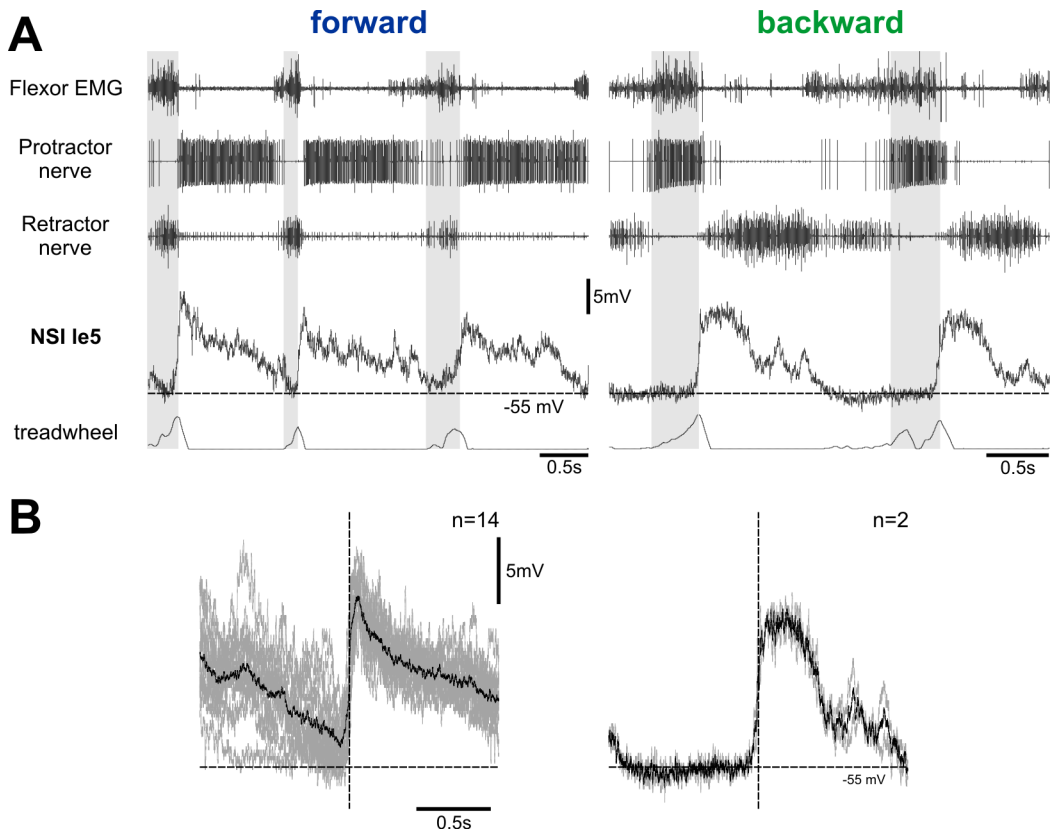

Figure 3.38 – Membrane potential modulation of NSI le5 during forward and backward walking. A: intracellular recording of le5 and extracellular traces of the flexor muscle (stance phase) and protractor and retractor nerves (indicating the walking direction). During both walking directions, le5 is quickly depolarized above RMP at the beginning of swing phase and slowly repolarizes until the onset of next stance. B: overdraws of the le5 membrane potential at the transition from stance to swing phase for single steps (gray) and the average potential (black). Forward n=14, backward n=2.

D). Le7 was successfully stained, the morphology is shown in Fig. 3.39E. The cell body is posterior and the main neurite processes in anterior direction and arborizes extensively in all directions.

The last type of NSIs, providing excitatory synaptic drive to levator MNS, is le8. It was recorded once and is shown because of its interesting physiology during forward and backward walking (Fig. 3.40). During forward walking le8 is depolarized during swing and stays at resting potential during the stance phase. This is true also during backward walking but, however, the amplitude of the depolarization is twice as high. This is emphasized in the overdrawn membrane potential modulations of single steps one second before and after the transition from stance to swing phase in Fig. 3.40C. The peak-to-peak amplitude of the averaged membrane potential modulation is 6.8 mV during forward walking and 11.8 mV during backward walking.

Thus, all recorded premotor nonspiking interneurons that have an excitatory in-

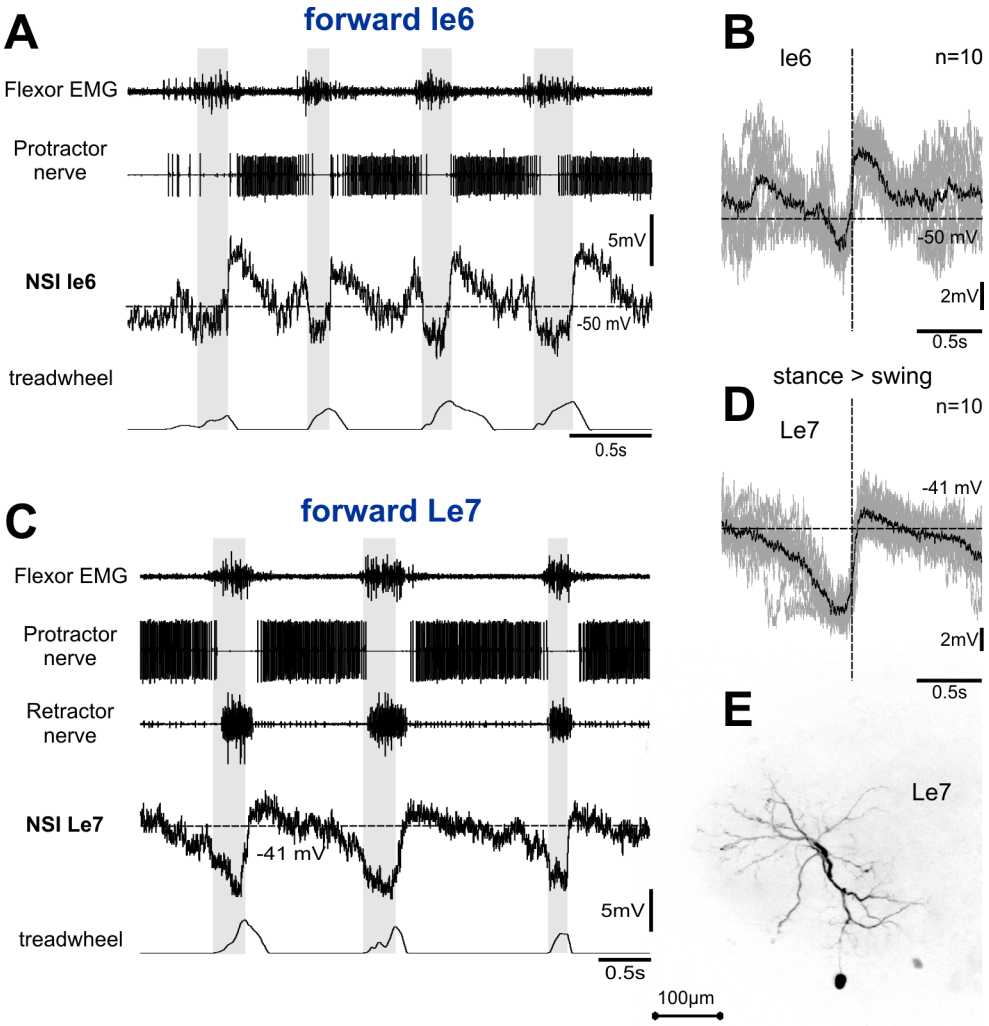

Figure 3.39 – Physiology of le6 and Le7 during forward stepping. A: NSI le6 is quickly depolarized at the start of the swing phase, repolarizes to RMP till mid-swing and is again depolarized until end of swing and then hyperpolarizes during stance. B: overdraws from 10 single steps (gray traces) and the averaged potential (black trace). C: NSI Le7 is at RMP or slightly depolarized at swing onset. It hyperpolarizes slightly until stance onset upon which it is quickly further hyperpolarized. At the stance-swing transition the MP rapidly repolarizes. D: overdraws of the membrane potential during forward stepping. E: morphology of Le7. The cell body is located at the posterior median margin ipsilaterally to the walking leg. The main neurite processes anteriorly and arborizes extensively in the hemiganglion.

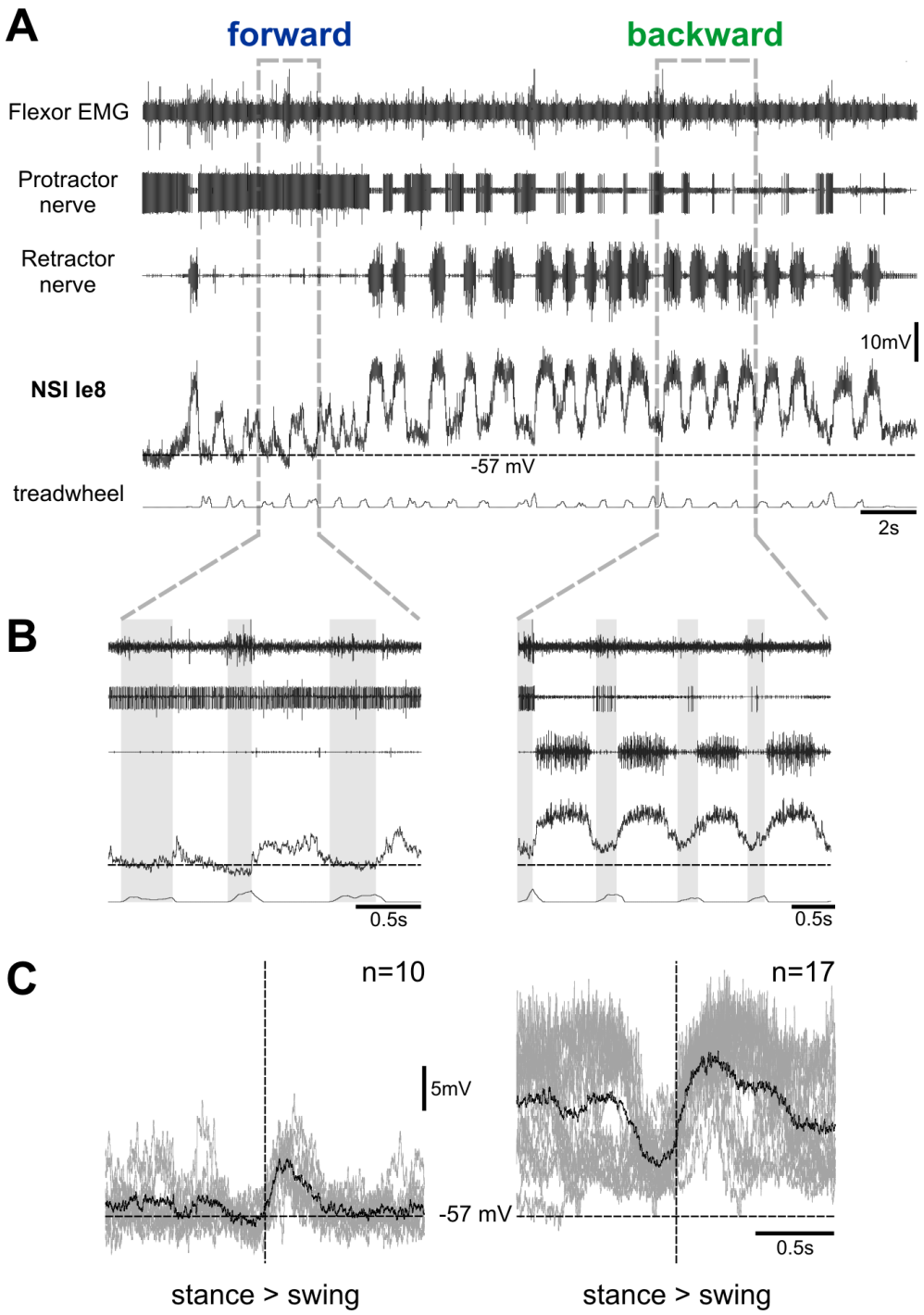

Figure 3.40 – Membrane potential modulation of NSI le8. A: intracellular recording of le8 during a long stepping sequence with forward directed steps in the first half of the recording and backward directed steps in the second half. B: extended views of the forward and backward stepping sequence. Note the two fold higher depolarization of the le8 MP during backward stepping. C: overdraws of single steps illustrate the stronger activation of le8 during backward walking.

fluence on levator motoneurons are active during the swing phase of the step cycle, both during forward and backward walking. One recorded NSI of this population, NSI le8, shows a difference in the depolarization amplitude during swing between the two walking directions. The one available staining of a levator NSI shows no resemblance with the only staining from Hess and Büschges (1997) for these types of NSIs.

Although the responses of the levator NSIs to the passive fCO-stimulation weren't used for NSI grouping, they will be stated here. All three le5 NSIs and le8 showed depolarizing responses both to elongation and relaxation. In one le6 this wasn't tested, the other le6 and Le7 showed ambiguous responses to elongation and a depolarizing response to relaxation of the fCO.

3.3.3 Nonspiking interneurons influencing the femur-tibia joint

Premotor nonspiking interneurons involved in the control of the femur-tibia leg joint movement are well investigated (Büschges, 1990; Driesang and Büschges, 1993; von Uckermann and Büschges, 2009). In a recent study by von Uckermann and Büschges (2009), NSIs from this population were recorded during single-leg forward stepping on a treadwheel and the membrane potential oscillations that occurred during walking were described. Here, some of those NSIs were recorded during forward as well as during backward walking, and the activity during those two walking directions was compared.

Nonspiking interneurons providing synaptic drive to flexor motoneurons Two previously described types of nonspiking interneurons, I1 (N=1) and I2 (N=2), were recorded and identified according to their established responses to fCO stimulation, their morphology (Büschges, 1990), and their membrane potential modulation during forward stepping on a treadwheel (von Uckermann and Büschges, 2009). Here, only an excitatory influence on flexor MNs could be stated. As extensor activity was not recorded, an influence on extensor MNs could not be shown.

The physiology during forward and backward stepping of NSI I1 (Büschges, 1990) is shown in Fig. 3.41A and B. During both walking directions, the membrane potential is at resting level (-48 mV) during stance phase and hyperpolarized (forward: -15.7 ± 0.8 mV, backward: 16.6 ± 1.5 mV) during swing phase to a constant level. The changes in membrane potential at the transitions from stance to swing and from swing to stance phase are very quick. In the study of von Uckermann and Büschges (2009), the modulation of the membrane potential had the same shape, but showed a stronger depolarization during stance and less hyperpolarization during swing. This difference is probably due to the lower resting membrane potential (-60 mV) in the study of von Uckermann and Büschges (2009). As described before (Büschges, 1990), also here the response to a passive fCO-stimulation was hyperpolarizing to an elongation stimulus and depolarizing to a relaxation. Furthermore, with the help of the neurobiotin-staining, this neuron could be identified as NSI I1 (Fig. 3.41C).

NSI I2 (Büschges, 1990) was recorded twice. One example of its physiology during forward and backward walking is shown in Fig. 3.42A and B. During forward walking the membrane potential was modulated around the resting membrane potential showing a depolarization during stance phase and an hyperpolarization in swing phase (peak-to-peak amplitude: 19.9 ± 8.5 mV). During backward walking the shape of the modulation stays the same but the membrane potential is shifted

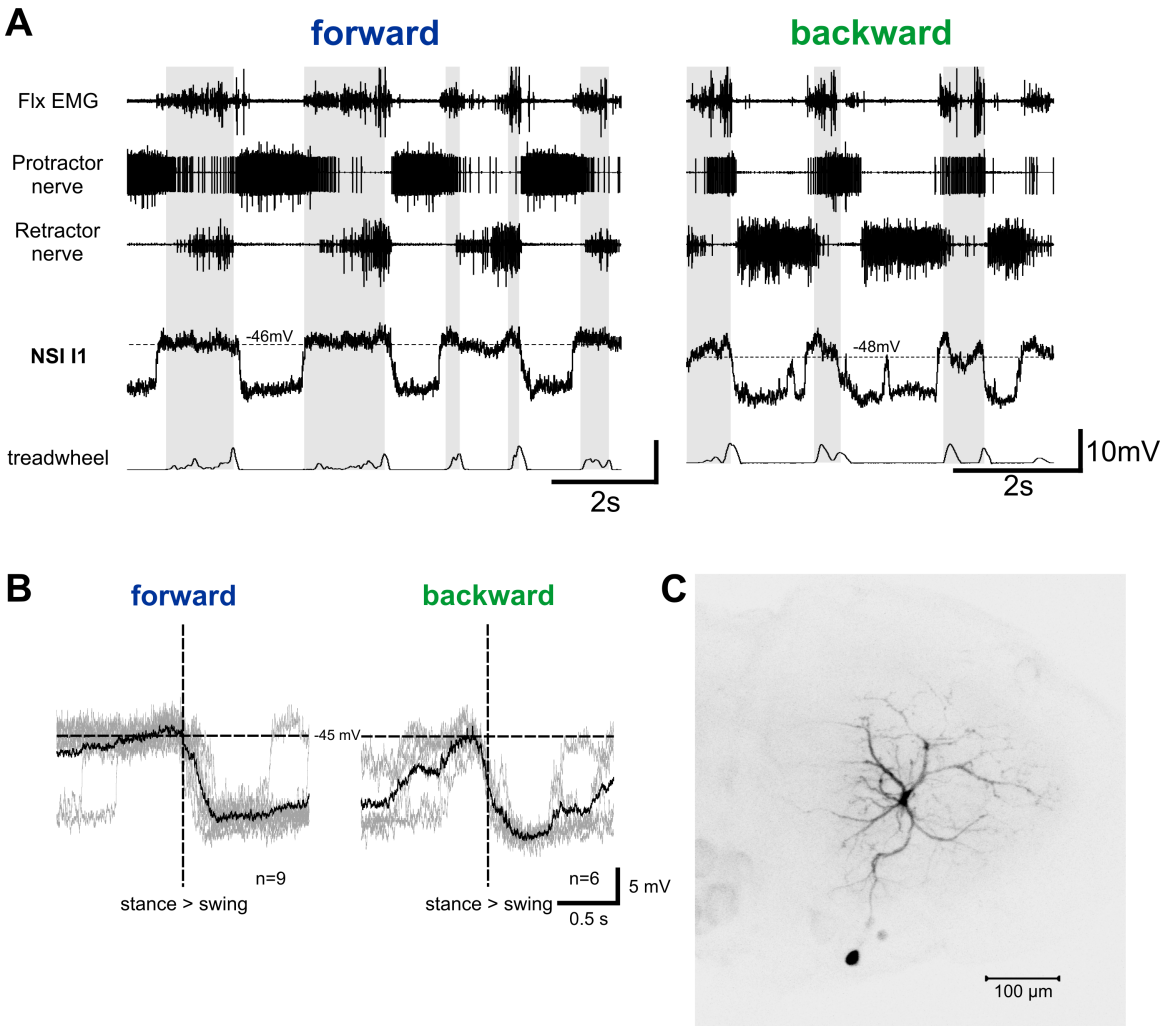

Figure 3.41 – Physiology and morphology of NSI I1. A: membrane potential modulation of I1 during forward and backward stepping. In both cases, I1 is at RMP during stance phase and quickly hyperpolarized at the start of swing and stays at this level during the complete swing phase. Shortly before the onset of stance, I1 is quickly depolarized to RMP. B: activity of I1 at the transition from stance to swing phase with aligned MPs during single steps (gray) and the averaged MP (black trace). C: morphology of I1 as revealed by a neurobiotin/streptavidin-Cy3 staining. The cell body is located posterior.

upwards so that only a depolarization during stance is apparent. During swing, the membrane potential stays at resting level or is only slightly depolarized (peak-peak 18.8 ± 1.7 mV). Because backward stepping could only be elicited in one of two I2 recordings, the difference between forward and backward walking could not be confirmed. The morphology of the recorded NSI is shown in Fig. 3.42C.

I1 and I2 are active during stance phase, hence a correlation to the stepping velocity might be the case (see Gabriel and Büschges, 2007 and sec. 3.2.2). Such a correlation was already shown for forward walking animals by von Uckermann and Büschges (2009) for I1 and I2 (and E1). A comparison of the peak and trough potentials and peak-to-trough amplitudes of I1 and I2 to the mean belt velocity is

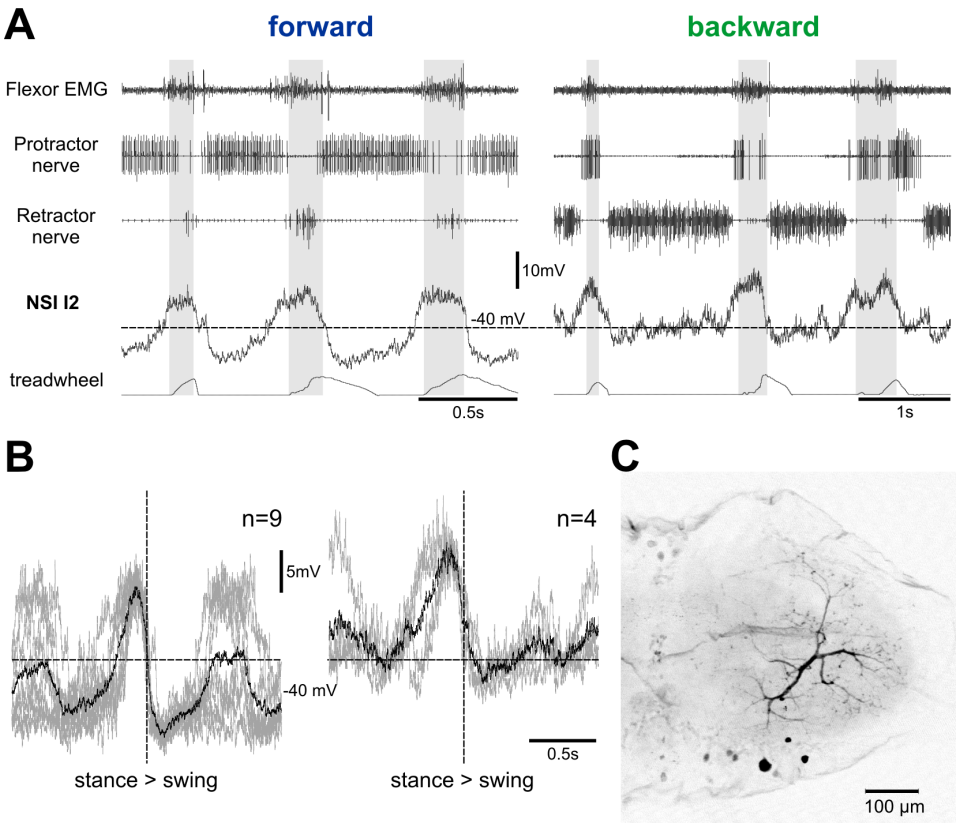

Figure 3.42 – Membrane potential modulation of NSI I2 during forward and backward walking. A: during both walking directions, I2 is depolarized during stance and hyperpolarized during swing. During backward walking, the hyperpolarization is only slightly below RMP. B: overdraws of the MP at the stance-swing transition emphasize that. C: identification of I2 via morphology, cell body posterior.

shown in Fig. 3.43. A significant correlation of the peak potential and the overall amplitude could only be shown for the backward stepping sequence of I1, ($p<0.05$, ANOVA). For I2 no such correlation was found.

Nonspiking interneurons providing synaptic drive to extensor motoneurons

NSIs premotoric to extensor MNs were also identified due to their known physiological and morphological properties. Here, they are described during forward and backward stepping. Firstly, the membrane potential modulation of identified NSI E3 (Büschges, 1990) will be described during walking. In Fig. 3.44A, the physiology during forward and backward stepping is shown. At the onset of swing, E3 is rapidly depolarized and then slowly repolarizes till the start of stance. In this example, also smaller depolarizations of the membrane potential during the stance phase or later in the swing phase are visible, most notably in the backward walking sequence. This is probably due to unmonitored movements of the leg. The overdrawn membrane potential modulations of E3 during single steps (Fig. 3.44D) clarify the same activity of E3 during both walking directions. When hyperpo-

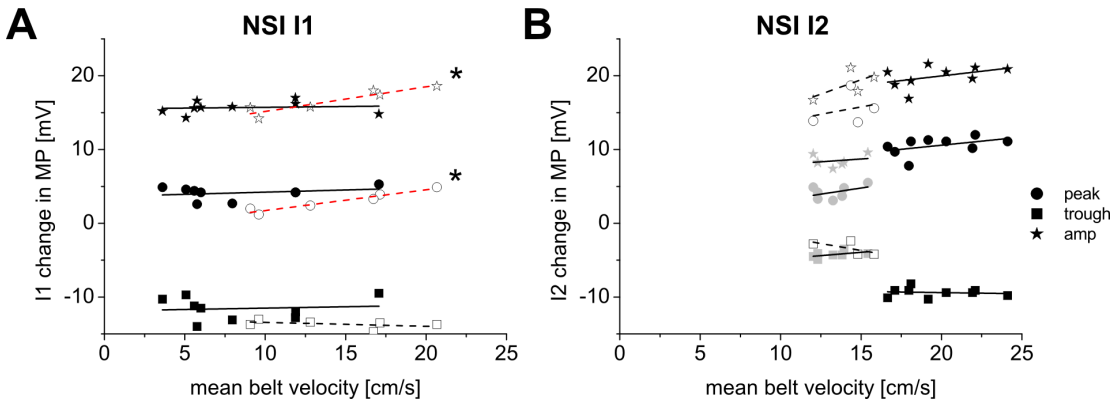

Figure 3.43 – Velocity dependency of NSI I1 and I2 activity. A: peak potentials, trough potentials and overall amplitude change of NSI I1 subtracted from RMP, plotted vs. mean belt velocity during forward and backward walking. Peak potentials and overall amplitude during backward walking are significantly correlated with stepping velocity (fwd+bwd N=1, fwd n=9, bwd n=6). B: peak, trough and peak-to-peak potentials of NSI I2 plotted vs. mean belt velocity. No significant correlations were found (fwd N=2, n=16; bwd N=1, n=4). Circles mark peak potentials, squares trough potentials, stars peak-to-peak MP amplitude during a step. Filled symbols and continuous regression lines denote forward, open symbols and dashed regression lines denote backward stepping. Red regression lines mark significance ($p < 0.05$, ANOVA).

larizing current (-3.9 nA) was injected into E3 and walking elicited, a clear tonic depolarization during the complete forward and backward stepping sequences was revealed (due to the changed electric driving force of the involved ions, see above). On top of this tonic depolarization, phasic depolarizations in swing with an increased amplitude are apparent (Fig. 3.44B). Holding E3 on a more depolarized level (+4 nA injected current) during walking revealed a hyperpolarizing input during the stance phase in both walking directions (Fig. 3.44C).

Another identified NSI, which provides excitatory drive to extensor motoneurons, is E5 (Büschges, 1990). The response to fCO-stimulation for E5 and E6 is very similar, depolarizing both to fCO elongation and relaxation. However, E5 and E6 have different morphologies, and von Uckermann and Büschges (2009) showed that E5 is depolarized in the swing phase and E6 in stance phase during single leg stepping on a treadwheel. Thus, the nonspiking neuron depicted in Fig. 3.45 could be identified as E5 (including a staining, not shown). Like E3, E5 is rapidly depolarized at the start of swing and repolarizes until stance onset. Furthermore, a small tonic depolarization during stepping is visible.

The third recorded type of NSI providing excitatory synaptic drive to extensor MNs is E7. It was firstly described by Sauer et al. (1996) and during walking by von Uckermann and Büschges (2009). E7 shows a hyperpolarizing response to fCO elongation and a depolarization response upon fCO relaxation. The membrane

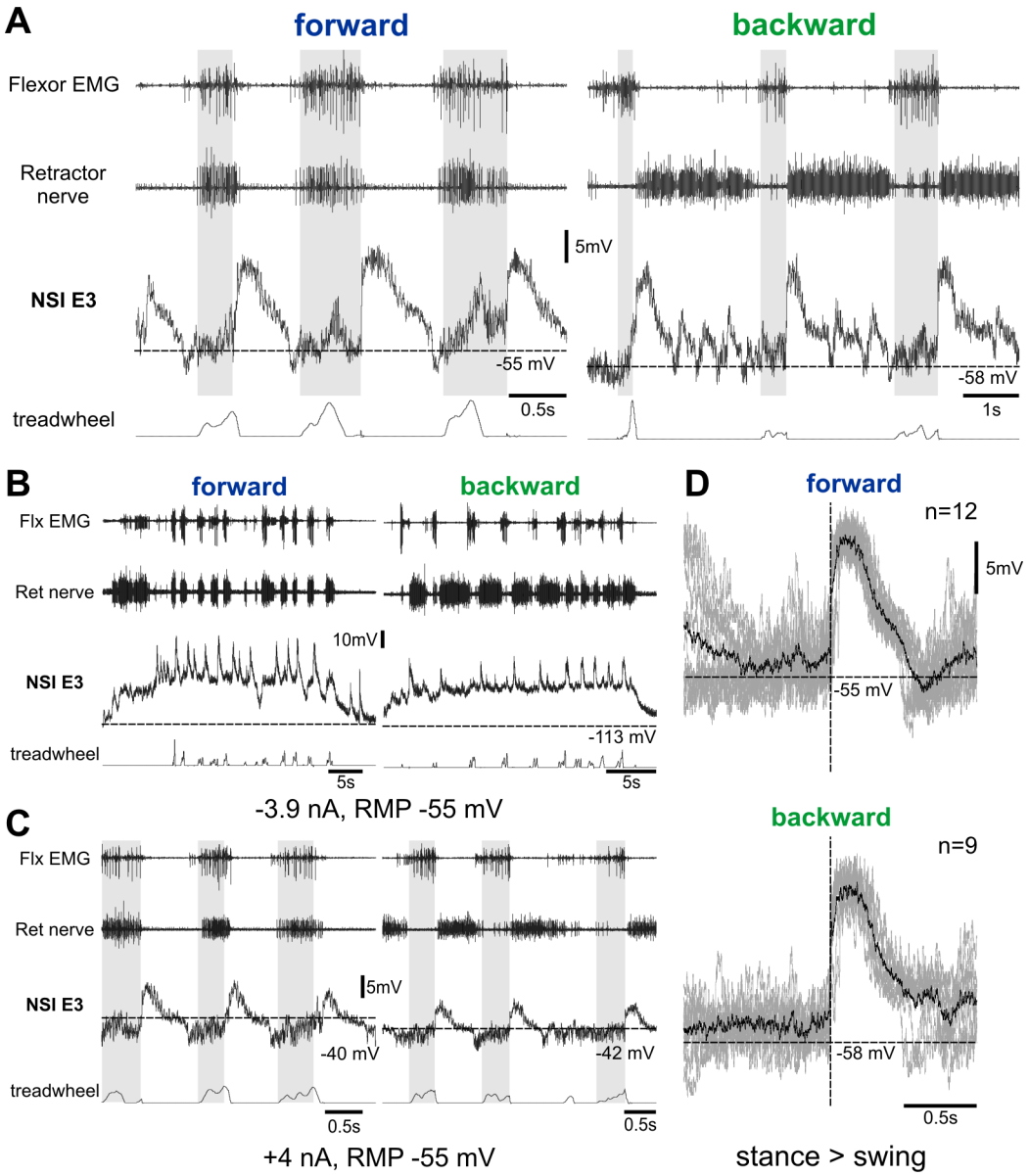

Figure 3.44 – Membrane potential modulation of NSI E3 during forward and backward walking. A: intracellular recording of E3 during forward and backward stepping. Note the unchanged activity during backward walking. B: intracellular recording of E3 while hyperpolarizing current (-3.9 nA) was injected. A tonic depolarization throughout the stepping sequences with phasic depolarizing inputs in swing becomes apparent during forward and backward walking. C: injecting depolarizing current (+4 nA) into E3 during walking shows a hyperpolarization of the MP during the stance phase. D: overdraws of the activity of E3 at the transition from stance to swing phase during forward (n=12) and backward stepping (n=9).

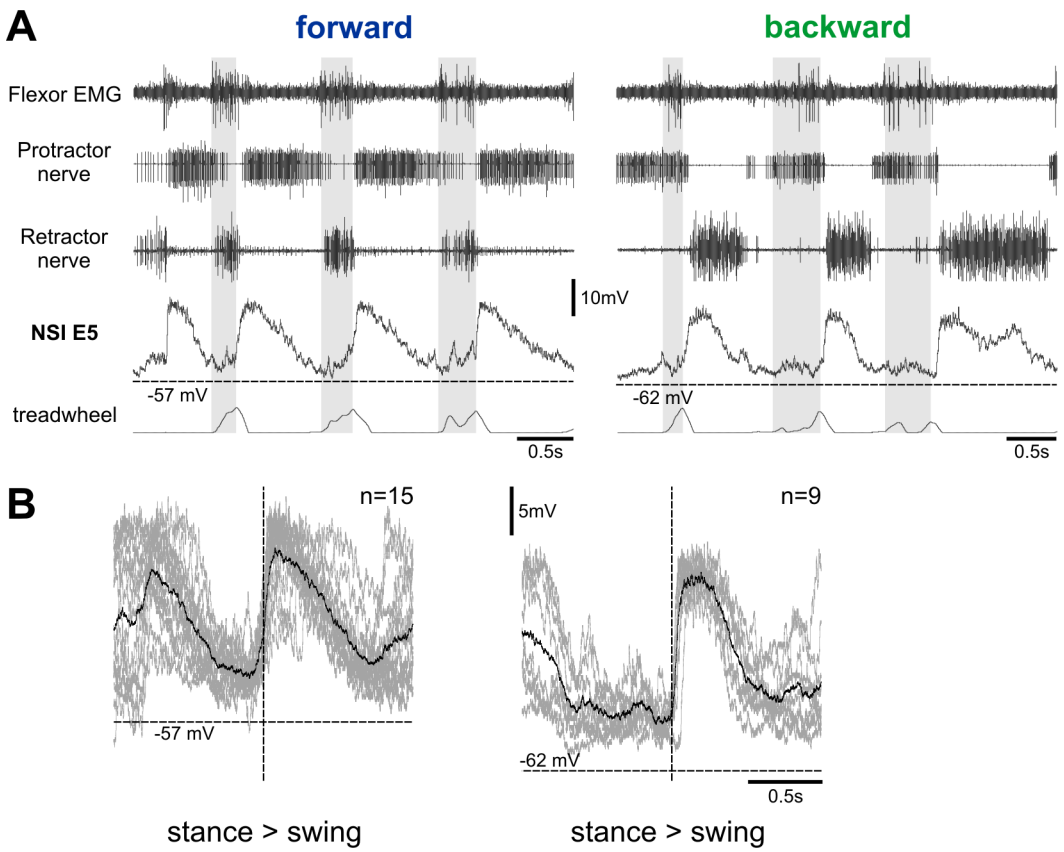

Figure 3.45 – Activity of NSI E5. A: intracellular recording of NSI E5 during forward and backward walking. During both walking directions, E5 is quickly depolarized at the onset of swing and slowly repolarizes to RMP (-62 mV) until stance onset. B: membrane potential modulation of E5 during single steps, aligned at the transition from stance to swing during forward (n=15) and backward (n=9) stepping.

potential modulation during forward and backward stepping is shown in Fig. 3.46A and B, the morphology in Fig. 3.46C. E7 remains at resting potential during stance and is hyperpolarized during swing in forward stepping. Unexpectedly for an NSI providing excitatory drive to extensor MNs, its phase of activity during backward stepping is reversed. Here, the membrane potential is slightly depolarized and many EPSP's are visible during swing. During stance, E7 is hyperpolarized. This is pointed out in the overdraws of membrane potential modulations for single steps (Fig. 3.46B).

3.3.4 Nonspiking interneurons influencing multiple leg joints

All recorded local nonspiking interneurons shown in this work so far either influence one or two MN pools of the same leg joint. However, previously described NSIs E4 and I4 influence MNs of more than one leg joint. E4 provides excitatory synaptic drive to extensor, levator, protractor MNs and CI1, and inhibitory drive

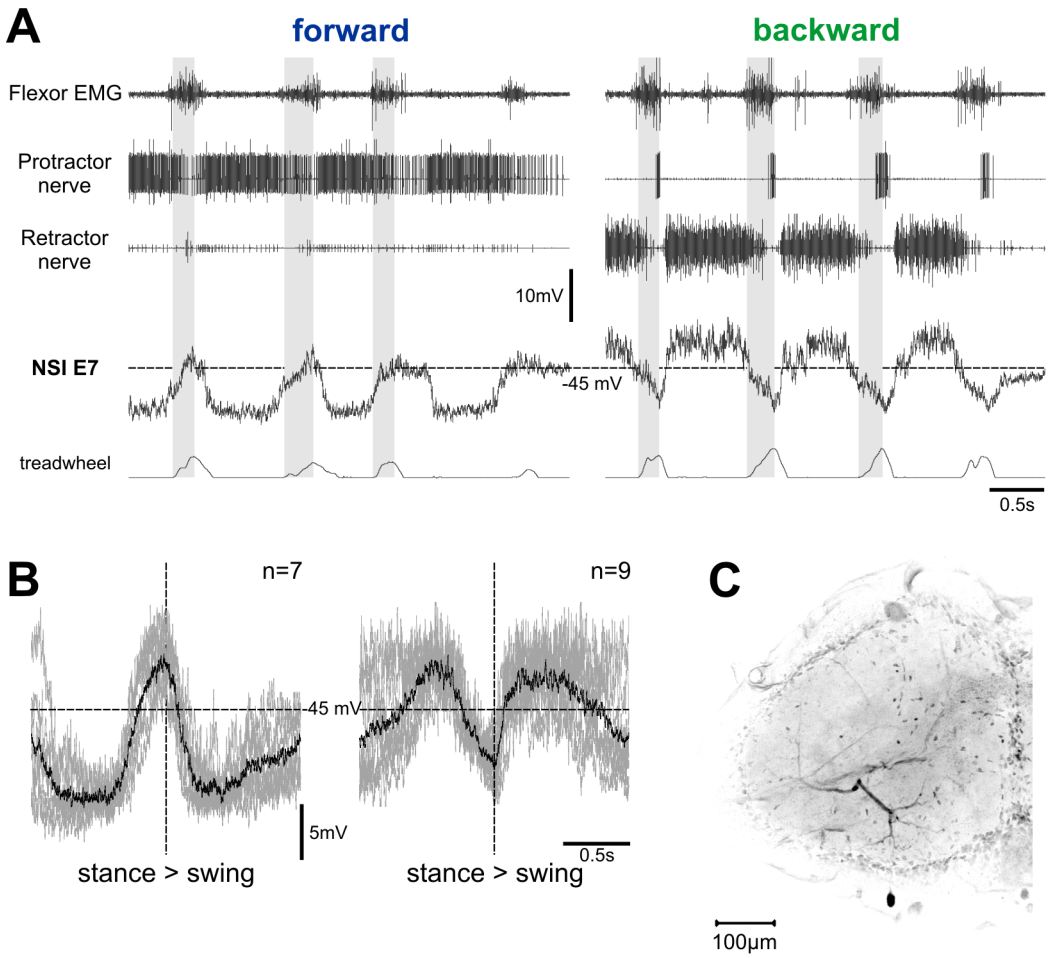

Figure 3.46 – Membrane potential modulation of NSI E7. A: intracellular recording of NSI E7 during forward and backward walking. During forward walking, E7 is at RMP or slightly depolarized in stance and hyperpolarized at the same level throughout swing. Conversely, during backward stepping E7 is depolarized (note the high amplitude EPSP's) during swing and hyperpolarized during stance. B: in the overdraws, the different phase of E7 activity is emphasized. C: morphology of E7, cell body posterior.

to depressor and retractor MNs. E4 is also thought to be part of the central pattern generating network of the leg joints (Büschges, 1990; Büschges et al., 1994; Büschges, 1995). Conversely, NSI I4 provides excitatory drive to flexor, depressor and common inhibitor1 MNs and inhibitory drive to extensor MNs (Sauer et al., 1996). Interestingly, the morphology of NSIs E4 and I4 is very similar (Büschges, 1990; Sauer et al., 1996).

In Fig. 3.47A, one of two intracellular recordings of NSI E4 is shown during forward and backward stepping. During both walking directions, E4 is rapidly depolarized at the onset of swing and slowly repolarizes until the start of stance, where the membrane potential stays at resting level. This is interesting, because, as stated earlier, E4 also provides excitatory drive to protractor MNs, which change their phase of activity during backward walking. The implications for conceivable net-

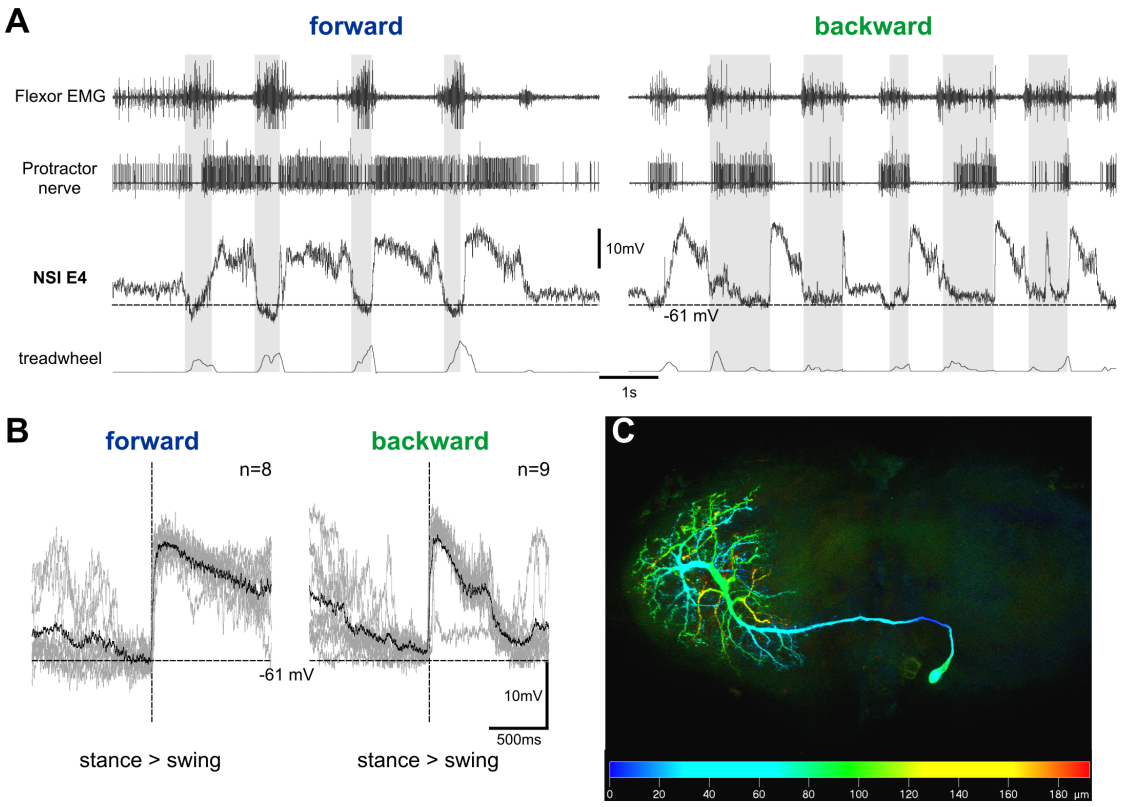

Figure 3.47 – Membrane potential modulation and morphology of NSI E4. A: E4 is depolarized during swing in forward and backward stepping. The MP remains at resting level during stance. B: overdraws of the MP at the transition from stance to swing phase for single steps during forward (n=8) and backward stepping (n=9). C: neurobiotin staining of E4 in a depth coded projection. Blue dorsal - red ventral. The cell body is located posterior in the hemiganglion contralateral to the recording site.

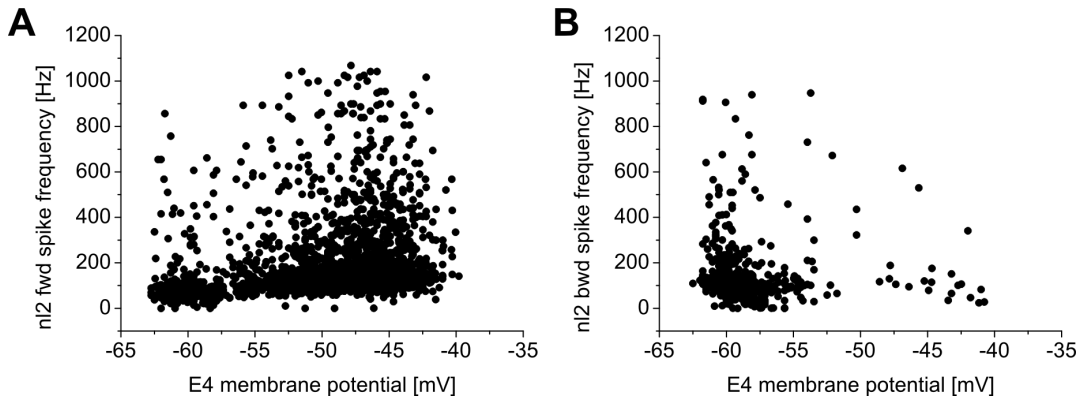

Figure 3.48 – Correlation between the membrane potential of E4 and protractor MN activity during walking. A: correlation of E4 membrane potential with protractor activity during forward walking (n=8). B: during backward walking (n=9). The instantaneous spike frequency of nl2 activity was determined and plotted against the E4 MP.

work connections will be followed up in the discussion. The morphology allows an unambiguous identification as E4. The cell body is located posterior in the hemiganglion contralateral to the recording site and the prominent primary neurite processes to the ipsilateral hemiganglion where it extensively ramifies (Fig. 3.47C). It was shown previously that the membrane potential of E4 during walking was barely correlated to the activity of protractor MNs (Büschges et al., 1994). Here, such a comparison also showed no strong correlation between E4 and protractor MN activity (Fig. 3.48).

Another neuron which provides excitatory synaptic drive to MNs of multiple leg joints, namely to extensor, levator and CI1 MNs, is shown in Fig. 3.49. This NSI was not described before, it is labeled Ee.Le1. Striking is the large tonic depolarization underlying both forward and backward directed stepping sequences. On top of that, a phasic depolarization during the swing phase is obvious. The morphology of this neuron is U-shaped with the cell body at the anterior lateral margin of the hemiganglion ipsilateral to the walking leg (Fig. 3.49C).

Finally, three single recordings of NSIs with excitatory influence to flexor, depressor and common inhibitor1 MNs are shown in Fig. 3.50. The NSIs in Fig. 3.50A and B are depolarized during the swing phase. The one in A remains depolarized at the same level throughout swing. The NSI in B is depolarized only in the first half of swing. The membrane potential during stance in both NSIs stays at resting level, respectively slightly hyperpolarized (Fig. 3.50A, B). For the NSI in Fig. 3.50A a backward stepping sequence was recorded in which the activity stayed the same. The NSI depicted in C is depolarized shortly before stance onset and hyperpolarizes after the onset of swing. This shows that in addition to I4, there are also other NSIs which influence the activity of stance phase MNs of more than

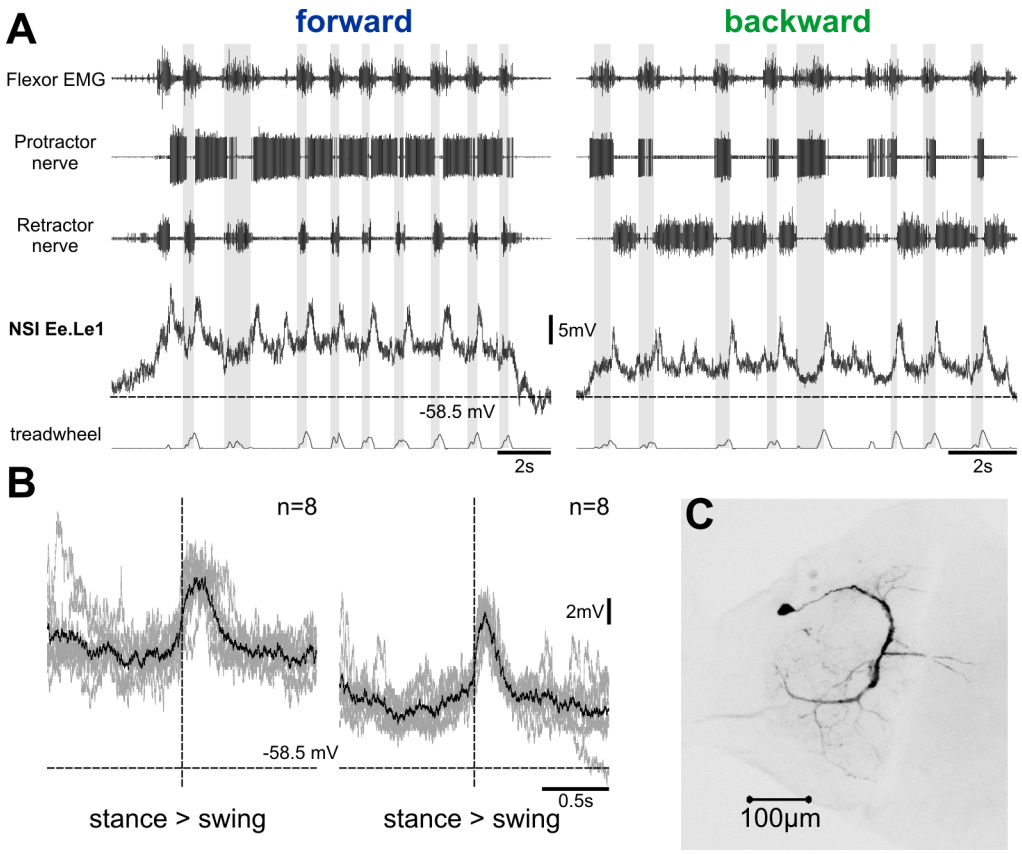

Figure 3.49 – Physiology and morphology of NSI Ee.Le1. A: intracellular recording of Ee.Le1 during forward and backward walking. The neuron receives phasic depolarizing inputs at the onset of swing on top of a tonic depolarization during forward and backward walking. B: overdraws emphasize the phasic depolarizing input shortly after the stance-swing phase transition during forward (n=8) and backward stepping (n=8). C: morphology of Ee.Le1 with the cell body in the anterior lateral margin and a U-shaped main neurite bending posterior-lateral.

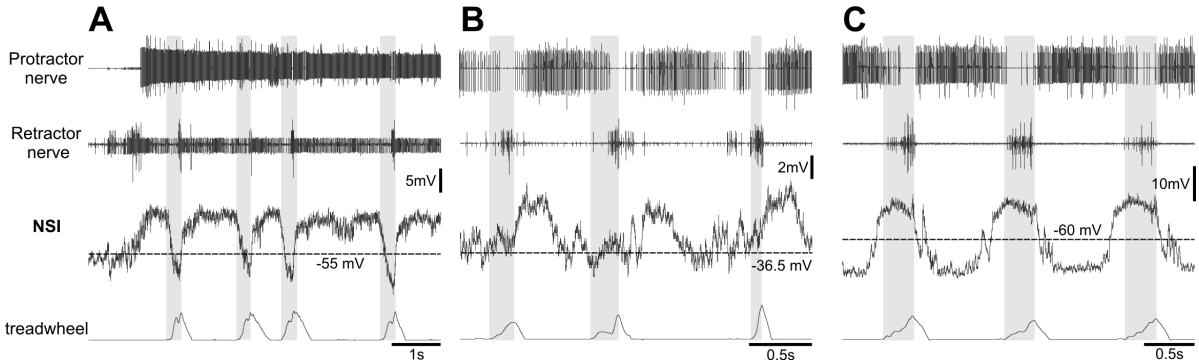

Figure 3.50 – Physiology of three single different neurons exhibiting excitatory influence on flexor, depressor and common inhibitor MNs. A: this neuron is steadily depolarized throughout swing and hyperpolarized slightly below RMP during stance. B: a neuron, which is depolarized during swing C: this neuron is depolarized during stance and hyperpolarized during swing.

Table 3.1 – Properties of recorded NSIs.

Interneuron	exc	inhib	rec fwd/bwd	fCO elong/relax	RMP	p-p fwd	p-p bwd
Pe1	pro	ret	2/0	dep/dep	-53; -51	15.7; 16.5	-
pe2	pro		1/1	-	-47	13.1	16.1
pe.re1	pro,ret		2/2	dep/dep,hyp	-53; -56	16.2; 20.3	19.4; 20.6
re1	ret	ret 2/5	5/3	hh(3),dd(1),d?(1)	-47.1±4.8	13.6±3.2	16.9±4.5
De2	dep	lev 1/5	5/2	hh(2),dd(1),hd(1),dh(1)	-44.9±3.3	14±1.8	17.4; 12.4
de3	dep	lev 1/5	4/3	hd(2),hh(1),?/h(1)	-41±3.1	14.2±1.8	13.7±0.6
de4	dep		3/1	hyp/dep(2)	-56; 50	13.6; 20	20.2
de5	dep		2/1	dep/dep	-50; -46	11.9; 8.8	14.1
De6	dep		1/1	hyp/hyp	-49	8	7
le5	lev		3/1	dep/dep	-53±4.5	12.1±4.4	11.6
le6	lev		2/-	?/dep(1)	-53; -51	9.1; 6.8	-
Le7	lev		1/-	?/dep	-41	8.5	-
le8	lev		1/1	dep/dep	-56	6.8	11.8
E3	ext		1/1	dep/hyp	-56	14.2	13.3
E4	ext,lev,pro		2/1	dep/dep	-58; -52	17.2; 17.4	17.1
E5	ext		3/3	dep/dep	-60±2.1	12.2±2.9	13.9±2.3
E7	ext		1/1	hyp/dep	-45	12.3	8.9
I1	flx		1/1	hyp/dep	-46	15.7±0.8	16.6±1.5
I2	flx		2/1	dep/dep	-40; -36.5	19.9; 8.5	18.8±1.7
Ee.Le1	ext,lev,CI		1/1	dep/dep	-57	6.6	7.6

In the table, excitatory (exc) and inhibitory (inhib) influences of the recorded NSIs are given, as well as the number of recordings during forward (rec fwd) and backward (bwd) walking. The responses to an elongation (fCO elong) and relaxation (relax) of the femoral chordotonal organ by passively bending and extending the leg on the treadwheel are listed. Furthermore, the resting membrane potentials (RMP) and the peak-to-peak amplitudes (p-p) of the membrane potential modulation during forward and backward walking are stated.

one leg joint.

In summary, intracellular recordings of a variety of previously identified and newly identified local premotor nonspiking interneurons were described in this chapter during forward and backward stepping of a single leg on a treadwheel. The membrane potential of all recorded neurons was modulated in close relation to the step cycle during forward and backward walking. This suggests that in the stick insect different motor programs can be achieved with the same set of nonspiking interneurons. Almost all NSIs involved in the control of the femur-tibia joint and the coxa-trochanter joint motor activity (except two exceptions with single recordings: E7 and le8) showed the same activity and, if tested, the same synaptic inputs during forward and backward walking. Newly identified NSIs involved in the control of the thorax-coxa joint were found to contribute to the change in protractor and retractor activity between forward and backward walking. Also for them, synaptic inputs, that is the tonic depolarization and phasic excitatory

and inhibitory inputs during walking, are similar but occur in different phases of the step cycle. Which inputs are actually responsible for this shift in activity still has to be elucidated. Furthermore, when stepping velocity was correlated to NSI activity and membrane potential modulations, significant correlations could only be found sporadically. This is true also for flexor NSI activity which was already shown to correlate with stepping velocity (von Uckermann and Büschges, 2009). That is probably due to a small number of recorded neurons and a small number of steps of I1 and I2 recorded here. Nevertheless, some significant correlations of NSI I1 activity and mean belt frequency during backward walking were found, which suggests that mechanisms controlling stepping velocity during forward walking also apply during backward walking.

4 Discussion

4.1 Leg muscle activity during walking on a slippery surface[1]

Kinematics / cycle period Multiple studies have investigated insect forward and curve walking (walking and turns on solid substrate: Wendler, 1966; Zolotov et al., 1975; Cruse, 1976b; Strauss and Heisenberg, 1990; Zollikofer, 1994; Jindrich and Full, 1999; Ridgel et al., 2007; Rosano and Webb, 2007; Cruse et al., 2009; air-cushioned Styrofoam ball: Frantsevich and Mokrushov, 1980; Jander, 1982; Dürr and Ebeling, 2005; Guo and Ritzmann, 2013; slippery surface: Camhi and Nolen, 1981; Mu and Ritzmann, 2005; Ridgel et al., 2007; Gruhn et al., 2009b; Hellekes et al., 2012). Backward walking has been investigated in crustacea (Ayers and Davis, 1977; Chasserat and Clarac, 1980), scorpions and spiders (Bowerman, 1981), and stick insects (Graham and Epstein, 1985). However, this quite early stick insect work was only qualitative and did not have precise measurements of stance-swing transitions. Furthermore, some modeling studies exist, which dealt with forward, backward, and curve walking in the stick insect (Rosano and Webb, 2007; Toth et al., 2012; Knops et al., 2012).

The data presented here confirm observations by Graham and Epstein (1985) that stick insects can perform coordinated backwards walks on a slippery surface. Our data shows that forward and backward steps are equally variable but backwards steps are significantly shorter and therefore more inward directed than forward

[1] Similar to the methods and results section, great parts of this section of the discussion are already published: Rosenbaum P, Wosnitza A, Büschges A, and Gruhn M. *Activity Patterns and Timing of Muscle Activity in the Forward Walking and Backward Walking Stick Insect* Carausius morosus. Journal of Neurophysiology 104: 1681-1695, 2010. The authors contributions for the paper are as followed: AB, MG, PR, and AW designed research; PR and AW performed experiments, analyzed data and prepared figures; AB, MG, PR, AW wrote the manuscript. Main parts of this section are taken from the paper literally. A discussion of the curve walking data is added in the appropriate sections. Furthermore, the discussion concerning the neural control of forward and backward walking, which was further investigated in the single-leg preparation, is adapted.

steps. Touch down positions were only slightly different in the transverse axis to the animal (y), and lift-off positions were unchanged, in forward and backward walking. This observation is consistent with the activity of the femur-tibia joint muscles, especially the flexor, being very similar in forward and backward walking, as it is flexor activity that determines y-position at stance end. It should be noted, though, that backward stepping was elicited by a continuous pull on the antennae, whereas forward walking was undisturbed. This may be an additional reason for some of the observed changes in vector length and direction. The kinematics of curve walking on a slippery surface have been studied previously (Gruhn et al., 2009b).

Cycle period depended only on stance duration in both forward and backward walking, as well as during curve walking on the slippery surface. This has been long known for stick insects walking forward on non-slippery substrates (Wendler, 1964; Graham, 1972, 1985), but it was unclear whether this relationship held for forward or backward walks on a slippery surface. The findings presented here confirm previous results (Büschges et al., 1995; Gabriel and Büschges, 2007; Gruhn et al., 2009a) showing that in pharmacologically activated neuron preparations only stance motor neuron firing duration varies with cycle period, and in single leg preparations stepping velocity was only correlated to leg MNs active in stance. It was not tested whether the onset of muscle bursting changes with the rate of walking. Such dependence has been shown in a previous study of muscle activities in cockroach (e.g. Delcomyn, 1989), where the phase of burst onsets in a leg stance phase muscle shifted with respect to the neighboring leg when walking speed increased, and bursting was initiated earlier during rapid walking. However, on the level of the single leg, such a shift has been shown to occur in flexor motor neurons in the stick insect middle leg, albeit not with respect to a neighboring leg (Gabriel and Büschges, 2007). It is therefore not unlikely that shifts in the muscle activity onset of stance related muscles in the stick insect exist with respect to neighboring legs.

Muscle activity and latencies in forward, backward, and curve walking Recent work on stick insect muscles (Guschlbauer et al., 2007; Hooper et al., 2007b, 2009) highlights the slow responses of these muscles to neural input, and hence the importance of direct measurement of muscle activation in describing how neural activity generates the motor output in this system. Our EMG recordings of the six main middle leg muscles showed that only the muscles controlling the thorax-coxa-joint (protractor, retractor) expressed changes in activity when stick insects reversed walking direction, or were walking a curve. For forward and backward walking, the leg muscle activity is summarized in Fig. 4.1, the curve walking results

are discussed in parallel. Fig. 4.1A shows the average onsets of muscle activities of the functional swing phase muscles, timed to lift-off, and Fig. 4.1B the average onsets of activities of the functional stance phase muscles timed to touch down, in both walking directions with their respective standard deviations (SDs). The levator and extensor muscles are always functional swing muscles and the depressor and flexor always stance muscles. This is true also during curve walking. The only difference during curve walking was the prolonged activity of the depressor muscle during an outside curve. The protractor and retractor muscles, alternatively, switched from being (respectively) functional swing/stance muscles to being stance/swing muscles when walking direction reversed (Fig. 4.1C; see also Fig. 4.1A which shows, in addition to swing onsets, the average end of retractor activity during stance in forward walking, and the average end of protractor activity during stance in backward walking). During curve walking, the activity of protractor and retractor is more diverse. Depending on the steepness of the curve, they are differentially activated. Hence, forward directed, backward directed, or lateral steps can occur. The activity of these muscles is thus determined by each muscle's function in the behavior that is being produced. Provided this switch is noted, the activation sequence of functional swing and stance muscles is the same in forward and backward walking: 1) all swing muscles are activated before lift-off, levator first, extensor second, and protractor (forward walking) or retractor (backward walking) third; 2) in stance the depressor is activated first (during swing) followed by the flexor at or shortly after touch down, and then the retractor (forward walking) or protractor (backward walking).

A general finding was that the onset of muscle activity was relatively imprecise for most muscles with standard deviations ranging from 10.2 (flexor in outside curve walking) to 64.2 ms (levator in forward walking). One reason for high levator and extensor variability could be that these muscles are timed to lift-off, and measurement of the lift-off signal can be less precise than that of the touch down signal. However, pro- and retractor muscle timing variability was similar in forward and backward walking despite different reference points being used in the two walking directions. During curve walking, protractor and retractor first muscle potentials were not determined due to the great variability of the muscle activity during curve walking. Furthermore, the flexor shows much higher variability in backward (28.6 ms) (reference point touch down) than forward walking (13.3 ms), and in an inside (16.8 ms) than an outside curve (10.2 ms). The opposite is the case for the depressor. These results suggest that variability differences do not result from a lack of precision in determining lift-off or touch down times, but are instead true differences in motor patterning.

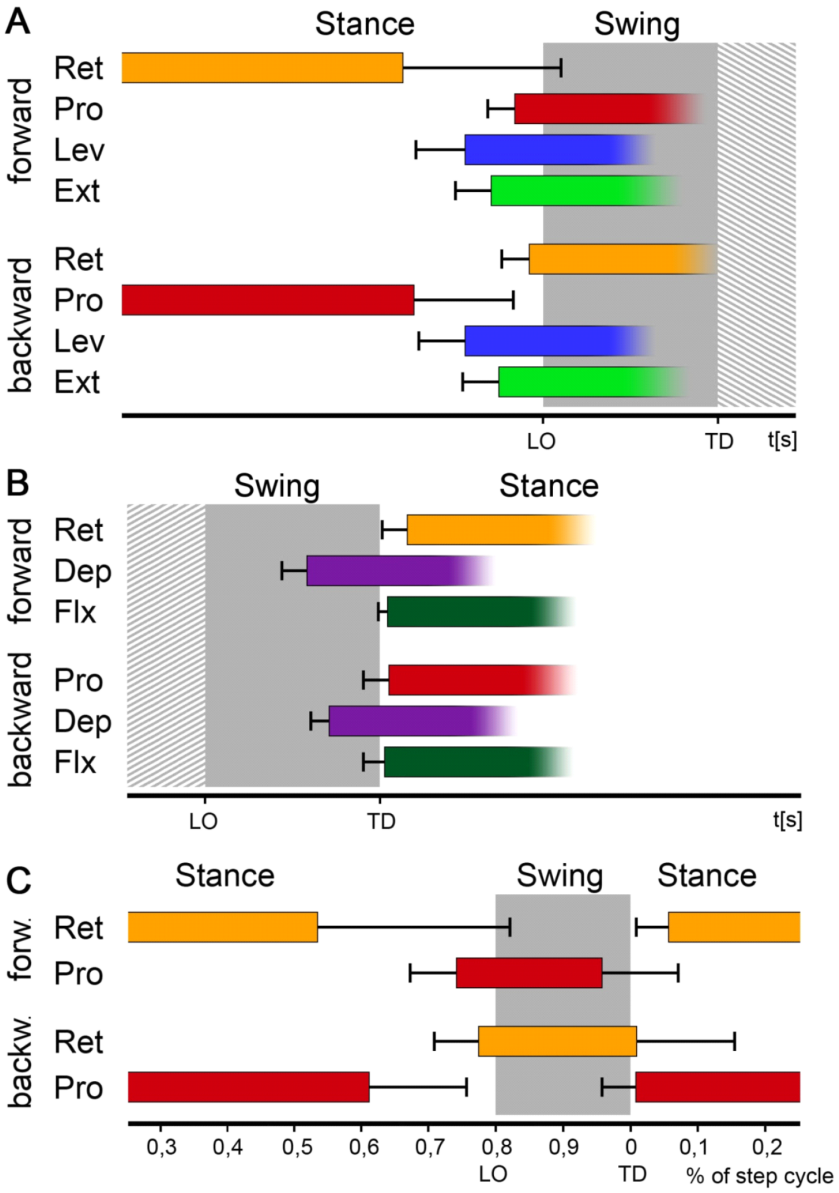

Figure 4.1 – Summary of right middle leg muscle timing in forward and backward walking in intact tethered animals walking on the slippery surface. A: comparison of the average beginning of activity in the protractor (fwd), retractor (bwd), levator (fwd and bwd), and extensor (fwd and bwd), and the average end of activity in the retractor (fwd) and protractor (bwd) with respect to lift-off (stance end). B: comparison of the average beginning of activity in the retractor (fwd), protractor (bwd), depressor (fwd and bwd) and flexor (fwd and bwd) muscles with respect to touch down (stance beginning). Gray areas mark swing duration; shaded areas standard deviation of swing duration. C: relative timing and duration of retractor and protractor activity in forward and backward walking animals with respect to mean cycle period calculated from first and last spikes and corresponding cycle periods of each step (swing marked with gray rectangle); error bars mark SD.

Another interesting observation in this context was the early activation of swing muscles before the actual kinematically observed onset of the swing movement, and the activation of stance muscles before or around touch down, and therefore before the kinematically observed stance movement. This finding can be explained with the muscle properties reported for stick insects and smaller animals in general (Guschlbauer et al., 2007; Hooper et al., 2007b, 2009). With decreasing diameter of a given muscle, the forces needed to overcome the passive forces of its antagonist become so large, that muscle activity has to start well before an observed movement that is caused by the muscle contraction (Hooper et al., 2009). In this case, as opposed to in large animals such as cat or human, the role of gravity in moving a limb becomes negligible, and therefore the early onset of muscle activity in levator and depressor is needed to counteract the respective antagonist before movement can begin.

Previous work has shown that signals from movement and load sensors are important for inducing stance-swing and swing-stance transitions during walking (Cruse et al., 2004; Büschges et al., 2008). In most of this work, however, motor activity timing was inferred from leg kinematics, which means that the measurement of sensory input timing with respect to motor output was rather imprecise. It is therefore useful to compare our precisely measured muscle activities and these previous data.

1) Tibia extension signals arising from the femur-tibia joint have been identified as a trigger for depressor activity in swing (Hess and Büschges, 1999; Bucher et al., 2003). The depressor activation times we measure, well into swing (93 ms prior to touch down), and at a time when the middle leg tibia is known to be well extended (e.g. von Uckermann and Büschges, 2009), are consistent with this conclusion (Fig. 4.1A,B). A recent study showed that the reflex reversal occurs more frequently in the inside than in the outside curve leg (Hellekes et al., 2012). This is not reflected in the recordings of muscle activities during curve walking presented here. However, in the study of Hellekes et al. (2012), the investigated leg was fixed and only the front legs were walking.

2) Leg loading, as occurring after touch down, has been reported to initiate retractor activity (in forward walking) as a result of signals from the trochanteral campaniform sensilla (Akay et al., 2004, 2007), and flexor activity as a result of signals from the femoral campaniform sensilla (Akay et al., 2001). While the mean activation times measured for these muscles agree with this hypothesis, first activation of both muscles was either prior to touch down or very shortly after, it seems unlikely that load signals from trochanteral or femoral campaniform sensilla alone are able to activate either muscle at stance onset.

3) Load signals arising from the trochanteral campaniform sensilla (Akay et al., 2007) have been reported to support ongoing depressor and retractor activity during stance (Bässler, 1967, 1972; Schmitz, 1986b). This matches the finding that depressor activity was increased and prolonged when the animal was lowered to the surface or walked freely on the slippery surface, compared to the normal height of the animal above the slippery surface.

4) The presented data shows that at swing onset the levator is activated first, then the extensor, and finally the protractor (Fig. 4.1A). This sequence matches the predicted effects of known sensory influences: leg unloading signaled by the femoral and trochanteral campaniform sensilla activates extensor (Akay et al., 2001) and protractor (Akay et al., 2004, 2007) motoneurons. The observed latency of about 40 ms between levator activation and activation of the other two swing muscles is ample time for sensory activation of the latter.

5) It was previously suggested that position signals from the coxa and unloading signals contribute to levator activation (Cruse, 1985). A recent study showed that sensory signals from trochanteral campaniform sensilla (trCS) are able to induce depressor activity and terminate levator activity (Borgmann et al., 2012).

In summary, our precisely measured data are generally consistent with prior interpretations of the role of sensory feedback in inducing step phase transitions. The only exceptions are the flexor and retractor (forward walking) and protractor (backward walking) muscles, which appear to activate too soon for the putative sensory triggering input to actually induce the activations.

Implications of pro- and retractor switch in forward, backward, and curve walking The finding that the timing of the pro- and the retractor muscles, which control the thorax-coxa joint, switched independently of that of the muscles for the other joints, and that it depended on the functional role of the muscle rather than on the muscle itself, raises questions about the neuronal control of forward and backward walking. Since single steps during curve walking can be seen as a continuum of possible movements between the extremes forward and backward walking, the question of its neuronal control is strongly connected. However, one needs to keep in mind that straight backward walking is a rather artificial situation, since it barely occurs in natural behaving stick insects. However, backward steps can occur during steep curve walking. So, how does the nervous system alter the control for the joint network to reverse the motor pattern and how is the similar timing of muscle activity achieved? This includes the question of how cycle period continues to depend on stance duration in backward walking even though under this condition the stance phase muscle at the thorax-coxa joint, and only at this

joint, switches.

One explanation for the retractor-protractor switch is that the phase coupling between the thorax-coxa joint pattern generator and the pattern generators of the other two joints is altered centrally. This would imply that neurons in the ThC-joint CPG which drive protractor MNs are active during stance in backward walking. Actually, I found nonspiking interneurons, which are responsible for the change in the protractor and retractor activity. Thus, they seem not to be involved in the CPG circuitry, although this can't be said with certainty. Now, the question arises, from where these NSIs receive inputs to switch their activity. Toth et al. (2012) proposed a mechanism, by which this switch can be achieved in a neuromechanical model, which will be discussed later. Furthermore, it has to be resolved, why cycle period continues to depend on stance duration in backward walking. For this, it would have to switch from depending on retractor interneuron activity to protractor interneuron activity. This could be explained if this dependency is not associated with retractor (forward walking) and protractor (backward walking) activity duration, but only with flexor and depressor durations. Flexor activity does indeed play an important role in determining cycle period (Gabriel and Büschges, 2007). Such an influence was not found for other stance phase MNs (depressor, retractor during forward walking, protractor during backward walking). This is shown in the next section. It is thus possible that the retractor-protractor switch does not pose a difficulty for understanding the dependency of cycle period on stance duration, because thorax-coxa joint activity is simply not a part of this process.

Another possibility is that the synaptic drive of the thorax-coxa pattern generator to the coxal motoneurons reverses in backward walking. This mechanism would explain why cycle period continues to depend on stance duration in backward walking. In both cases, pattern generator cycle period would continue to depend on the burst durations of the same set of interneurons, with these interneurons driving different motor neurons in forward and backward walking, but nonetheless always stance phase motor neurons.

This change in central drive could be assisted by altering the effects of leg derived sensory input (reviewed in Büschges et al., 2008) such that these changes result in the observed switch. In this case, for example, parallel pathways from load sensors like the trochanteral campaniform sensilla to the premotor interneurons and the two motor neuron pools of retractor and protractor could be weighted differently during forward and backward walking and thereby reverse the effect of the sensory signal. Similar mechanisms have been demonstrated to alter several sensorimotor processes (Büschges and Manira, 1998; Clarac et al., 2000) and Akay

et al. (2007) have indeed shown that trochanteral campaniform sensilla activity initiates retractor muscle during forward stepping, but protractor muscle during backward stepping.

Inter-leg influences on muscle activity in the forward walking animal Reducing leg number caused only relatively small alterations in overall leg muscle activity but shifted the average latency of the first muscle spikes in the pro/retractor, in the extensor and the flexor muscles, and the depressor, while no effect was seen on levator activity. These data are consistent with kinematics analyses of straight walking and turning in stick insects showing that single legs produced leg movements with changes in the precise leg positioning, when the number of legs was reduced (Gruhn et al., 2009b). These changes are also in line with considerable evidence suggesting that inter-leg influences could play a prominent role in shaping leg motor output (Ludwar et al., 2005a; Borgmann et al., 2007, 2009, 2012). In the data presented here, the greatest changes in forward walking between intact and reduced animals were in the extensor and retractor muscles, where the onset of activity shifted by about 25-30 ms towards lift-off, and therefore activation started later than in the intact animal. In case of the flexor, the effect was a shift of 5-10 ms, yet, also this muscle was activated significantly later in the reduced preparations. Interestingly, the effect of the reduction was not always a delay in the activation, but in the case of the retractor and the depressor muscle a significantly earlier activation, demonstrating that potentially sensory derived intersegmental effects affect the timing in both directions and, in the case of the depressor, even the ablation of the contralateral leg and the lack of its sensory input may have an effect on timing. The activity of the above muscles may be especially influenced by inter-leg influences because they largely determine the leg's anterior and posterior extreme positions, and stance and swing phase duration, all extremely important components of inter-leg coordination (Cruse, 1990; Cruse et al., 1998). The origins of the sensory input from the neighboring legs exerting these influences is unclear, although Ludwar et al. (2005a) have demonstrated that flexion signals from the front leg femoral chordotonal organ can facilitate middle leg retractor activity and also contralateral influences have been shown to exist, although not for the depressor muscle (Stein et al., 2006).

Local influence on depressor muscle activity When the animals were tethered $\geq$ 10 mm above the slippery surface, depressor activity strongly decreased very early in stance, but in animals tethered at a lower height, depressor activity continued throughout the greater part of stance. Increased depressor duration was also seen in freely walking animals. These data suggest that sensory input in

freely walking animals prolongs depressor activity so that, in addition to lowering the leg at swing end, the muscle also helps to support the animal during stance. Work in stick insect and other insects suggest that the sense organs most likely responsible for this effect are again the campaniform sensilla, the same organs involved in switching protractor to retractor activity at touch down (see above and Akay et al., 2004, 2007; Borgmann et al., 2012). However, the role of campaniform sensilla in the magnitude control of motor neuron activity in stick insects is much less understood. Cruse et al. (1993) have demonstrated in double treadwheel experiments that stick insects walking with small distances between body and wheel push the wheel away from the body resulting in increased depressor activity. In the cockroach, different subgroups of tibial campaniform sensilla react to increases or decreases in body load (Noah et al., 2004; Zill et al., 2009) and fire prolonged spike trains when legs actively support the body. Increased load also increases cockroach trochanteral extensor motoneuron firing, the functional analog of stick insect depressor motoneurons (Quimby et al., 2006). Additionally, position signals from the fCO (Bucher et al., 2003), and from the trochanteral hair plate also play a role in the control of depressor activity (Schmitz, 1986b,a; Berg et al., 2013). These results and data presented here suggest that local mechanisms controlling depressor activity are a major component of the support of body load and maintenance of body height.

Conclusions The activity and timing of all major middle leg muscles during forward, backward, and curve walking in the tethered stick insect was described. As the animal switched from forward to backward walking, the major change observed was that the functional stance muscle of the thorax-coxa-joint switched from retractor to protractor, with both muscles showing the same activity times when serving as stance muscles. During curve walking, also intermediate changes between those two could occur. These findings demonstrate again the modular structure of the neuronal networks driving leg movement. They also suggest potential ways in which the central nervous system controls adaptive walking behaviors and how sensory input may be differentially modulated depending on the behavioral task.

4.2 Patterning of motoneuron and interneuron activity during single-leg stepping on a treadwheel

4.2.1 Synaptic inputs to MNs

In the second part of this thesis, synaptic inputs to leg MNs during single leg forward and backward stepping on a treadwheel were investigated. Previous studies showed for forward walking, that leg MNs receive tonic depolarizing synaptic inputs during walking, originating from descending and/or intersegmental sources (Ludwar et al., 2005b). Additionally, the MNs receive phasic inhibitory inputs from the leg CPGs, and phasic excitatory and inhibitory inputs from leg sense organs (Büschges et al., 2004; Schmidt et al., 2001). Here, it could be shown that the synaptic inputs to leg MNs are very similar during forward and backward walking. However, phasic inputs to protractor and retractor MNs occur in another phase of the step cycle, and thus the activity of these MNs changes with walking direction.

The tonic depolarization was found in all recorded leg MNs. Either it was immediately apparent during walking (protractor MNs: Fig. 3.16, depressor MNs: Fig. 3.17, levator MNs: Fig. 3.18), or it could be revealed by injecting hyperpolarizing current into MNs during walking (retractor MN: Fig. 3.15, flexor MN: Fig. 3.19). Also during backward walking, the tonic depolarization is apparent and does not seem to be altered in amplitude (protractor MN Fig. 3.16). Fig. 4.2 shows a schematic of the synaptic input leg MNs receive during walking. In Fig. 4.2A, the tonic and phasic synaptic inputs to leg MNs during stepping are depicted. In Fig. 4.2B, the influence of current injection into the neuron on its membrane potential during walking is schematized. The amplitude of the tonic depolarization is increased when the membrane potential is more hyperpolarized, and decreased when the membrane potential is more depolarized. As explained earlier (sec. 3.2.1.1), this is due to the changed electrochemical driving force, and the reversal potential of the involved ions. The change in the peak-to-peak phasic modulation is small, because inhibitory and excitatory synaptic inputs are changed differently. The implications of these mechanism are manifold. Fast flexor MNs, e.g., have a more hyperpolarized resting membrane potential than slow flexor MNs, so they are recruited later during faster movements (Gabriel et al., 2003). The amplitude and duration of the tonic depolarization was not investigated quantitatively here. These properties strongly depend on the quality of the recording and the walking sequences. The amplitude depends on the resting membrane potential of the recorded MN, and the measurable duration on how fast the animal is stepping. If

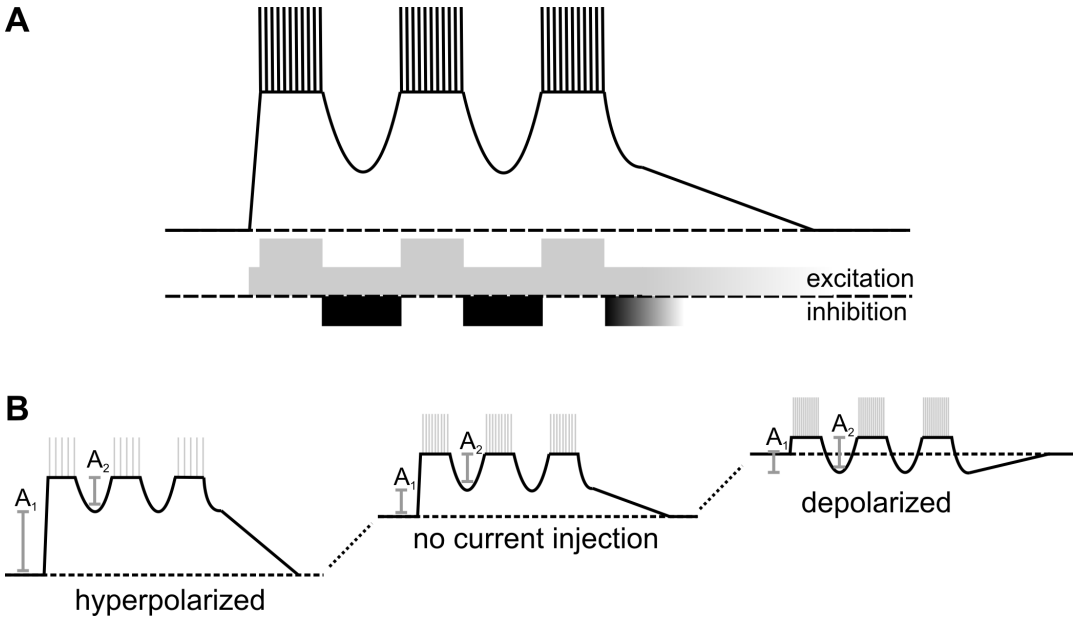

Figure 4.2 – Schematic overview of the synaptic inputs to leg motoneurons during walking. A: overview of the synaptic inputs leg motoneurons receive during walking. Throughout stepping, MNs are tonically depolarized by descending/intersegmental input (long gray bar). Additionally, the MNs receive phasic excitation (gray bars) in the swing or stance phase of the step cycle, and phasic inhibition when the antagonist is active (black bars). B: change of synaptic inputs when artificially altering the membrane potential by current injection. A_1 is the amplitude of the tonic depolarization and A_2 the amplitude of the phasic inhibitory and excitatory inputs. When hyperpolarizing current is injected into a motoneuron during walking (left), the amplitude of the tonic depolarization is increased. The net change in phasic inputs is small, because excitation and inhibition amplitude are differently changed (see text), compared to the normal situation (middle). Injecting depolarizing current into a leg MN during walking leads to a decreased amplitude of the tonic depolarization (right). Figure adapted from Gabriel (2005).

for example two steps occur quickly after one another, the tonic depolarization has not repolarized completely before the next step begins and thus cannot be measured exactly. This is visible in the protractor MN recording (Fig. 3.16), in which a fast stepping sequence is shown during forward and a slow during backward walking. The tonic depolarization is supposed to be a cellular correlate of arousal which brings MNs closer to their spiking threshold (Ludwar et al., 2005b). It was thoroughly investigated in experiments in which mesothoracic leg MNs were recorded intracellularly while a front leg was stepping. In the study of Ludwar et al. (2005b), the tonic depolarization exhibited an increase in the membrane potential of up to 5 mV during walking, depending on the membrane potentials of the recorded neurons. Its reversal potential was between -32 to -47 mV, which suggests that an mixed inward/outward current of Na^+ and K^+ ions is responsible for the change in membrane potential (Ludwar et al., 2005b; Gabriel, 2005). It was shown that the transmitter released to induce the tonic depolarization is acetylcholine (ACh), acting on metabotropic ACh receptors. Furthermore, the tonic depolarization is increased in amplitude by the neuromodulator octopamine, which is possibly influencing the premotor nonspiking interneurons (Westmark et al., 2009).

The phasic modulation of the MN membrane potential during walking has two origins. The phasic inhibitory input in the phase, in which the antagonistic MNs are active, is presently thought to mainly derive from synaptic inputs of the central pattern generating network (Büschges et al., 2004). The excitatory inputs to the MNs derive from sensory information, either via direct inputs from sense organs or via nonspiking and spiking interneurons (e.g. signals from femoral campaniform sensilla: Akay et al., 2001, reviews: Bässler and Büschges, 1998; Büschges et al., 2008). Furthermore, intersegmental information from stepping legs of other segments can influence the motor output of leg MNs (e.g. Ludwar et al., 2005a; Borgmann et al., 2007, 2009, 2012). Also in other systems, a tonic depolarization and phasic inhibitory and excitatory inputs has been found to underlie rhythmic locomotor activity (locust flight: Hedwig and Pearson, 1984; crayfish: Mulloney, 2003; lamprey: Wallén et al., 1993; tadpole: Soffe and Roberts, 1982).

Another observation that was made in leg MN recordings was that the change of the membrane potential at the transition from stance to swing was often very quick and quicker than at the transition from swing to stance. This has been exemplified in the overdraws of the membrane potential during single steps at the stance-swing transition (e.g. Fig. 3.16B). The same observation has also been made in several previous investigations (e.g. Schmitz et al., 1991a; Gabriel, 2005; Gabriel and Büschges, 2007). In a study, in which vibrational stimuli were applied to the

fCO, phase transitions in the activity of antagonistic MN pools could be elicited. It was found that the latency for the transition from flexor to extensor activity was smaller than from extensor to flexor activity (Bässler et al., 2003). This suggests that the transition from stance to swing might be generated faster than the transition from swing to stance, which would be in accordance with the above mentioned results. The activity of the inhibitory MN CI1 could be of importance in this case. In the locust (Wolf, 1990) and in the stick insect (Büschges et al., 1994, personal observation), CI1 is active in the swing phase of the step cycle during both forward and backward walking. Wolf (1990) could show that the activity of CI1 contributes to a fast activation and speed of the leg protraction, that is the swing movement. During backward walking, such an influence of CI1 on the leg retraction exists (Ansgar Büschges, unpublished data), which during backward walking generates the swing movement. What the functional implication for this observation is, and how this could be achieved at the premotor/central level has to be elucidated. One could imagine, that a stick insect which is climbing in a bush and finds an unsuitable foothold quickly initiates a new swing phase to move the leg away from that to find a new foothold.

The activity of all leg MNs and also of the NSIs is strongly coupled to the step phase transitions. The latencies for the muscle activities, however, sometimes showed negative latencies in relation to step phase transitions, e.g. the levator and protractor muscles were activated before the onset of swing movement. This might be due to the experimental situation in the single-leg preparation. Here, specific sensory signals measuring the position of the thorax-coxa are influenced, because the ThC-joint is fixed and the motor nerves nl2 and nl5 deafferented. Such signals are conveyed by coxal hair plates and hair rows (Cruse et al., 1984). In fact, projections from those run through nerves nl3, C1, and C2 (Schmitz et al., 1991b; Goldammer et al., 2012), but certainly coxal hair fields and hair rows are influenced by fixating the ThC-joint. Thus, the 'fictive' forward and backward walking activity of protractor and retractor MNs could be more stereotyped in the single-leg preparation.

4.2.2 Velocity dependence of MN and NSI activity in the single-leg preparation

In the single-leg preparation, the stepping velocity on the treadwheel is largely correlated only with flexor MN activity. This is the case also during backward walking. For forward walking, this is in accordance with results of Gabriel and Büschges (2007). In the single-leg preparation, these authors found a correlation

of the treadwheel velocity with flexor MN activity, but not with extensor MN activity. Stick insects alter their walking speed by a change in the stance phase duration (Wendler, 1964), sec. 3.1.2). So at least for the other stance phase MNs, the depressor, the retractor during forward, and the protractor during backward walking, this could have been hypothesized. But none of them showed more than an occasional correlation of their membrane potential to the mean belt velocity. As was pointed out earlier (sec. 3.2.1), an analysis of the joint kinematics of single-leg stepping on a treadwheel showed that the major movement is based on an angular change in the FTi-joint, and only slight joint angle changes occur in the CTr-joint (von Uckermann and Büschges, 2009). Protractor and retractor muscles are not involved in the movement of the leg in the single-leg preparation. This is probably the main reason for the result that stepping velocity on the treadwheel is only correlated to flexor MN activity. Thus, it would be interesting to look if a correlation of the activity of other than the flexor MNs to stepping velocity exists in other preparations, in which the leg moves more naturally.

However, the question arises, how the leg is able to step in different speeds, but no other leg MN pools except flexor MNs seem to be involved. In my preparation, the nerves nl2 and nl5, which contain the axons of protractor and retractor MNs, are crushed distally to the recording site. Some sensory afferents, whose projection pattern resembles that of tactile hairs, also run through the nerves nl2 and nl5. Their origin is, however, unclear (Goldammer et al., 2012). Thus, no sensory information from leg sense organs of this joint seem to be necessary for the control of walking speed. But, because fictive forward and backward walking can be elicited in this preparation, sensory information that is necessary for the appropriate coordination of ThC-MN activity to the activity of the two moving leg joints must be intact. Responsible for that are sensory signals from trochanteral campaniform sensilla (trCS), which are necessary for the coupling of ThC-MN activity to those of the more distal leg joints (Akay et al., 2004). Furthermore, it has been shown that signals from the trCS are also modificated with the change in walking direction (Akay et al., 2007). However, they do not seem to be involved in conveying signals of different stepping velocities. MNs of the CTr-joint are involved in the generation of the movement on the treadwheel. FTi- and CTr-joint activity influence each other via different sense organs (e.g. Hess and Büschges, 1997, 1999; Akay et al., 2001; Akay and Büschges, 2006). But apparently, no sensory signals about stepping velocity seem to be transmitted by the fCO to MNs of the CTr-joint (and ThC-joint). Thus, not all joint CPGs contribute equally to the generation of different stepping velocities, and sensory signals reporting changes in walking speed do not influence different joint-CPGs in the same manner. This further supports the modular construction of the stick insects leg joint control

system and its weak coupling. However, neuronal mechanisms responsible for the change in stepping velocity are also involved in the change of stepping velocity during backward walking.

Gabriel and Büschges (2007) found an initial depolarization of flexor MNs underlying slow and fast steps and a subsequent faster depolarization which was velocity-dependent. They suggested that the initial depolarization results from the release from inhibition of the flexor MNs after swing in combination with the tonic depolarization. The second, velocity dependent depolarization could be generated by reinforcement of flexor MN activity from strain and movement signals. I did not find an initial depolarization to that extent Gabriel and Büschges (2007) did, neither in flexor MNs nor in other stance phase MNs. This difference could be due to a much smaller number of consecutive steps, as well as higher mean belt velocities in my experiments. Especially the antennal stimulation to induce backward walking is a strong stimulus, which often elicits comparably fast steps.

As a next step, the activity of NSIs that contribute to the generation of leg stance was compared with the stepping velocity on the treadwheel. Here, only occasionally correlations of NSI activity with stepping velocity were found, including NSIs I1 and I2, which provide excitatory drive to flexor MNs. In contrast, von Uckermann and Büschges (2009) found a correlation of stepping velocity to the latter two. The result here may be due to a a small number of steps in the recordings. Since no correlation of depressor MN activity and belt velocity was found, it is not too surprising that I also did not find a systematic correlation between depressor NSI activity and belt velocity. Though, in one depressor NSI, de5, the peak amplitudes of the membrane potential during two of four forward walking sequences were significantly correlated to stepping velocity. Von Uckermann & Büschges observed that only NSIs which were depolarized during stance (I1, I2 and E1) showed a correlation to the stepping velocity. Since the majority of depressor NSIs is only slightly depolarized during stance but strongly hyperpolarized during swing, a similar, unknown mechanism may apply.

The neural control of locomotion velocity is studied in a variety of organisms. A previous study, in which swimming in *Xenopus* tadpoles was investigated, showed that the basic motor pattern was not altered with varying swimming frequencies, and that a change in background excitation and phasic inhibition is responsible for a change in swim frequency (Li and Moult, 2012). Also in mice, a phasic inhibition of motoneurons plays an important role for the control of the CPG frequency (Gosgnach et al., 2006). Studies in zebrafish suggest, that in the vertebrate spinal cord motoneurons and interneurons are recruited differently at increasing swimming frequency (McLean et al., 2008; Gabriel et al., 2011; Ausborn et al., 2012).

How the phasic and tonic inputs to MNs and NSIs are related to the change of stepping velocity in the stick insect, remains unclear. The study of Gabriel and Büschges (2007) mentioned earlier makes first suggestions.

4.2.3 Premotor nonspiking interneurons

In the third part of this thesis, premotor nonspiking interneurons were recorded during single-leg forward and backward walking on a treadwheel to further investigate how the change in walking direction is generated by the leg control network. The membrane potential modulation of NSIs providing synaptic drive to motoneurons from all three main leg joints during walking was described. NSIs were found, which can contribute to the change in protractor and retractor motoneuron activity between forward and backward walking. Besides NSIs which provide synaptic input to tibial MNs, already described during forward stepping (E3, E4, E5, E7, I1 and I2; von Uckermann and Büschges, 2009), also newly described NSIs involved in the thorax-coxa and coxa-trochanter joint control regime were analyzed. These are Pe1, pe2 and pe.re1 providing excitatory synaptic drive to protractor MNs, and re1 and pe.re1 exciting retractor MNs; De2, de3, de4, de5 and De6 for depressor MNs and le5, le6, Le7 and le8 exciting levator MNs. All these NSIs showed an activity strongly coupled to the step cycle of the walking leg during both walking directions. The scheme in Fig. 4.3 summarizes the activity of the NSIs that were recorded, only the net membrane potential changes during the swing and stance phase of the step cycle are depicted. Only NSIs controlling the thorax-coxa joint were found to have a different phase of activity during forward and backward stepping (pe2 and re1), though not all NSIs of this joint show a change in the phase of activity (pe.re1). Unexpectedly, also an NSI providing excitatory drive to extensor MNs, E7, showed a changed activity in backward stepping compared to forward stepping. Furthermore, NSI le8 which provides excitatory drive to levator MNs is more strongly modulated during backward as during forward stepping.

NSIs De2, de4, de5 and I2 are depolarized during stance and hyperpolarized during swing phase in both forward and backward stepping. The membrane potential of re1 also shows this pattern during forward stepping but changes its phase of activity during backward stepping. As shown in the example figures for the NSI types in the result section, the depolarization of NSIs influencing depressor MNs differs strongly in amplitude. De2 is only slightly depolarized during stance phase, whereas the depolarization amplitude in de4 is higher. A large group of NSIs is depolarized during swing, whereas their membrane potential remains at resting level during stance in both walking directions: le5, le8, E3, E4, E5, Ee.Le1, pe.re1 and Pe1 (for E3, E4 and E5 cf. von Uckermann and Büschges, 2009). All of

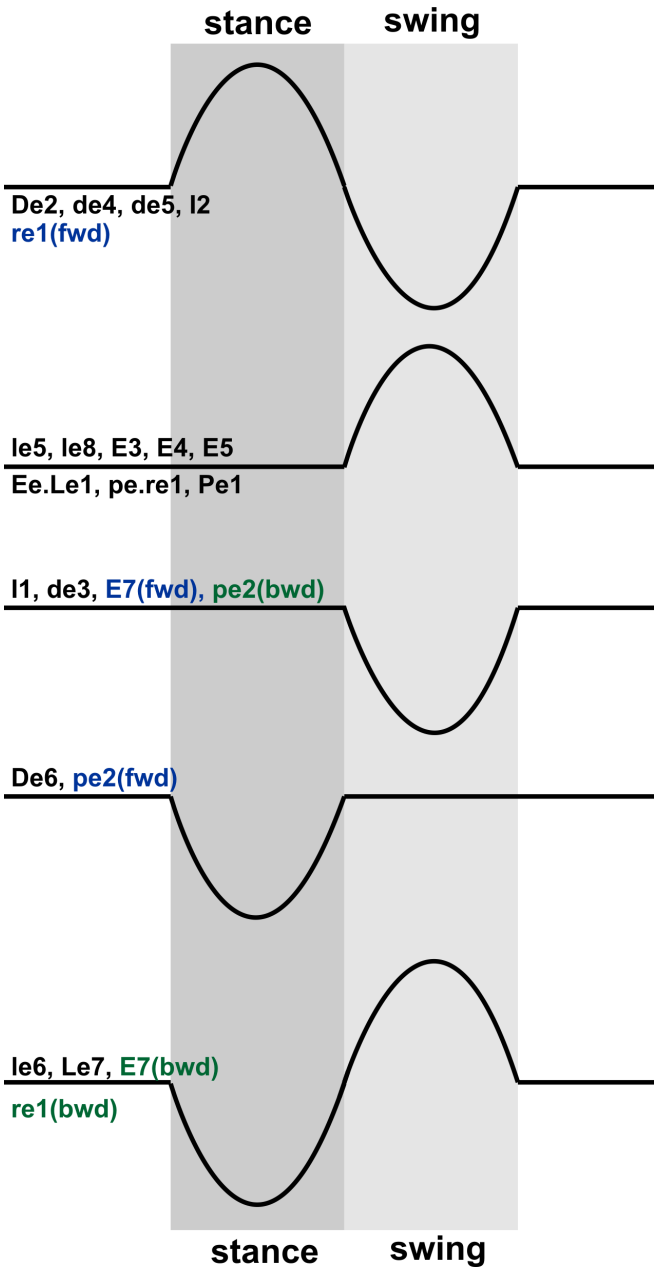

Figure 4.3 – Schematic overview of NSI activity. Membrane potential modulation patterns during single-leg stepping on a treadwheel are depicted schematically during stance and swing phase of the step cycle. NSIs De2, de4, de5, I2 and re1(forward) show a depolarization of the membrane potential in stance and a hyperpolarization in swing. Ie5, Ie8, E3, E4, E5, Ee.Le1, pe.re1 and Pe1 are depolarized during swing. I1, de3 E7(forward) and pe2(backward) are hyperpolarized during swing. De6 and pe2(fwd) are hyperpolarized during stance. Ie6, Le7, E7(backward) and re1(backward) are hyperpolarized in stance and depolarized in swing. NSIs in black show the same activity during both forward and backward walking. NSIs in blue show the assigned activity only during forward walking, NSIs in green only during backward walking.

these NSIs provide synaptic output to motoneuron pools which are active in the swing phase of the step cycle during both walking directions. In Pe1, no backward stepping sequences could be recorded. Also the shape of the membrane potential modulation of most of these neurons looks similar. E3, E4, E5, le5 and pe.re1 are rapidly depolarized at the start of swing phase and slowly repolarize to the resting membrane potential until the beginning of stance. NSIs I1 and de3 are hyperpolarized during swing and remain at resting potential during stance phase, but, however, the shape of their membrane potential modulation is very different. The course of the membrane potential of I1 is almost rectangular pulse-shaped with a very quick hyperpolarization at the start of the swing phase, a stable membrane potential during swing and a very quick hyperpolarization at the onset of stance, in which the membrane potential stays at resting level (cf. Fig. 13E in Bässler and Büschges, 1998). de3, on the contrary, slowly repolarizes already early in swing. Two other NSIs also show this modulation pattern but only during one walking direction: E7 during forward and pe2 during backward stepping. During forward stepping, the membrane potential of pe2 is hyperpolarized in stance. This is also the case for De6, but for both walking directions. At last, NSIs le6 and Le7 are hyperpolarized during stance and depolarized during swing phase. This is the case during both walking directions in le6 and Le7, and in E7 and re1 during backward stepping.

Some previous studies dealt with the physiology of NSIs during forward and backward walking in insects. Büschges and Wolf (1995) recorded tibial NSIs in a semi-intact locust walking on a double-treadwheel. All investigated NSIs showed the same morphology and physiology as in the corresponding NSIs in the stick insect. No difference in the membrane potential modulation was found for all investigated NSIs in the locust (E4, I4, E5, I1, I5 and E9) between the two different walking directions.

Similar to the motoneurons, also all nonspiking interneurons receive a tonic depolarization of their membrane potential during stepping, which was phasically excitatory and inhibitory modulated. Often, the tonic depolarization was hidden by the strong phasic modulations, but could be demasked via injection of hyperpolarizing current (e.g. Fig. 3.44). This suggests that phasic inputs from leg sense organs and the rhythm generating network, as well as the tonic depolarization, are summated on the level of the NSIs and than further transmitted to the MNs. That also means that the tonic and phasic synaptic inputs to the MNs are most likely mediated via parallel connections.

Burrows (1987); Laurent and Burrows (1988, 1989); Siegler (1981) showed in the thoracic nervous system of locusts that NSIs integrate signals from sense organs

and from descending interneurons. They receive synaptic inputs from sense organs, spiking interneurons and intersegmental interneurons, which themselves receive inputs from sense organs from the same leg and from other legs. The integration of these information likely leads to the typical pattern of membrane potential modulations of the NSIs during walking. Thereby one can suggest that the shape of the NSIs during walking is related to the function of the respective interneuron in providing synaptic drive to MNs in the step cycle. Some might be responsible for the activity at the transition from stance to swing phase or vice versa, some for the velocity of the actual stepping movement, and some for the angular changes in a specific leg joint during walking (Schmitz et al., 1991a; Wolf and Büschges, 1995; Kittmann et al., 1996).

The resting membrane potentials and peak-to-peak membrane potential changes of the recorded NSIs during forward and backward walking are shown in table Tab. 3.1. Resting membrane potentials in the recorded interneurons varied from -35 to -60 mV. Thus, they are on average higher than the resting membrane potentials of insect leg motoneurons. This is in agreement with previous studies, which stated a more depolarized resting membrane potential of NSIs. This allows them to reach the threshold for the release of transmitters already after small voltage changes (Burrows and Siegler, 1978; Wilson and Phillips, 1983; Siegler, 1985; Büschges, 1990). Examining the membrane potential modulation of the recorded NSIs during stepping, one can see that there are no big differences in the peak-to-peak amplitudes between forward and backward stepping (Tab. 3.1), except for one case, le8, which shows a two-fold increased amplitude in backward stepping compared to forward stepping. The measured peak-to-peak amplitudes of E3, E4, E5, I1 and I2 are in the same range as those measured by von Uckermann and Büschges (2009). One exception is E7, which is here found to have a stronger modulation during stepping. However, the physiology of E7 has to be confirmed, because E7 was only recorded once here, and only twice by von Uckermann and Büschges (2009). Other studies, which investigated the membrane potential modulation of NSIs during stepping in animals walking with six legs showed mostly smaller amplitude changes in the membrane potential (stick insect: 5-10 mV, Schmitz et al., 1991a, up to 15 mV Büschges et al., 1994; locust: 5-10 mV Büschges and Wolf, 1995). If these differences in amplitude are due to intersegmental signals from other legs has to be further elucidated.

Nonspiking interneurons providing synaptic drive to ThC-joint MNs A comparison of the membrane potential modulation of NSIs pe1 (only forward, N=2) and pe2 (forward and backward, N=1) with the spikes in the extracellular recording of nerve nl2 showed a correlation. This suggests, that these NSIs contribute to

the patterning of the motor output of protractor MNs. The membrane potential modulation of NSI re1 also showed a correlation to the retractor MN activity during forward and backward walking, but to differing extents. This might be due to two issues. First, only the physiology during walking was used to group re1 neurons, since good morphological data is missing. Thus, it is not certain if the five recorded neurons are really one type of neuron. Second, the membrane potential of re1 was compared with the instantaneous spike frequency of all units in the nl5 nerve recording. The retractor muscle is innervated by 16-17 MNs (recording site: branch A+B, Goldammer et al., 2012), and not all might get inputs from re1, so there certainly is some kind of imprecision in the correlation.

Nonspiking interneurons, influencing the activity of subcoxal MNs were described previously. Schmitz et al. (1991a) recorded NSIs in a preparation in which the animal was walking with all legs on a double-wheel treadmill. Although the output of the NSIs on MNs was not specifically tested, current injection into the NSIs changed the activity of protractor and retractor MNs during walking. The membrane potential modulation of the NSIs was shown to be tightly coupled to the step cycle. The morphology of these NSIs has no similarities with the morphology of the stained ThC-joint NSIs shown here, but rather resembles NSIs I1 and I2. In another study, NSIs related to subcoxal MN activity were recorded under the influence of pilocarpine (Brunn, 1998). The membrane potential modulation observed in this condition showed a strong coupling to the modulation of protractor or retractor MN activity. None of those NSIs can be related to NSIs recorded here.

Nonspiking interneurons providing synaptic drive to CTr-joint MNs NSIs involved in the control regime of the coxa-trochanter joint were studied by Hess and Büschges (1997); Hess (1998). They recorded interneurons in a completely restrained animal and applied ramp-and-hold stimuli to the femoral chordotonal organ (fCO) to study the interjoint reflex responses of trochanteral MNs and NSIs. Hess and Büschges (1997) grouped NSIs according to their responses to fCO-stimulation and their morphology. In my study, as described in the results section, NSIs were grouped according to the synaptic drive they provided to MN pools, their membrane potential modulation pattern during walking, and, if possible, by their morphology. Thus, some NSIs were grouped which showed differing responses to fCO-stimulation: pe.re1, re1, De2 and de3 (cf. Tab. 3.1). On the one hand, it is not absolutely clear if NSIs other than those involved in the FTi-joint control system also have stereotyped responses to fCO-elongation and -relaxation. Results from Hess and Büschges (1997); Hess (1998) suggest that. For subcoxal NSIs, this wasn't investigated before. On the other hand, the fCO-stimulation performed here strongly differs from those in previous studies that described NSI activity (i.e.

Büschges, 1990; Sauer et al., 1997; Hess and Büschges, 1997). In those studies, the fCO was stimulated by fixating the femur and clamping the fCO-receptor apodeme to a stimulator (Büschges, 1989). Thus, ramp-and-hold displacement stimuli could be applied to the fCO with velocities up to 2000°/s or even higher (a displacement of the receptor apodeme of 100µm corresponds to roughly 20° in the angle between femur and tibia). Some of the responses of NSIs to these stimuli were recorded at high velocities and sometimes even changed with stimulus velocity (Hess and Büschges, 1997). High stimulation velocities could not be achieved with the passive treadwheel stimulation in the single-leg preparation. Here, a movement of the treadwheel towards or away from the animal mimicked a flexion/elongation or relaxation/extension of the leg, respectively (Büschges et al., 1994; von Uckermann and Büschges, 2009). Sometimes the responses to this 'passive' fCO-stimulation I recorded were very weak, if present at all, or could only hardly be identified. Hess and Büschges (1997) showed that a stimulation of the fCO with a velocity of 200°/s led to barely visible responses in Li2, whereas a much faster stimulation velocity (2000°/s) led to clear hyperpolarizing responses to both elongation as well as relaxation of the fCO (Hess and Büschges, 1997). Therefore, previously described NSI Li2 (Hess and Büschges, 1997) might be the same neuron as De2, although responses to fCO-stimuli in De2 vary. Furthermore, the morphology of Li2 and De2 (Fig. 3.32) share some similarities, and also in one case an inhibition of levator MN activity by depolarization of De2 could be observed, which fits to the physiological properties of Li2.

As mentioned before, trochanteral campaniform sensilla (trCS) contribute to the patterning of depressor and levator MN activity (Borgmann et al., 2012). A way to characterize NSIs influencing those MNs could be to record their responses to trCS stimulation, and see if also stereotyped responses exist, as was shown for NSIs providing synaptic inputs to extensor and flexor MNs to a fCO-stimulation. Akay (2002) investigated the influence of a fCS-stimulation to tibial MNs and NSIs, but due to a small number of recordings no general conclusion could be drawn.

Nonspiking interneurons providing synaptic drive to FTi-joint MNs and to MNs of multiple leg joints Nonspiking interneurons providing synaptic drive to extensor and flexor MNs were thoroughly described previously, also during single-leg-stepping on a treadwheel (Büschges, 1990; Büschges and Schmitz, 1991; Schmitz et al., 1991a; Driesang and Büschges, 1993; Büschges et al., 1994; Büschges, 1995; Sauer et al., 1996; von Uckermann and Büschges, 2009).

Especially the role of NSI E4 is interesting during forward and backward walking. E4 provides excitatory synaptic drive to extensor, levator, protractor and common

inhibitor1 MNs as well as inhibitory synaptic drive to retractor and depressor MNs (Büschges, 1990; Büschges et al., 1994; Büschges, 1995). The physiological properties of E4 do not depend on intrinsic properties of the neuron, such as voltage-gated ion channels, but are due to synaptic inputs to E4 (Driesang and Büschges, 1993). This fits the observation that the membrane potential modulation of NSIs is due to a tonic excitation throughout stepping and phasic excitatory and inhibitory synaptic inputs in the appropriate phase of the step cycle phases, as was already shown for the MNs. During walking, the membrane potential modulation of E4 is almost linearly correlated with extensor and CI1 MN activity. Conversely, protractor MN activity was not clearly correlated to the actual membrane potential of E4 during walking (Büschges et al., 1994), also in my recordings. Under the influence of the muscarinic acetylcholine agonist pilocarpine (Büschges, 1995), E4 showed oscillations of its membrane potential, but with smaller peak-to-peak amplitudes of 10-11 mV, compared to 17-19 mV during walking (Tab. 3.1, von Uckermann and Büschges, 2009). This is probably due to missing inputs from leg sense organs. Furthermore, the membrane potential oscillation of E4 showed no obvious correlation to extensor MN activity anymore, but to some extent to depressor MNs. Not only E4 but also other FTi-NSIs received strong synaptic drive from rhythm generating networks activated by pilocarpine. Furthermore, E4 seems to be associated or even a part of the leg joint CPG. When depolarizing current is injected into E4, the pilocarpine induced rhythm was resetted in depressor and extensor MNs (Büschges, 1995). The injected current probably reflects the role of synaptic inputs from sense organs in a 'real' walking situation, which would affect the locomotor output in order to adapt to the actual requirements. Here, it was shown that the membrane potential modulation of E4 stays the same during both forward and backward walking. This suggests that the excitatory influence of E4 on protractor MNs during backward walking is inhibited or at least diminished. Accordingly, the inhibitory influence of E4 to retractor MNs could be reversed during backward walking. This could either be explained by a presynaptic inhibition of synaptic connections from E4 to protractor and retractor MNs, or by the 'parliamentary principle' (Bässler, 1993), which will be explained later. Thus, during the change of walking direction, the synaptic input from sense organs to NSIs could be changed and therefore generate a different, distributed output to the leg MNs via parallel antagonistic pathways to achieve backward walking. This has been shown for signals from trochanteral campaniform sensilla to subcoxal MNs (Akay et al., 2007). Because NSIs re1 and pe2 actually show a changed activity, signals from those could 'overrule' the output of E4 to protractor MNs in backward stepping. The synaptic output of E4 to extensor and levator MNs during backward walking would be uninfluenced by that, because in these MN pools no qualitative change

in activity occurred during the changed walking direction. Since already during forward walking no strong correlation of the membrane potential of E4 and protractor MNs could be shown, the fact that this is also the case during backward walking is not an argument for the assumptions made above.

Related to the switch in walking direction, a recent study by Toth et al. (2012) introduced a neuromechanical model of the stick insect neuromuscular system. They presented a mechanism, by which the switch from forward to backward walking could be achieved. In the model, the ThC-joint CPG has excitatory connections to interneurons which inhibit the protractor and retractor MNs pools and thus control their motor output. A switch in the ThC-joint control system is generated by introducing additional connections to these intercalated interneurons, reversed to the original connections, and a presynaptic inhibition of the original connections via central, descending input. Therefore, the activity of the CPG does not have to be changed to achieve a switch in the walking direction. Toth et al. (2012) argued that a change of the oscillatory state of the CPG neurons to change the walking direction would result in a too long transition time to achieve step-to-step switches from forward to backward walking. This can occur in curve walking, where, depending on the steepness of the curve, a backward directed step can occur directly after a forward directed step. They suggest that this hypothesis could be tested by recordings of NSI E4 during forward and backward stepping, because E4 could be part of the CPG related to the ThC-joint. If no change in the activity of E4 would occur, this would prove their hypothesis. Results from my experiments confirm the hypothesis, but since E4 is only known to be part of the CPGs related to the CTr- and FTi-joint (Büschges, 1995), it has to be further investigated in how far E4 contributes to the pattern generation of the ThC-joint.

General features of premotor nonspiking interneurons In Fig. 4.4, synaptic connections of NSIs recorded in this study to leg MN pools are depicted. It is apparent that the majority of NSIs either found here or previously described, only influence one or two MN pools of one leg joint. Only some NSIs provide synaptic drive to MN pools of two or even three leg joints (E4, I4, Ee.Le1, DFs). This suggests that the majority of nonspiking interneurons in the stick insect mesothoracic ganglion have connections to MN pools of only one leg joint. The total number of local nonspiking interneurons in an insect ganglion can only be estimated. Siegler (1985) suggested that there are 100 NSIs in each hemiganglion. Wilson (1981) showed that at least some NSIs are uniquely identifiable and exist as individuals. However, at least two copies of NSI E4 exist in the stick insect mesothoracic ganglion (Büschges et al., 1994). The morphology of NSIs can be diverse, and the location of the cell body has no implications for the physiology

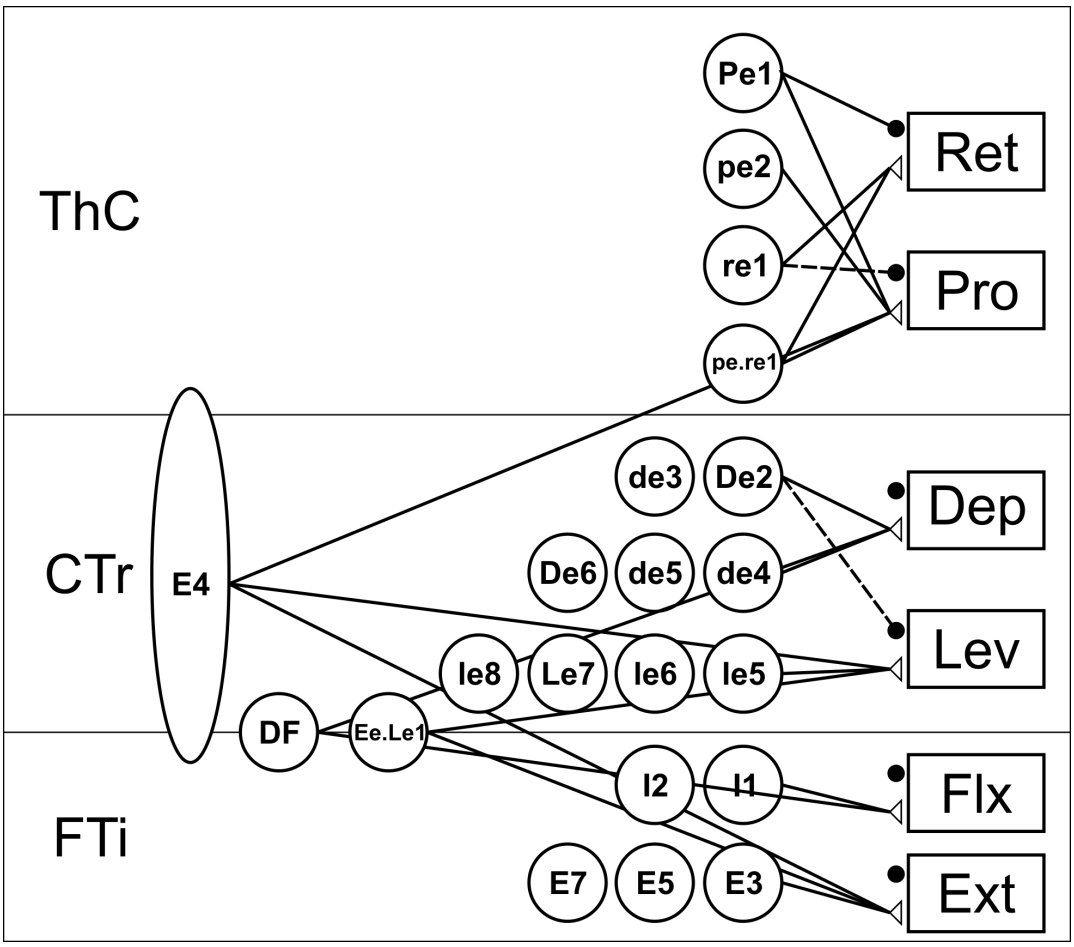

Figure 4.4 – Scheme of the synaptic connections of recorded NSIs. The three big boxes each symbolize the leg joint control system for a joint: thorax-coxa (ThC), coxa-trochanter (CTr) and femur-tibia (FTi) joint. In circles, NSI types, which were recorded in this thesis, are shown with their synaptic connections to MN pools (small boxes). Open triangles mark excitatory connections, filled circles inhibitory connections. NSIs with the same synaptic connections are drawn on one horizontal line. NSIs which are part of more than one leg joint control network (DF, Ee.Le1, E4) are drawn on the borders of the boxes. Dashed lines show connections that were not found in every recorded neuron of this type. It is unclear, if all of the connections are monosynaptical. Neurons presynaptic to the NSIs are not shown.

or connectivity of a neuron. Yet, the neurites of NSIs are known to overlap with the neurites of motor neurons, local and intersegmental interneurons, and sensory neurons (Burrows, 1996). Furthermore, pre- and postsynaptic sites on NSIs can be mixed in the same regions, which provides an anatomical basis for restricted local processing (Wilson and Phillips, 1983). This would have major implications for the understanding of the local network, since in this case not only the connectivity between single neurons would be necessary to reveal the network function, but single compartments of neurons would also have the ability to locally compute distinct network functions.

Some of the nonspiking interneurons, which provide excitatory drive to depressor motoneurons (De2, de4), are modulated with stepping such that an inhibition at the start of the swing phase is apparent, and sometimes a slight depolarization in the stance phase, while their membrane potential is a resting level in the bigger part of the step cycle. Only at the onset of swing, depressor activity has to be inhibited because the leg has to lift. But, in the main course of the step cycle, an active depression is needed, because the leg has to be depressed at late swing and during stance to support the weight of the animal (see sec. 3.1.6). In consistence with that, the slow depressor MN (Fig. 3.17B) is spiking throughout the step cycle with an inhibition only during early swing, and an increased spike frequency in stance. This suggests, that the slow depressor MN receives constant synaptic input from some of its premotor NSIs. Studies from Burrows and Siegler (1978); Wilson and Phillips (1982, 1983) showed that some premotor NSIs in the locust tonically release transmitter and thus continuously excite postsynaptic MNs. One type of NSI for which this applied was necessary for maintaining posture (Burrows and Siegler, 1978). For NSIs De2, de3 and/or de4 this might be the case in the stick insect.

The 'parliamentary principle' or distributed processing NSIs providing excitatory synaptic input to extensor MNs can be active in the phase of the step cycle that is opposed to the synaptic drive they exert. For example NSI E6 excites extensor MNs, which are active in the swing phase of the step cycle. However, E6 is depolarized in stance during single leg stepping on a treadwheel (von Uckermann and Büschges, 2009). This is also true for NSI E7 during forward stepping. In my thesis, also one depressor NSI is shown, De6, whose phase of activity in the step cycle opposes its synaptic output to depressor MNs. It was already mentioned, that NSIs integrate signals from sense organs and descending sources, and contribute to the control of timing and magnitude of the motor output. The observation that a population of NSIs which show differing responses to these inputs but still show a clear influence on a postsynaptic MN pool, was termed the parlia-

mentary principle by Bässler (1993). It originally described information pathways participating in the generation of the resistance reflex. Thus, such a neural network includes not only parallel but also antagonistic pathways (e.g. see Bässler and Büschges, 1998; Büschges et al., 1999). This kind of information processing is also called 'distributed processing' and was investigated in many other systems. It was thoroughly described for the leech bending behavior (Lockery and Kristan, 1990a,b, reviewed in Kristan et al., 1995; Kristan and Shaw, 1997). Thus, the term distributed processing must be distinguished from a dedicated processing, in which connections between neurons only support one motor response. Kristan et al. (1995) also pointed out the advantages of a distributed network. It is very efficient, because if a combination of interneurons produces different behaviors, the theoretical number of generated behaviors is very high (see also Bässler, 1993). Furthermore, such a network of neurons is able to fine control a certain movement very well over a wide range by weighting the contributions of the involved neurons, a strategy which is called population coding. Since a stick insect, navigating through bushes, needs a continuum of possible leg positions, this mechanism is able to ensure such a behavior.

Neural control of forward and backward walking In the present study, all investigated NSIs showed activity modulated with the step cycle for two different, but very related behaviors, forward and backward walking. Only in NSIs controlling the ThC-joint, a change in the activity phase could be observed. Thus, the change in movement is achieved by the same set of NSIs, MNs, and muscles. This has been also shown for other invertebrates and vertebrates, at least for MNs and muscles (e.g. lamprey: Grillner et al., 1995). However, a recent study in the nematode C. elegans, which locomotes by a sequential contraction of body wall motoneurons, showed that two populations of motoneurons are coactive during forward locomotion, but only one of those is active during backward locomotion (Haspel et al., 2010). This suggests, that there are motoneurons which are dedicated to either of the tested locomotion directions. A recent study in the lamprey investigated the descending inputs from reticulospinal neurons to spinal motor networks (Zelenin, 2011). Those glutamatergic neurons project from the reticular formation in the brainstem to motor centers in the spinal cord, where they activate motoneurons and interneurons. The higher the level of activity in these reticulospinal neurons, the faster the animal will locomote (Grillner et al., 1995; Deliagina et al., 2000). Lamprey backward swimming underlies the same activation of the motor system but has few kinematical changes (Islam et al., 2006). That is similar to the the zebrafish (Zhu et al., 2009), which implies that, at least for vertebrate swimming, the change in the swim direction is not simply a reversed motor program for forward

swimming (Zhu et al., 2009; Orger et al., 2008). However, Zelenin (2011) showed that the majority of reticulospinal neurons activated during locomotion were active during forward and backward swimming, a bigger portion only during forward, and a smaller portion only during backward swimming. This suggests that descending drive from reticulospinal neurons discriminates between swim directions.

In insects, it remains largely unclear if signals responsible for the switch in walking direction derive from head ganglia or are generated in the thoracic nerve cord, and in which manner descending signals contribute to different motor outputs. Some studies dealt more generally with that issue. Gal and Libersat (2006) showed in lesioning experiments with cockroaches, in which they were able to separately remove descending inputs from the brain, the subesophageal ganglion (SEG), or both, that brain inputs inhibit walking and SEG inputs are needed for the initiation of walking. SEG inputs also seem to be necessary for an appropriate inter-leg coordination during walking (Gal and Libersat, 2006). Furthermore, emergency behaviors like escape, righting or swimming can be elicited without inputs from either of the head ganglia. Another study investigated the effect of cutting the neck connectives (and thus disconnecting the brain and the SEG) and showed an alteration of thoracic reflexes (Mu and Ritzmann, 2008a,b). One important structure in the insect brain which controls higher locomotor functions is the central complex (Strauss, 2002). In the cockroach central complex, cell ensembles were found whose activity corresponded to turning behavior, and preceded changes in turning speed (Guo and Ritzmann, 2013). Furthermore, potential higher order neurons which control the walking direction were found recently in the fruit fly *Drosophila melanogaster* (Bidaye, 2012). A recent study even suggested a homology of the central complex with the basal ganglia in vertebrates (Strausfeld and Hirth, 2013).

In conclusion, in this thesis I described the contributions of premotor nonspiking interneurons, leg motoneurons, and leg muscles in the generation of different walking directions and walking speeds. In the single-leg preparation, in which fictive forward and backward walking can be reliably elicited, all investigated NSIs contribute to the generation of the leg motor output during both walking directions. Furthermore, newly described NSIs which provide synaptic drive to MNs of the ThC-joint were shown to contribute to a change in subcoxal MN activity between forward and backward walking. Leg motoneurons receive similar synaptic inputs during both walking directions, a tonic depolarizing input throughout walking and phasic excitatory and inhibitory inputs in the according phase of the step cycle. Only the phase of activity in which phasic inputs occur reverses in protractor and retractor MNs with a change in walking direction. Furthermore,

the stepping velocity of the single leg, stepping on a treadwheel, was shown to be correlated only to flexor MN activity, but not to the activity of other stance phase MNs. Analyses of muscle activity and timing in stick insects freely walking on a slippery surface showed that also in a more naturally walking situation the most pronounced changes in muscle activity during forward, backward, and curve walking occur in protractor and retractor muscles which are responsible for an anterior and posterior directed movement of the leg.

Bibliography

Akay, T., 2002. The Role of Sensory Signals for Interjoint Coordination in Stick Insect Legs (Carausius morosus and Cuniculina impigra). Phd thesis, University of Cologne.

Akay, T., Bässler, U., Gerharz, P., Büschges, A., Feb. 2001. The role of sensory signals from the insect coxa-trochanteral joint in controlling motor activity of the femur-tibia joint. Journal of Neurophysiology 85 (2), 594–604.

Akay, T., Büschges, A., Dec. 2006. Load signals assist the generation of movement-dependent reflex reversal in the femur-tibia joint of stick insects. Journal of Neurophysiology 96 (6), 3532–7.

Akay, T., Haehn, S., Schmitz, J., Büschges, A., Jul. 2004. Signals from load sensors underlie interjoint coordination during stepping movements of the stick insect leg. Journal of Neurophysiology 92 (1), 42–51.

Akay, T., Ludwar, B. C., Göritz, M. L., Schmitz, J., Büschges, A., Mar. 2007. Segment specificity of load signal processing depends on walking direction in the stick insect leg muscle control system. Journal of Neuroscience 27 (12), 3285–94.

Alexander, R. M., Oct. 1989. Optimization and gaits in the locomotion of vertebrates. Physiological reviews 69 (4), 1199–227.

Ashley-Ross, M. A., Lauder, G. V., Dec. 1997. Motor patterns and kinematics during backward walking in the pacific giant salamander: evidence for novel motor output. Journal of Neurophysiology 78 (6), 3047–60.

Ausborn, J., Mahmood, R., El Manira, A., Dec. 2012. Decoding the rules of recruitment of excitatory interneurons in the adult zebrafish locomotor network. Proceedings of the National Academy of Sciences of the United States of America 109 (52), E3631–9.

Ayers, J. L., Davis, W. J., 1977. Neuronal control of locomotion in the lobster,Homarus americanus. Journal of Comparative Physiology A 115 (1), 1–27.

Bässler, U., Aug. 1967. On the regulation of the position of the femur-tibial joint of the walking-stick insect Carausius morosus at rest and in motion. Kybernetik 4 (1), 18–26.

Bässler, U., Jul. 1972. "Knee-tendon reflex" in Carausius morosus: transition function and frequency. Kybernetik 11 (1), 32–50.

Bässler, U., 1993. The femur-tibia control system of stick insects–a model system for the study of the neural basis of joint control. Brain Research Reviews 18 (2), 207–26.

Bässler, U., Büschges, A., Jun. 1998. Pattern generation for stick insect walking movements-multisensory control of a locomotor program. Brain Research Reviews 27 (1), 65–88.

Bässler, U., Sauer, A. E., Büschges, A., Aug. 2003. Vibration signals from the FT joint can induce phase transitions in both directions in motoneuron pools of the stick insect walking system. Journal of Neurobiology 56 (2), 125–38.

Berens, P., 2009. CircStat: A MATLAB toolbox for circular statistics. J Stat Software 31, 1–21.

Berg, E., Büschges, A., Schmidt, J., Mar. 2013. Single perturbations cause sustained changes in searching behavior in stick insects. Journal of Experimental Biology 216 (Pt 6), 1064–74.

Bidaye, S. S., 2012. Neuronal basis for directed walking in Drosophila melanogaster. Dissertation, University of Wien.

Blaesing, B., Cruse, H., Mar. 2004. Stick insect locomotion in a complex environment: climbing over large gaps. Journal of Experimental Biology 207 (Pt 8), 1273–86.

Borgmann, A., Hooper, S. L., Büschges, A., Mar. 2009. Sensory feedback induced by front-leg stepping entrains the activity of central pattern generators in caudal segments of the stick insect walking system. Journal of Neuroscience 29 (9), 2972–83.

Borgmann, A., Scharstein, H., Büschges, A., Sep. 2007. Intersegmental coordination: influence of a single walking leg on the neighboring segments in the stick insect walking system. Journal of Neurophysiology 98 (3), 1685–96.

Borgmann, A., Toth, T. I., Gruhn, M., Daun-Gruhn, S., Büschges, A., Jan. 2012. Dominance of local sensory signals over inter-segmental effects in a motor system: experiments. Biological Cybernetics (2011), 399–411.

Bowerman, R. F., 1981. Arachnid locomotion. In: Locomotion and Energetics in Arthropods. Plenum Press, New York, pp. 73–102.

Bräunig, P., Pflüger, H.-J., 2001. The Unpaired Median Neurons of Insects. Advances in Insect Physiology 28, 185–IN2.

Brunn, D. E., Jun. 1998. Cooperative mechanisms between leg joints of Carausius morosus I. Nonspiking interneurons that contribute to interjoint coordination. Journal of Neurophysiology 79 (6), 2964–76.

Brunn, D. E., Heuer, A., Jun. 1998. Cooperative mechanisms between leg joints of Carausius morosus II. Motor neuron activity and influence of conditional bursting interneuron. Journal of Neurophysiology 79 (6), 2977–85.

Bucher, D., Akay, T., DiCaprio, R. A., Büschges, A., Mar. 2003. Interjoint coordination in the stick insect leg-control system: the role of positional signaling. Journal of Neurophysiology 89 (3), 1245–55.

Buford, J. a., Smith, J. L., Sep. 1990. Adaptive control for backward quadrupedal walking. II. Hindlimb muscle synergies. Journal of Neurophysiology 64 (3), 756–66.

Buford, J. a., Zernicke, R. F., Smith, J. L., Sep. 1990. Adaptive control for backward quadrupedal walking. I. Posture and hindlimb kinematics. Journal of Neurophysiology 64 (3), 745–55.

Burrows, M., Jul. 1979. Graded synaptic interactions between local premotor interneurons of the locust. Journal of Neurophysiology 42 (4), 1108–23.

Burrows, M., Oct. 1987. Inhibitory interactions between spiking and nonspiking local interneurons in the locust. Journal of Neuroscience 7 (10), 3282–92.

Burrows, M., Sep. 1989. Processing of mechanosensory signals in local reflex pathways of the locust. Journal of Experimental Biology 146, 209–27.

Burrows, M., 1996. The Neurobiology of an insect brain. Oxford University Press, Oxford.

Burrows, M., Siegler, M. V. S., 1976. Transmission without spikes between locust interneurones and motoneurons. Nature.

Burrows, M., Siegler, M. V. S., Dec. 1978. Graded synaptic transmission between local interneurones and motor neurones in the metathoracic ganglion of the locust. Journal of Physiology 285, 231–55.

Büschges, A., 1989. Processing of sensory input from the femoral chordotonal organ by spiking interneurones of stick insects. Journal of Experimental biology 111, 81–111.

Büschges, A., 1990. Nonspiking pathways in a joint-control loop of the stick insect Carausius morosus. Journal of Experimental biology 160, 133–160.

Büschges, A., Aug. 1995. Role of local nonspiking interneurons in the generation of rhythmic motor activity in the stick insect. Journal of Neurobiology 27 (4), 488–512.

Büschges, A., Mar. 2005. Sensory control and organization of neural networks mediating coordination of multisegmental organs for locomotion. Journal of Neurophysiology 93 (3), 1127–35.

Büschges, A., Akay, T., Gabriel, J. P., Schmidt, J., Jan. 2008. Organizing network action for locomotion: insights from studying insect walking. Brain Research Reviews 57 (1), 162–71.

Büschges, A., Gruhn, M., 2008. Mechanosensory feedback in walking: from joint control to locomotor patterns. Advances in Insect Physiology 34 (07).

Büschges, A., Kittmann, R., Schmitz, J., Jun. 1994. Identified nonspiking interneurons in leg reflexes and during walking in the stick insect. Journal of Comparative Physiology A 174 (6), 685–700.

Büschges, A., Ludwar, B. C., Bucher, D., Schmidt, J., DiCaprio, R. A., Apr. 2004. Synaptic drive contributing to rhythmic activation of motoneurons in the deafferented stick insect walking system. European Journal of Neuroscience 19 (7), 1856–62.

Büschges, A., Manira, A. E., Dec. 1998. Sensory pathways and their modulation in the control of locomotion. Current Opinion in Neurobiology 8 (6), 733–9.

Büschges, A., Sauer, A. E., Bässler, U., 1999. Flexibility of a propioreceptive feedback system results from its "parliamentary" (distributed) organization. Prerational intelligence: adaptive behavior and intelligent systems without symbols and logic 1, 267–286.

Büschges, A., Schmitz, J., Apr. 1991. Nonspiking pathways antagonize the resistance reflex in the thoraco-coxal joint of stick insects. Journal of Neurobiology 22 (3), 224–37.

Büschges, A., Schmitz, J., Bässler, U., Jan. 1995. Rhythmic patterns in the thoracic nerve cord of the stick insect induced by pilocarpine. Journal of Experimental Biology 198 (Pt 2), 435–56.

Büschges, A., Wolf, H., May 1995. Nonspiking local interneurons in insect leg motor control. I. Common layout and species-specific response properties of femur-tibia joint control pathways in stick insect and locust. Journal of Neurophysiology 73 (5), 1861–75.

Camhi, J. M., Nolen, T. G., 1981. Properties of the escape system of cockroaches during walking. Journal of Comparative Physiology A 142 (3), 339–346.

Chasserat, C., Clarac, F., 1980. Interlimb coordinating factors during driven walking in Crustacea. Journal of Comparative Physiology A 139 (4), 293–306.

Clarac, F., Cattaert, D., Le Ray, D., May 2000. Central control components of a 'simple' stretch reflex. Trends in Neurosciences 23 (5), 199–208.

Cruse, H., 1976a. The control of body position in the stick insect (Carausius morosus), when walking over uneven surfaces. Biological Cybernetics 24 (1), 25–33.

Cruse, H., 1976b. The function of the legs in the free walking stick insect,Carausius morosus. Journal of Comparative Physiology A 112 (2), 235–262.

Cruse, H., 1985. Coactivating influences between neighbouring legs in walking insects. Journal of Experimental Biology 114 (1), 513–519.

Cruse, H., Jan. 1990. What mechanisms coordinate leg movement in walking arthropods? Trends in Neurosciences 13 (1), 15–21.

Cruse, H., Bartling, C., Sep. 1995. Movement of joint angles in the legs of a walking insect, Carausius morosus. Journal of Insect Physiology 41 (9), 761–771.

Cruse, H., Dean, J., Suilmann, M., Sep. 1984. The contributions of diverse sense organs to the control of leg movement by a walking insect. Journal of Comparative Physiology A 154 (5), 695–705.

Cruse, H., Ehmanns, I., Stübner, S., Schmitz, J., Mar. 2009. Tight turns in stick insects. Journal of Comparative Physiology. A, Neuroethology, sensory, neural, and behavioral physiology 195 (3), 299–309.

Cruse, H., Kindermann, T., Schumm, M., Dean, J., Schmitz, J., Oct. 1998. Walknet-a biologically inspired network to control six-legged walking. Neural networks : the official journal of the International Neural Network Society 11 (7-8), 1435–1447.

Cruse, H., Kühn, S., Park, S., Schmitz, J., Dec. 2004. Adaptive control for insect leg position: controller properties depend on substrate compliance. Journal of Comparative Physiology. A, Neuroethology, sensory, neural, and behavioral physiology 190 (12), 983–91.

Cruse, H., Pflüger, H.-J., 1981. Is the position of the femur-tibia joint under feedback control in the walking stick insect ? II. Electrophysiological recordings. Journal of experimental biology (92), 97–107.

Cruse, H., Schmitz, J., Braun, U., Schweins, A., 1993. Control of body height in a stick insect walking. Journal of Experimental biology 155, 141–155.

Dean, J., Schmitz, J., Dec. 1992. The two groups of sensilla in the ventral coxal hairplate of Carausius morosus have different roles during walking. Physiological Entomology 17 (4), 331–341.

Delcomyn, F., Mar. 1989. Walking in the American cockroach: the timing of motor activity in the legs during straight walking. Biological Cybernetics 60 (5).

Deliagina, T. G., Zelenin, P. V., Fagerstedt, P., Grillner, S., Orlovsky, G. N., Feb. 2000. Activity of reticulospinal neurons during locomotion in the freely behaving lamprey. Journal of Neurophysiology 83 (2), 853–63.

Driesang, R. B., Büschges, A., 1993. The neural basis of catalepsy in the stick insect IV . Properties of nonspiking interneurons. Journal of Comparative Physiology A: Sensory, Neural, and Behavioral Physiology.

Dürr, V., Ebeling, W., Jun. 2005. The behavioural transition from straight to curve walking: kinetics of leg movement parameters and the initiation of turning. Journal of Experimental Biology 208 (Pt 12), 2237–52.

Eckert, R., 2000. Tierphysiologie. Georg Thieme Verlag.

Epstein, S., Graham, D., 1983. Behaviour and motor output of stick insects walking on a slippery surface: I. Forward walking. Journal of Experimental Biology 105, 215–229.

Fischer, H., Schmidt, J., Haas, R., Büschges, A., Jan. 2001. Pattern generation for walking and searching movements of a stick insect leg. I. Coordination of motor activity. Journal of Neurophysiology 85 (1), 341–53.

Frantsevich, L. I., Mokrushov, P. A., 1980. Turning and righting in Geotrupes (Coleoptera, Scarabaeidae). Journal of Comparative Physiology A 136 (4), 279–289.

Frye, M. A., Dickinson, M. H., Nov. 2001. Fly flight: a model for the neural control of complex behavior. Neuron 32 (3), 385–8.

Frye, M. a., Dickinson, M. H., Dec. 2004. Closing the loop between neurobiology and flight behavior in Drosophila. Current opinion in neurobiology 14 (6), 729–36.

Gabriel, J. P., 2005. Activity of leg motoneurons during single leg walking of the stick insect : From synaptic inputs to motor performance.

Gabriel, J. P., Ausborn, J., Ampatzis, K., Mahmood, R., Eklöf-Ljunggren, E., El Manira, A., Jan. 2011. Principles governing recruitment of motoneurons during swimming in zebrafish. Nature Neuroscience 14 (1), 93–9.

Gabriel, J. P., Büschges, A., Jan. 2007. Control of stepping velocity in a single insect leg during walking. Philosophical transactions. Series A, Mathematical, physical, and engineering sciences 365 (1850), 251–71.

Gabriel, J. P., Scharstein, H., Schmidt, J., Büschges, A., Sep. 2003. Control of flexor motoneuron activity during single leg walking of the stick insect on an electronically controlled treadwheel. Journal of Neurobiology 56 (3), 237–51.

Gal, R., Libersat, F., Sep. 2006. New vistas on the initiation and maintenance of insect motor behaviors revealed by specific lesions of the head ganglia. Journal of comparative physiology. A, Neuroethology, sensory, neural, and behavioral physiology 192 (9), 1003–20.

Getting, P. A., Lennard, P. R., Hume, R. I., Jul. 1980. Central pattern generator mediating swimming in Tritonia. I. Identification and synaptic interactions. Journal of Neurophysiology 44 (1), 151–64.

Goldammer, J., Büschges, A., Schmidt, J., Feb. 2012. Motoneurons, DUM cells, and sensory neurons in an insect thoracic ganglion: a tracing study in the stick insect Carausius morosus. Journal of Comparative Neurology 520 (2), 230–57.

Gosgnach, S., Lanuza, G. M., Butt, S. J. B., Saueressig, H., Zhang, Y., Velasquez, T., Riethmacher, D., Callaway, E. M., Kiehn, O., Goulding, M., Mar. 2006. V1 spinal neurons regulate the speed of vertebrate locomotor outputs. Nature 440 (7081), 215–9.

Goulding, M., Jul. 2009. Circuits controlling vertebrate locomotion: moving in a new direction. Nature reviews. Neuroscience 10 (7), 507–18.

Grabowska, M., Godlewska, E., Schmidt, J., Daun-Gruhn, S., Dec. 2012. Quadrupedal gaits in hexapod animals - inter-leg coordination in free-walking adult stick insects. Journal of Experimental Biology 215 (Pt 24), 4255–66.

Graham, D., 1972. A behavioural analysis of the temporal organisation of walking movements in the 1st instar and adult stick insect (Carausius morosus). Journal of Comparative Physiology 81 (1), 23–52.

Graham, D., 1985. Pattern and control of walking in insects. Academic Press, London.

Graham, D., Epstein, S., 1985. Behaviour and motor output for an insect walking on a slippery surface: II. Backward walking. Journal of Experimental Biology 296, 287–296.

Grillner, S., Dec. 1999. Bridging the gap - from ion channels to networks and behaviour. Current opinion in neurobiology 9 (6), 663–9.

Grillner, S., Jul. 2003. The motor infrastructure: from ion channels to neuronal networks. Nature reviews. Neuroscience 4 (7), 573–86.

Grillner, S., Deliagina, T. G., Ekeberg, O., El Manira, A., Hill, R. H., Lansner, A., Orlovsky, G. N., Wallén, P., Jun. 1995. Neural networks that co-ordinate

locomotion and body orientation in lamprey. Trends in neurosciences 18 (6), 270–9.

Grillner, S., Zangger, P., Jan. 1979. On the central generation of locomotion in the low spinal cat. Experimental Brain Research 34 (2), 241–261.

Gruhn, M., Hoffmann, O., Dübbert, M., Scharstein, H., Büschges, A., Dec. 2006. Tethered stick insect walking: a modified slippery surface setup with optomotor stimulation and electrical monitoring of tarsal contact. Journal of Neuroscience Methods 158 (2), 195–206.

Gruhn, M., Rosenbaum, P., Bollhagen, H.-P., Büschges, A., Jan. 2011. Studying the neural basis of adaptive locomotor behavior in insects. Journal of visualized experiments : JoVE (50), 1–6.

Gruhn, M., von Uckermann, G., Westmark, S., Wosnitza, A., Büschges, A., Borgmann, A., Aug. 2009a. Control of stepping velocity in the stick insect Carausius morosus. Journal of Neurophysiology 102 (2), 1180–92.

Gruhn, M., Zehl, L., Büschges, A., Jan. 2009b. Straight walking and turning on a slippery surface. Journal of Experimental Biology 212 (Pt 2), 194–209.

Guo, P., Ritzmann, R. E., Mar. 2013. Neural activity in the central complex of the cockroach brain is linked to turning behaviors. Journal of Experimental Biology 216 (Pt 6), 992–1002.

Guschlbauer, C., Scharstein, H., Büschges, A., Mar. 2007. The extensor tibiae muscle of the stick insect: biomechanical properties of an insect walking leg muscle. Journal of Experimental Biology 210 (Pt 6), 1092–108.

Haspel, G., O'Donovan, M. J., Hart, A. C., Aug. 2010. Motoneurons dedicated to either forward or backward locomotion in the nematode Caenorhabditis elegans. Journal of Neuroscience 30 (33), 11151–6.

Hedwig, B., Pearson, K. G., Sep. 1984. Patterns of synaptic input to identified flight motoneurons in the locust. Journal of Comparative Physiology A 154 (5), 745–760.

Hellekes, K., Blincow, E., Hoffmann, J., Büschges, A., Jan. 2012. Control of reflex reversal in stick insect walking: effects of intersegmental signals, changes in direction, and optomotor-induced turning. Journal of Neurophysiology 107 (1), 239–49.

Hengstenberg, R., Nov. 1977. Spike responses of 'non-spiking' visual interneurone. Nature 270 (5635), 338–40.

Hess, D., 1998. Neuronale Grundlagen der sensomotorischen Informationsverarbeitung zwischen zwei Beingelenken in der Stabheuschrecke. Dissertation, University of Kaiserslautern.

Hess, D., Büschges, A., Dec. 1997. Sensorimotor pathways involved in interjoint reflex action of an insect leg. Journal of Neurobiology 33 (7), 891–913.

Hess, D., Büschges, A., Apr. 1999. Role of proprioceptive signals from an insect femur-tibia joint in patterning motoneuronal activity of an adjacent leg joint. Journal of Neurophysiology 81 (4), 1856–65.

Hooper, S. L., Guschlbauer, C., Blümel, M., Rosenbaum, P., Gruhn, M., Akay, T., Büschges, A., Apr. 2009. Neural control of unloaded leg posture and of leg swing in stick insect, cockroach, and mouse differs from that in larger animals. Journal of Neuroscience 29 (13), 4109–19.

Hooper, S. L., Guschlbauer, C., von Uckermann, G., Büschges, A., Feb. 2007a. Different motor neuron spike patterns produce contractions with very similar rises in graded slow muscles. Journal of Neurophysiology 97 (2), 1428–44.

Hooper, S. L., Guschlbauer, C., von Uckermann, G., Büschges, A., Sep. 2007b. Slow temporal filtering may largely explain the transformation of stick insect (Carausius morosus) extensor motor neuron activity into muscle movement. Journal of Neurophysiology 98 (3), 1718–32.

Hughes, G. M., 1952. The Co-Ordination of Insect Movements. I. The Walking Movements of Insects. Journal of Experimental Biology 29 (2), 267–285.

Islam, S. S., Zelenin, P. V., Orlovsky, G. N., Grillner, S., Deliagina, T. G., Jul. 2006. Pattern of motor coordination underlying backward swimming in the lamprey. Journal of Neurophysiology 96 (1), 451–60.

Jander, J. P., 1982. Untersuchungen zum Mechanismus und zur zentralnervösen Steuerung des Kurvenlaufs bei Stabheuschrecken (Carausius morosus). Dissertation, University of Cologne.

Jindrich, D. L., Full, R. J., Jun. 1999. Many-legged maneuverability: dynamics of turning in hexapods. Journal of Experimental Biology 202 (Pt 12, 1603–23.

Jing, J., Sasaki, K., Perkins, M. H., Siniscalchi, M. J., Ludwar, B. C., Cropper, E. C., Weiss, K. R., Oct. 2011. Coordination of distinct motor structures through remote axonal coupling of projection interneurons. Journal of Neuroscience 31 (43), 15438–49.

Kiehn, O., Jan. 2006. Locomotor circuits in the mammalian spinal cord. Annual Review of Neuroscience 29, 279–306.

Kittmann, R., Schmitz, J., Büschges, A., Dec. 1996. Premotor interneurons in generation of adaptive leg reflexes and voluntary movements in stick insects. Journal of Neurobiology 31 (4), 512–32.

Knops, S. A., Toth, T. I., Guschlbauer, C., Gruhn, M., Daun-Gruhn, S., Nov. 2012. A neuro-mechanical model for the neural basis of curve walking in the stick insect. Journal of Neurophysiology (November 2012), 679–691.

Kristan, W. B., Calabrese, R. L., Friesen, W. O., Aug. 2005. Neuronal control of leech behavior. Progress in Neurobiology 76 (5), 279–327.

Kristan, W. B., Lockery, S. R., Lewis, J. E., Jul. 1995. Using reflexive behaviors of the medicinal leech to study information processing. Journal of Neurobiology 27 (3), 380–9.

Kristan, W. B., Shaw, B. K., Dec. 1997. Population coding and behavioral choice. Current Opinion in Neurobiology 7 (6), 826–31.

Lamb, T., Yang, J. F., May 2000. Could different directions of infant stepping be controlled by the same locomotor central pattern generator? Journal of Neurophysiology 83 (5), 2814–24.

Laurent, G., Burrows, M., Sep. 1988. Direct excitation of nonspiking local interneurones by exteroceptors underlies tactile reflexes in the locust. Journal of Comparative Physiology A 162 (5), 563–572.

Laurent, G., Burrows, M., Sep. 1989. Intersegmental interneurons can control the gain of reflexes in adjacent segments of the locust by their action on nonspiking local interneurons. Journal of Neuroscience 9 (9), 3019–29.

Li, W.-C., Moult, P. R., May 2012. The control of locomotor frequency by excitation and inhibition. Journal of Neuroscience 32 (18), 6220–30.

Lockery, S. R., Kristan, W. B., Jun. 1990a. Distributed processing of sensory information in the leech. I. Input-output relations of the local bending reflex. Journal of Neuroscience 10 (6), 1816–29.

Lockery, S. R., Kristan, W. B., Jun. 1990b. Distributed processing of sensory information in the leech. II. Identification of interneurons contributing to the local bending reflex. Journal of Neuroscience 10 (6), 1816–29.

Ludwar, B. C., Göritz, M. L., Schmidt, J., Mar. 2005a. Intersegmental coordination of walking movements in stick insects. Journal of Neurophysiology 93 (3), 1255–65.

Ludwar, B. C., Westmark, S., Büschges, A., Schmidt, J., Oct. 2005b. Modulation of membrane potential in mesothoracic moto- and interneurons during stick insect front-leg walking. Journal of Neurophysiology 94 (4), 2772–84.

Marder, E., Bucher, D., Nov. 2001. Central pattern generators and the control of rhythmic movements. Current Biology 11 (23), R986–96.

Marder, E., Bucher, D., Jan. 2007. Understanding circuit dynamics using the stomatogastric nervous system of lobsters and crabs. Annual Review of Physiology 69, 291–316.

Marder, E., Calabrese, R. L., Jul. 1996. Principles of rhythmic motor pattern generation. Physiological reviews 76 (3), 687–717.

Marder, E., Eisen, J. S., Jun. 1984. Electrically coupled pacemaker neurons respond differently to same physiological inputs and neurotransmitters. Journal of Neurophysiology 51 (6), 1362–74.

McLean, D. L., Masino, M. a., Koh, I. Y. Y., Lindquist, W. B., Fetcho, J. R., Dec. 2008. Continuous shifts in the active set of spinal interneurons during changes in locomotor speed. Nature Neuroscience 11 (12), 1419–29.

Mendelson, M., Mar. 1971. Oscillator neurons in crustacean ganglia. Science 171 (3976), 1170–3.

Mu, L., Ritzmann, R. E., Nov. 2005. Kinematics and motor activity during tethered walking and turning in the cockroach, Blaberus discoidalis. Journal of Comparative Physiology. A, Neuroethology, sensory, neural, and behavioral physiology 191 (11), 1037–54.

Mu, L., Ritzmann, R. E., Mar. 2008a. Interaction between descending input and thoracic reflexes for joint coordination in cockroach: I. descending influence on thoracic sensory reflexes. Journal of Comparative Physiology. A, Neuroethology, sensory, neural, and behavioral physiology 194 (3), 299–312.

Mu, L., Ritzmann, R. E., Mar. 2008b. Interaction between descending input and thoracic reflexes for joint coordination in cockroach. II comparative studies on tethered turning and searching. Journal of comparative physiology. A, Neuroethology, sensory, neural, and behavioral physiology 194 (3), 299–312.

Mulloney, B., Jul. 2003. During fictive locomotion, graded synaptic currents drive bursts of impulses in swimmeret motor neurons. Journal of Neuroscience 23 (13), 5953–62.

Mulloney, B., Smarandache-Wellmann, C., Feb. 2012. Neurobiology of the crustacean swimmeret system. Progress in Neurobiology 96 (2), 242–67.

Musienko, P. E., Zelenin, P. V., Lyalka, V. F., Gerasimenko, Y., Orlovsky, G. N., Deliagina, T. G., Nov. 2012. Spinal and supraspinal control of the direction of stepping during locomotion. Journal of Neuroscience 32 (48), 17442–53.

Noah, J. A., Quimby, L., Frazier, S. F., Zill, S. N., Mar. 2004. Sensing the effect of body load in legs: responses of tibial campaniform sensilla to forces applied to the thorax in freely standing cockroaches. Journal of Comparative Physiology. A, Neuroethology, sensory, neural, and behavioral physiology 190 (3), 201–15.

Nusbaum, M. P., Blitz, D. M., Swensen, A. M., Wood, D., Marder, E., Mar. 2001. The roles of co-transmission in neural network modulation. Trends in neurosciences 24 (3), 146–54.

Orger, M. B., Kampff, A. R., Severi, K. E., Bollmann, J. H., Engert, F., Mar. 2008. Control of visually guided behavior by distinct populations of spinal projection neurons. Nature Neuroscience 11 (3), 327–33.

Orlovsky, G. N., Deliagina, T. G., Grillner, S., 1999. Neuronal control of locomotion: from mollusc to man. Oxford University Press Oxford.

Pearson, K. G., Fourtner, C. R., Jan. 1975. Nonspiking interneurons in walking system of the cockroach. Journal of Neurophysiology 38 (1), 33–52.

Pick, S., Strauss, R., Aug. 2005. Goal-driven behavioral adaptations in gap-climbing Drosophila. Current Biology 15 (16), 1473–8.

Quimby, L., Amer, A. S., Zill, S. N., Mar. 2006. Common motor mechanisms support body load in serially homologous legs of cockroaches in posture and walking. Journal of Comparative Physiology. A, Neuroethology, sensory, neural, and behavioral physiology 192 (3), 247–66.

Ridgel, A. L., Alexander, B. E., Ritzmann, R. E., Apr. 2007. Descending control of turning behavior in the cockroach, Blaberus discoidalis. Journal of Comparative Physiology. A, Neuroethology, sensory, neural, and behavioral physiology 193 (4), 385–402.

Ridgel, A. L., Ritzmann, R. E., Jun. 2005. Effects of neck and circumoesophageal connective lesions on posture and locomotion in the cockroach. Journal of Comparative Physiology. A, Neuroethology, sensory, neural, and behavioral physiology 191 (6), 559–73.

Ritzmann, R. E., Büschges, A., Dec. 2007. Adaptive motor behavior in insects. Current Opinion in Neurobiology 17 (6), 629–36.

Roberts, A., Li, W.-C., Soffe, S. R., Wolf, E. S., Jan. 2008. Origin of excitatory drive to a spinal locomotor network. Brain Research Reviews 57 (1), 22–8.

Roberts, A., Soffe, S. R., Wolf, E. S., Yoshida, M., Zhao, F. Y., Nov. 1998. Central circuits controlling locomotion in young frog tadpoles. Annals of the New York Academy of Sciences 860, 19–34.

Robertson, R. M., Pearson, K. G., Jan. 1985. Neural circuits in the flight system of the locust. Journal of Neurophysiology 53 (1), 110–28.

Rosano, H., Webb, B., Sep. 2007. A dynamic model of thoracic differentiation for the control of turning in the stick insect. Biological Cybernetics 97 (3), 229–46.

Rosenbaum, P., Wosnitza, A., Büschges, A., Gruhn, M., Sep. 2010. Activity patterns and timing of muscle activity in the forward walking and backward walking stick insect Carausius morosus. Journal of Neurophysiology 104 (3), 1681–95.

Sauer, A. E., Büschges, A., Stein, W., Apr. 1997. Role of presynaptic inputs to proprioceptive afferents in tuning sensorimotor pathways of an insect joint control network. Journal of Neurobiology 32 (4), 359–76.

Sauer, A. E., Driesang, R. B., Büschges, A., Bässler, U., Sep. 1996. Distributed processing on the basis of parallel and antagonistic pathways simulation of the femur-tibia control system in the stick insect. Journal of computational neuroscience 3 (3), 179–98.

Schaefer, P. L., Ritzmann, R. E., Oct. 2001. Descending influences on escape behavior and motor pattern in the cockroach. Journal of Neurobiology 49 (1), 9–28.

Scharstein, H., 1989. A universal projector for optomotor stimulation. In: Elsner, N., Singer, W. (Eds.), Dynamics and Plasticity in neuronal Systems. Proceedings of the 17th Göttingen Neurobiology Conference. Thieme, p. 116.

Schmidt, J., Fischer, H., Büschges, A., Jan. 2001. Pattern generation for walking and searching movements of a stick insect leg. II. Control of motoneuronal activity. Journal of Neurophysiology 85 (1), 354–61.

Schmitz, J., Oct. 1986a. Properties of the feedback system controlling the coxatrochanter joint in the stick insect Carausius morosus. Biological Cybernetics 55 (1), 35–42.

Schmitz, J., Oct. 1986b. The depressor trochanteris motoneurones and their role in the coxo-trochanteral feedback loop in the stick insect Carausius morosus. Biological Cybernetics 55 (1), 25–34.

Schmitz, J., Büschges, A., Kittmann, R., Dec. 1991a. Intracellular recordings from nonspiking interneurons in a semiintact, tethered walking insect. Journal of Neurobiology 22 (9), 907–21.

Schmitz, J., Dean, J., Kittmann, R., Mar. 1991b. Central projections of leg sense organs inCarausius morosus (Insecta, Phasmida). Zoomorphology 111 (1), 19–33.

Schmitz, J., Delcomyn, F., Büschges, A., 1991c. Oil and Hook Electrodes for en paasant recording from small nerves. Methods in Neuroscience 4, 266–278.

Siegler, M. V. S., Aug. 1981. Posture and history of movement determine membrane potential and synaptic events in nonspiking interneurons and motor neurons of the locust. Journal of Neurophysiology 46 (2), 296–309.

Siegler, M. V. S., 1985. Nonspiking interneurons and motor control in insects. Advances in Insect Physiology, 249–304.

Soffe, S. R., Roberts, A., Dec. 1982. Tonic and phasic synaptic input to spinal cord motoneurons during fictive locomotion in frog embryos. Journal of Neurophysiology 48 (6), 1279–88.

Stein, W., Büschges, A., Bässler, U., Sep. 2006. Intersegmental transfer of sensory signals in the stick insect leg muscle control system. Journal of Neurobiology 66 (11), 1253–69.

Strausfeld, N. J., Hirth, F., Apr. 2013. Deep homology of arthropod central complex and vertebrate basal ganglia. Science 340 (6129), 157–61.

Strauss, R., Dec. 2002. The central complex and the genetic dissection of locomotor behaviour. Current Opinion in Neurobiology 12 (6), 633–638.

Strauss, R., Heisenberg, M., Aug. 1990. Coordination of legs during straight walking and turning in Drosophila melanogaster. Journal of Comparative Physiology. A, Sensory, neural, and behavioral physiology 167 (3), 403–12.

Toth, T. I., Knops, S. A., Daun-Gruhn, S., Jun. 2012. A neuromechanical model explaining forward and backward stepping in the stick insect. Journal of Neurophysiology 107 (12), 3267–80.

Tryba, A. K., Ritzmann, R. E., Jun. 2000a. Multi-joint coordination during walking and foothold searching in the Blaberus cockroach. I. Kinematics and electromyograms. Journal of Neurophysiology 83 (6), 3323–36.

Tryba, A. K., Ritzmann, R. E., Jun. 2000b. Multi-joint coordination during walking and foothold searching in the Blaberus cockroach. II. Extensor motor neuron pattern. Journal of Neurophysiology 83 (6), 3337–50.

van Deursen, R., Flynn, T., McCrory, J., Morag, E., May 1998. Does a single control mechanism exist for both forward and backward walking? Gait & posture 7 (3), 214–224.

von Uckermann, G., 2008. Role of local premotor nonspiking interneurons in walking pattern generation of the stick insect Carausius morosus. Ph.D. thesis, University of Cologne.

von Uckermann, G., Büschges, A., Sep. 2009. Premotor interneurons in the local control of stepping motor output for the stick insect single middle leg. Journal of Neurophysiology 102 (3), 1956–75.

Wallén, P., Shupliakov, O., Hill, R. H., Oct. 1993. Origin of phasic synaptic inhibition in myotomal motoneurons during fictive locomotion in the lamprey. Experimental Brain Research 96 (2), 194–202.

Watson, J. T., Ritzmann, R. E., Pollack, A. J., Feb. 2002a. Control of climbing behavior in the cockroach, Blaberus discoidalis. II. Motor activities associated with joint movement. Journal of comparative physiology. A, Neuroethology, sensory, neural, and behavioral physiology 188 (1), 55–69.

Watson, J. T., Ritzmann, R. E., Zill, S. N., Pollack, A. J., Feb. 2002b. Control of obstacle climbing in the cockroach, Blaberus discoidalis. I. Kinematics. Journal of comparative physiology. A, Neuroethology, sensory, neural, and behavioral physiology 188 (1), 39–53.

Weidler, D. J., Diecke, F. P. J., Sep. 1969. The role of cations in conduction in the central nervous system of the herbivorous insect Carausius morosus. Zeitschrift fuer Vergleichende Physiologie 64 (4), 372–399.

Wendler, G., 1964. Laufen und Stehen der Stabheuschrecke Carausius morosus: Sinnesborstenfelder in den Beingelenken als Glieder von Regelkreisen. Journal of Comparative Physiology A: Neuroethology, ... 250, 198–250.

Wendler, G., Jan. 1966. The co-ordination of walking movements in arthropods. Symposia of the Society for Experimental Biology 20, 229–49.

Westmark, S., Oliveira, E. E., Schmidt, J., Aug. 2009. Pharmacological analysis of tonic activity in motoneurons during stick insect walking. Journal of Neurophysiology 102 (2), 1049–61.

Wildman, M., Ott, S. R., Burrows, M., Dec. 2002. GABA-like immunoreactivity in nonspiking interneurons of the locust metathoracic ganglion. Journal of Experimental Biology 205 (Pt 23), 3651–9.

Wilson, J. A., Jul. 1981. Unique, identifiable local nonspiking interneurons in the locust mesothoracic ganglion. Journal of Neurobiology 12 (4), 353–66.

Wilson, J. A., Phillips, C. E., Jan. 1982. Locust local nonspiking interneurons which tonically drive antagonistic motor neurons: physiology, morphology, and ultrastructure. Journal of Comparative Neurology 204 (1), 21–31.

Wilson, J. A., Phillips, C. E., Jan. 1983. Pre-motor non-spiking interneurons. Progress in Neurobiology 20 (1-2), 89–107.

Wolf, H., 1990. Activity patterns of inhibitory motoneurones and their impact on leg movement in tethered walking locusts. Journal of Experimental Biology 304, 281–304.

Wolf, H., Büschges, A., May 1995. Nonspiking local interneurons in insect leg motor control. II. Role of nonspiking local interneurons in the control of leg swing during walking. Journal of Neurophysiology 73 (5), 1861–75.

Wosnitza, A., Bockemühl, T., Dübbert, M., Scholz, H., Büschges, A., Feb. 2013. Inter-leg coordination in the control of walking speed in Drosophila. Journal of Experimental Biology 216 (Pt 3), 480–91.

Zelenin, P. V., Mar. 2011. Reticulospinal neurons controlling forward and backward swimming in the lamprey. Journal of Neurophysiology 105 (3), 1361–71.

Zelenin, P. V., Deliagina, T. G., Orlovsky, G. N., Karayannidou, A., Stout, E. E., Sirota, M. G., Beloozerova, I. N., Jun. 2011. Activity of motor cortex neurons during backward locomotion. Journal of Neurophysiology 105 (6), 2698–714.

Zhu, P., Narita, Y., Bundschuh, S. T., Fajardo, O., Schärer, Y.-P. Z., Chattopadhyaya, B., Bouldoires, E. A., Stepien, A. E., Deisseroth, K., Arber, S., Sprengel, R., Rijli, F. M., Friedrich, R. W., Jan. 2009. Optogenetic Dissection of Neuronal Circuits in Zebrafish using Viral Gene Transfer and the Tet System. Frontiers in Neural Circuits 3 (December), 21.

Zill, S. N., Keller, B. R., Duke, E. R., May 2009. Sensory signals of unloading in one leg follow stance onset in another leg: transfer of load and emergent coordination in cockroach walking. Journal of Neurophysiology 101 (5), 2297–304.

Zill, S. N., Schmitz, J., Chaudhry, S., Büschges, A., Sep. 2012. Force encoding in stick insect legs delineates a reference frame for motor control. Journal of Neurophysiology 108 (5), 1453–72.

Zollikofer, C., Jul. 1994. Stepping patterns in ants - influence of speed and curvature. Journal of Experimental Biology 192 (1), 95–106.

Zolotov, V., Frantsevich, L. I., Falk, E.-M., 1975. Kinematik der phototaktischen Drehung bei der HonigbieneApis mellifera L. Journal of Comparative Physiology A 97 (4), 339–353.

List of Figures

List of Tables

Teilpublikationen

Publications

1. Gruhn M, Rosenbaum P, Bollhagen HP, Büschges A (2011) Studying the neural basis of adaptive locomotor behavior in insects. J Vis Exp 50, doi: 10.3791/2629
2. Rosenbaum P, Wosnitza A, Büschges A, Gruhn M (2010) Activity patterns and timing of muscle activity in the forward walking and backward walking stick insect, Carausius morosus. J Neurophysiol 104: 1681-1695
3. Hooper SL, Guschlbauer C, Blümel M, Rosenbaum P, Gruhn M, Akay T, Büschges A (2009) Neural control of unloaded leg posture and of leg swing in stick insect, cockroach and mouse differs from that in larger animals. J Neurosci 29:4109-4119

Conference Abstracts

1. Rosenbaum P and Büschges A (2013) Neural control of forward and backward walking in insects. 10th Göttingen meeting of the German Neuroscience Society, Göttingen Germany
2. Gruhn M, Rosenbaum P, Borgmann A, Büschges A (2013) Body side specificity of descending control of leg motor activity during turning in an insect. 10th Göttingen meeting of the German Neuroscience Society, Göttingen Germany
3. Knops S, Tóth T, Rosenbaum P, Guschlbauer C, Gruhn M, Daun-Gruhn S (2012) Neuro-mechanical control of forwards, backwards and sidewards walking. Neurovisionen NRW, Aachen, Germany
4. Rosenbaum P, Schmitz J, Büschges A (2012) Neural control of adaptive locomotor behavior. 105th Annual meeting of the German Zoological Society, Konstanz, Germany
5. Rosenbaum P, Schmitz J, Büschges A (2012) Neural control of adaptive locomotor behavior. 23rd Annual Neurobiology Doctoral Student Workshop, Marburg, Germany
6. Rosenbaum P, Hellekes K, Gruhn M, Büschges A (2011) Neural mechanisms underlying turning in the stick insect. 41st Annual meeting of the Society for Neuroscience, Washington DC, USA

7. Gruhn M, Rosenbaum P, Hellekes K, Büschges A (2011) Neural mechanisms of turning in an insect. Janelia Farm Conference: Neural Basis of motor control, Janelia Farm, USA
8. Rosenbaum P, Schmitz J, Büschges A (2011) Changing of walking direction in the stick insect. Interdisciplinary College, Guenne, Germany
9. Gruhn M, Borgmann A, Rosenbaum P, Büschges A (2011) Descending control of turning in the stick insect Carausius morosus. 9th Göttingen meeting of the German Neuroscience Society, Göttingen Germany
10. Büschges A, Rosenbaum P, Wosnitza A, Gruhn M (2010) Activity and timing of leg muscles in the forward and backward walking stick insect. 40th Annual meeting of the Society for Neuroscience, San Diego, USA
11. Wosnitza A, Rosenbaum P, Büschges A, Gruhn M (2010) Leg muscle activity and timing in the forward and backward walking stick insect Carausius morosus. 9th meeting of the Society for Neuroethology, Salamanca, Spain
12. Rosenbaum P, Büschges A, Gruhn M (2009) Muscle activity of antagonistic leg muscles in a turning insect. Neurovisionen NRW, Bochum, Germany
13. Rosenbaum P, Zehl L, Büschges A, Gruhn M (2009) Muscle activity of antagonistic leg muscles in the walking stick insect. 8th Göttingen meeting of the German Neuroscience Society, Göttingen, Germany

Danksagung

Bei folgenden Personen möchte ich mich ganz besonders bedanken:

- Prof. Dr. Ansgar Büschges für die Vergabe des Themas, die sehr gute Betreuung und für seine ansteckende Begeisterung für die Wissenschaft,
- Prof. Dr. Peter Kloppenburg für die freundliche Übernahme des Zweitgutachtens und viele interessante Gespräche,
- Dr. Till Bockemühl, Eva Berg und Jens Goldammer für das Korrekturlesen der Arbeit und ihrer Editierung,
- Eva Berg, Jens Goldammer und Dr. Katja Hellekes für viele interessante und unterhaltsame Gespräche in unserem gemeinsamen Büro,
- Dr. Jochen Schmidt, Dr. Matthias Gruhn, Dr. Carmen Wellmann und Prof. Dr. Scott Hooper für viele Tipps und Tricks und Unterstützung im Verlauf der Doktorarbeit,
- Dipl. Ing. Michael Dübbert, Jan Sydow, Hans-Peter Bollhagen, Sima Seyed-Nejadi, Sherylane Seeliger und Lydia Berlingen für essentielle Unterstützung im Labor- und Unialltag,
- der gesamten Arbeitsgruppe Büschges, Wellmann und Gruhn für die großartige Atmosphäre im Labor und darüber hinaus,
- meinen Eltern, Geschwistern und Freunden für die tolle Unterstützung während der gesamten Doktorarbeitszeit.

Erklärung

Ich versichere, dass ich die von mir vorgelegte Dissertation selbstständig angefertigt, die benutzten Quellen und Hilfsmittel vollständig angegeben und die Stellen der Arbeit - einschließlich Tabellen, Karten und Abbildungen -, die anderen Werken im Wortlaut oder dem Sinn nach entnommen sind, in jedem Einzelfall als Entlehnung kenntlich gemacht habe; dass diese Dissertation noch keiner anderen Fakultät oder Universität zur Prüfung vorgelegen hat; dass sie - abgesehen von oben angegebenen Teilpublikationen - noch nicht veröffentlicht worden ist sowie, dass ich eine solche Veröffentlichung vor Abschluss des Promotionsverfahrens nicht vornehmen werde. Die Bestimmungen dieser Promotionsordnung sind mir bekannt. Die von mir vorgelegte Dissertation ist von Prof. Dr. Ansgar Büschges betreut worden.

Köln, den 01. August 2013